Study of the Behavior of the Daily Maximum Rainfall Regime in the Colombian Caribbean Region

Master Thesis

Orlando Manuel Viloria Marimón

With the approval of the directors:

Álvaro González Álvarez, Ph.D. **Andrés M. Vélez Pereira, Ph.D.**

Master Program in Engineering with an Emphasis in Civil and Environmental Engineering
School of Engineering
Universidad Tecnológica de Bolívar
Cartagena de Indias
November, 2019

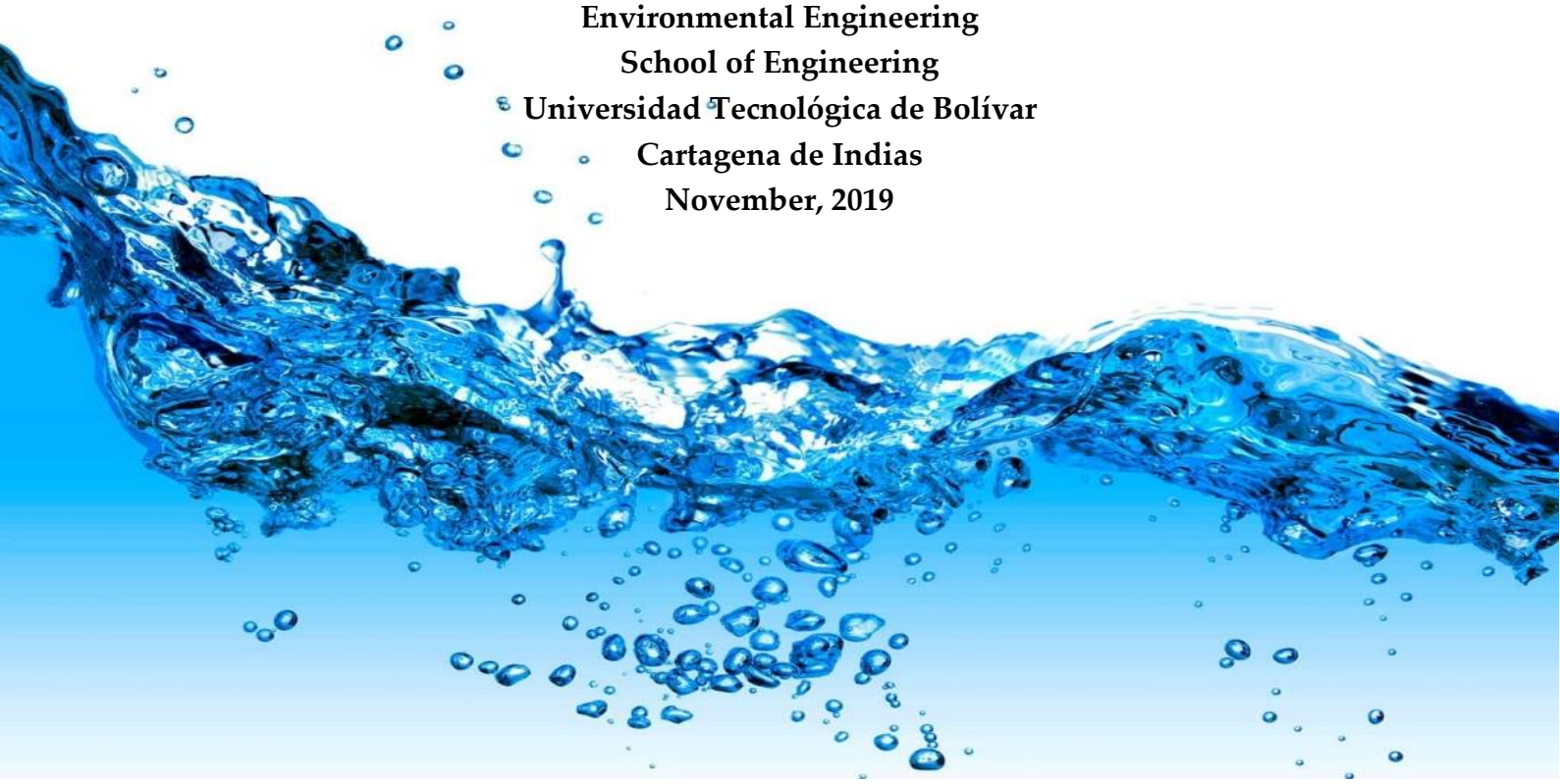

Table of Contents

List of Figures

List of Tables

Acknowledgments

Initially, I want to thank Professor ***Álvaro González*** who has been not only a mentor but almost a father to me. He was the one who allowed this process to begin and I am sure that without his guide, advice, constructive criticism, and phone calls, this process would not have ended today. For this reason, I want to use these lines to say: "*infinitas gracias*" and that "*lo siento profe*" for all the time you put into to make sure I always excelled in all I did. *Profe*, I do not know if one day I will exceed your expectations; however, I will always do my best and well…. The sky is the limit!

With these words, I also want to thank: (a) ***Universidad Tecnológica de Bolivar*** for granting the scholarship that allowed me to complete this stage in my life, (b) ***IDEAM*** for providing rainfall information for the development of this investigation, (c) ***my parents and family***, for their infinite support during this process, (d) ***Andres Velez*** for its guidance always aimed at improving this research, and (e) ***Dayana Rada*** (my girlfriend) who never stopped believing in me and was always there to support me and encourage me in moments of weakness, (e) my friends ***Vita, Vaca, Franzua, Robe, Peña, Luis, and Tatis*** for giving me the moments of joy, relax, and fun that my mind needed.

Finally, I want to dedicate this research to my grandfather ***Julio Cesar Marimón Ayola*** who always believed in me, even more than I thought. Thank you for your support during all these years.

General introduction

I. Introduction

Rainfall is one of the most important hydrometeorological variables. It is directly related to the availability of water resources in the territories owing to its influence on the process of runoff generation and, consequently, the recharge of streams and aquifers [1–3]. For these reasons, the estimation of rainfall values is fundamental for the development of projects that involve water resource management, such as: evaluation and design of structures for the management of stormwater, delimitation of flood-prone areas, territorial planning, determination of volumes of water for irrigation, among others [4–7].

The rainfall value used in the development of such projects is often called design rainfall [8]. For its estimation, time series of maximum daily rainfall are the most important input [9]. The design rainfall is used by hydrologists in the estimation of design flows, which are typically calculated through rainfall-runoff models [10]. However, the estimation of design rainfall values is one of the challenges hydrologists face, mainly due to, among others: (a) the spatial-temporal variability of rainfall, (b) the low density of rainfall gauges, and (c) errors during the rainfall frequency analysis. These problems become more challenging in ungauged regions where rainfall data has to be retrieved from neighboring rain gauges that probably do not have the same rainfall behavior [11].

In order to address the unavailability of information on spatial-temporal variability in a given ungauged area (or with low density of rain gauges), some studies have focused on applying a regional approach to the analysis of extreme rainfall events based on the concept of homogeneity so that rainfall data within a particular region can be safely assumed as similar. The concept of homogeneity permits to have more reliable results than those obtained with the traditional rain gauge selection method [12–16].

After selecting the rain gauge, another problem that typically arises is performing the rainfall frequency analysis (typically, under stationary conditions). This analysis consists in establishing a relationship between the magnitude of a rainfall event and its probability of occurrence. For this, a probability distribution function (PDF) (e.g. normal distribution, log-normal distribution, Pearson Type III, exponential function, Gumbel distribution, and generalized extreme value distribution (GEV)) needs to be selected so that the data analyzed fits best [15,17,18]. If an inappropriate PDF is selected the design rainfall values will be either over- or underestimated, which causes both project cost overruns in the and/or the collapse of a hydraulic structure during extreme rain events [19]. For this reason, many studies in different countries have focused on defining the PDF that show best fit to their rain gauges networks [9,20]. It is important to highlight that the rainfall frequency analysis under stationary conditions considers that the probability of occurrence of extreme event of rain remains constant over time and a geometric distribution can be used for its estimation [7,21]. Despite the fact the stationary frequency analysis has been widely used, studies in the United States, Canada, Brazil, South Korea, India, African cities and other regions of the world have shown the presence of changes in the rainfall regime [22–28], which demonstrates that the recurrence interval between rain events that equal or exceed the design rain, may be due to inhomogeneous geometric distributions [21]. This should oblige engineers to first perform an analysis to demonstrate whether a frequency analysis under non-stationary (which considers a non-homogeneous geometric distribution) is more convenient than a stationary one.

In the Colombian Caribbean region, there are few studies focused on generating information capable of preventing these setbacks at a regional scale (all departments that compose the Colombian Caribbean region) in the estimation of design rainfall derived from daily maximum rainfall ($P_{max\text{-}24h}$). For this reason, this research tries to contribute to the generation of this information through two stages/phases. During the first stage (Chapter 1), the study is focused on (a) determining the probabilistic distribution function that best fits the time series of the rain gauges within the Colombian Caribbean region according to the goodness of fit test, (b) evaluating the interpolation method with the better fit for the space distribution of the rain gauges of Colombian Caribbean region, and (c) generating isohyetals maps of $P_{max\text{-}24h}$ for return periods of 2, 5, 10, 20, 25, 50 and 100 years for the Colombian Caribbean region. The second stage (Chapter 2), corresponds to a case study focused on analyzing the behavior of maximum daily rainfall at a more local scale in the department of Atlántico (one of the departments of the Colombian Caribbean region). This part of the research deals with: (a) determining possible increasing/decreasing trends over time in the rain gauges of this department, (b) identifying regions with homogeneous behavior of $P_{max\text{-}24h}$ in the department of Atlántico, (c) assessing whether the time series are better suited under either a stationary or non-stationary frequency analyze via Akaike Information Criterion (AIC) test, and (d) generating isohyetal maps for different return periods using the $P_{max\text{-}24h}$ under stationary non-stationary and mixed conditions (stationary and non-stationary $P_{max\text{-}24h}$ based on the AIC test results).

The methodology developed in these two stages is expected to be lay the foundation of future studies in other areas of Colombia so as to have a better understanding of a key variable used in many water related projects.

II. Objectives

This study aims at analyzing the behavior of daily maximum rainfall multi-annual time series in the Colombian Caribbean region, which was carried out in two stages (explained in two separate chapters) each with specific objectives:

Chapter 1: *Isohyetal Maps of Daily Maximum Rainfall for Different Return Periods for the Colombian Caribbean Region.* The specific objective of this stage were to:

- Determine the probabilistic distribution function that best fit to the records of the rain gauges of the Colombian Caribbean region according to the goodness of fit test;
- Evaluate the interpolation method the best fit to the space distribution of the rain gauges of Colombian Caribbean region; and
- Generate isohyetals maps of $P_{max\text{-}24h}$, through the Geographic Information System (GIS), for return periods of 2, 5, 10, 20, 25, 50 and 100 years for the Colombian Caribbean region.

Chapter 2: *Analysis of the Behavior of Daily Maximum Rainfall within the Department of Atlántico, Colombia.* The specific objectives of this stage were to:

- Determine possible increasing/decreasing trends over time in the rain gauges of department of Atlántico;
- Identify regions with homogeneous behavior of $P_{max\text{-}24h}$ in the department of Atlántico.
- Assess whether the time series are better suited under either a stationary or non-stationary frequency analyze via Akaike Information Criterion (AIC) test; and
- Generate isohyetals maps for different return periods using the $P_{max\text{-}24h}$ under stationary, non-stationary and mixed conditions (stationary and non-stationary $P_{max\text{-}24h}$ based on the AIC test results).

III. References

1. Guillén Bolaños, T.; Máñez Costa, M.; Nehren, U. Development of a Prioritization Tool for Climate Change Adaptation Measures in the Forestry Sector—A Nicaraguan Case Study. In *Economic Tools and Methods for the Analysis of Global Change Impacts on Agriculture and Food Security*; Quiroga, S., Ed.; Springer International Publishing: Cham, 2018; pp. 165–177 ISBN 978-3-319-99462-8.
2. Młyński, D.; Wałęga, A.; Petroselli, A.; Tauro, F.; Cebulska, M. Estimating Maximum Daily Precipitation in the Upper Vistula Basin, Poland. *Atmosphere* **2019**, *10*, 43.
3. Schmocker-Fackel, P.; Naef, F. More frequent flooding? Changes in flood frequency in Switzerland since 1850. *J. Hydrol.* **2010**, *381*, 1–8.
4. Chorley, R.J. *Introduction to geographical hydrology: Spatial aspects of the interactions between water occurrence and human activity*; Routledge, 2019; ISBN 1-00-000023-0.
5. Abdallah, W.; Allani, M.; Mezzi, R.; Jlassi, R.; Romdhane, A.; Faidi, F.; Daouthi, Z.; Amara, A.; Selmi, H.; Zouabi, A. A Contribution to an Advisory Plan for Integrated Irrigation Water Management at Sidi Saad Dam System (Central Tunisia): From Research to Operational Support. In *Embedding Space in African Society*; Springer, 2019; pp. 65–79.
6. Gurjar, G.; Swami, S. Impacts of irrigation and rainfall on agricultural production under climate change. *Int. J. Chem. Stud.* 3.
7. Chow, V.T.; Maidment, D.R.; Mays, L.W. *Applied hydrology*; 1st ed.; McGraw-Hill: New York, NY, USA, 1998;
8. Koutsoyiannis, D.; Baloutsos, G. Analysis of a long record of annual maximum rainfall in Athens, Greece, and design rainfall inferences. *Nat. Hazards* **2000**, *22*, 29–48.
9. Koutsoyiannis, D. Statistics of extremes and estimation of extreme rainfall: I. Theoretical investigation / Statistiques de valeurs extrêmes et estimation de précipitations extrêmes: I. Recherche théorique. *Hydrol. Sci. J.* **2004**, *49*, null-590.
10. Ledingham, J.; Archer, D.; Lewis, E.; Fowler, H.; Kilsby, C. Contrasting seasonality of storm rainfall and flood runoff in the UK and some implications for rainfall-runoff methods of flood estimation. *Hydrol. Res.* **2019**, *50*, 1309–1323.
11. Luna Vera, J.A.; Domínguez Mora, R. Un método para el análisis de frecuencia regional de lluvias máximas diarias: aplicación en los Andes bolivianos. *Ingeniare Rev. Chil. Ing.* **2013**, *21*, 111–124.
12. Paulo Terassi; Emerson Galvani Identification of Homogeneous Rainfall Regions in the Eastern Watersheds of the State of Paraná, Brazil. *Climate* **2017**, *5*, 53.
13. Pelczer, I.; Ramos, J.; Domínguez, R.; González, F. Establishment of regional homogeneous zones in a watershed using clustering algorithms. 10.
14. Saikranthi, K.; Rao, T.N.; Rajeevan, M.; Bhaskara Rao, S.V. Identification and Validation of Homogeneous Rainfall Zones in India Using Correlation Analysis. *J. Hydrometeorol.* **2013**, *14*, 304–317.
15. Hoskins, J.; Wallis, J. *Regional frequency analysis: An approach based on l-moments*; Cambridge University, 1997; ISBN 0-521-01940-0.
16. Arellano-Lara, F.; Escalante-Sandoval, C.A. Multivariate delineation of rainfall homogeneous regions for estimating quantiles of maximum daily rainfall: A case study of northwestern Mexico. *Atmósfera* **2014**, *27*, 47–60.
17. Singh, B.; Rajpurohit, D.; Vasishth, A.; Singh, J. Probability analysis for estimation of annual one day maximum rainfall of Jhalarapatan Area of Rajasthan. 9.
18. Salinas, J.L.; Castellarin, A.; Kohnová, S.; Kjeldsen, T.R. Regional parent flood frequency distributions in Europe – Part 2: Climate and scale controls. *Hydrol. Earth Syst. Sci.* **2014**, *18*, 4391–4401.

19. Haddad, K.; Rahman, A. Selection of the best fit flood frequency distribution and parameter estimation procedure: a case study for Tasmania in Australia. *Stoch. Environ. Res. Risk Assess.* **2011**, *25*, 415–428.
20. Wdowikowski, M.; Kaźmierczak, B.; Ledvinka, O. Maximum daily rainfall analysis at selected meteorological stations in the upper Lusatian Neisse River basin. *Meteorol. Hydrol. Water Manag.* **2016**, *4*, 53–63.
21. Gonzalez-Alvarez, A.; Coronado-Hernández, O.; Fuertes-Miquel, V.; Ramos, H. Effect of the Non-Stationarity of Rainfall Events on the Design of Hydraulic Structures for Runoff Management and Its Applications to a Case Study at Gordo Creek Watershed in Cartagena de Indias, Colombia. *Fluids* **2018**, *3*, 27.
22. Westra, S.; Fowler, H.J.; Evans, J.P.; Alexander, L.V.; Berg, P.; Johnson, F.; Kendon, E.J.; Lenderink, G.; Roberts, N.M. Future changes to the intensity and frequency of short-duration extreme rainfall. *Rev. Geophys.* **2014**, *52*, 522–555.
23. Sarhadi, A.; Soulis, E.D. Time-varying extreme rainfall intensity-duration-frequency curves in a changing climate. *Geophys. Res. Lett.* **2017**, *44*, 2454–2463.
24. Mailhot, A.; Duchesne, S.; Caya, D.; Talbot, G. Assessment of future change in intensity–duration–frequency (IDF) curves for Southern Quebec using the Canadian Regional Climate Model (CRCM). *J. Hydrol.* **2007**, *347*, 197–210.
25. Sugahara, S.; Rocha, R.P. da; Silveira, R. Non-stationary frequency analysis of extreme daily rainfall in Sao Paulo, Brazil. *Int. J. Climatol.* **2009**, *29*, 1339–1349.
26. Lima, C.H.R.; Kwon, H.-H.; Kim, J.-Y. A Bayesian beta distribution model for estimating rainfall IDF curves in a changing climate. *J. Hydrol.* **2016**, *540*, 744–756.
27. Mondal, A.; Mujumdar, P.P. Modeling non-stationarity in intensity, duration and frequency of extreme rainfall over India. *J. Hydrol.* **2015**, *521*, 217–231.
28. De Paola, F.; Giugni, M.; Topa, M.E.; Bucchignani, E. Intensity-Duration-Frequency (IDF) rainfall curves, for data series and climate projection in African cities. *SpringerPlus* **2014**, *3*, 133.

Chapter 1: Isohyetals Maps of Daily Maximum Rainfall for Different Return Periods for the Colombian Caribbean Region

The final result of this stage of the research was a manuscript already published (shown below) in the Journal Water (MDPI) under the same title with the following citation:

González-Álvarez, Á.; Viloria-Marimón, O.M.; Coronado-Hernández, Ó.E.; Vélez-Pereira, A.M.; Tesfagiorgis, K.; Coronado-Hernández, J.R. Isohyetal Maps of Daily Maximum Rainfall for Different Return Periods for the Colombian Caribbean Region. *Water* 2019, *11*, 358 (available at: https://www.mdpi.com/2073-4441/11/2/358)

Abstract: In Colombia, daily maximum multiannual series are one of the main inputs for design streamflow calculation, which requires performing a rainfall frequency analysis that involves several prior steps: (a) requesting the datasets, (b) waiting for the information, (c) reviewing the datasets received for missing or data different from the requested variable, and (d) requesting the information once again if it is not correct. To tackle these setbacks, 318 rain gauges located in the Colombian Caribbean region were used to first evaluate whether or not the Gumbel distribution was indeed the most suitable by performing frequency analyses using three different distributions (Gumbel, Generalized Extreme Value (GEV), and Log-Pearson 3 (LP3)); secondly, to generate daily maximum isohyetal maps for return periods of 2, 5, 10, 20, 25, 50, and 100 years; and, lastly, to evaluate which interpolation method (IDW, spline, and ordinary kriging) works best in areas with a varying density of data points. GEV was most suitable in 47.2% of the rain gauges, while Gumbel, in spite of being widely used in Colombia, was only suitable in 34.3% of the cases. Regarding the interpolation method, better isohyetals were obtained with the IDW method. In general, the areal maximum daily rainfall estimated showed good agreement when compared to the true values.

1-1. Introduction

Designing hydraulic structures for stormwater management encompasses several tasks, among which are: (a) watershed morphometric analysis, (b) estimation of the time of concentration, (c) calculation of the design rainfall via frequency analysis (typically, under stationary conditions), (d) design flow computation, (e) sizing the hydraulic structure per se, and (f) hydraulic modeling to evaluate the structure's hydraulic performance under various return periods. The design flow may be estimated via either a rainfall-runoff model or regression equations (in ungauged watersheds), or stationary frequency analysis of streamflow data, if available.

Unlike streamflow data, rainfall observations are the most abundant hydrometeorological variable available. Rainfall observations, as a result, are most commonly used when estimating the flow value in ungauged watersheds (via rainfall-runoff models) to design hydraulic structures for runoff management. The Institute of Hydrology, Meteorology, and Environmental Studies of Colombia (IDEAM in Spanish) has hundreds of rain gauges (pluviometers and pluviographs) within Colombia. However, there are certain limitations when it comes to the availability of the rainfall data. The most common are: areas not covered due to either the absence of a rain gauge, or rain gauges no longer in service, or the rain gauges are mostly pluviometers (not pluviographs). The latter limits the ability to: (a) try to understand the real (measured) rainfall's behavior during a day (its temporal distribution) and (b) derive, for instance, Intensity-Duration-Frequency (IDF) curves directly from registered time increments of daily rainfall (from pluviographs). Instead, synthetic IDF curves are typically derived [1–3], which often need multiannual 24-h maximum rainfall ($P_{24h\text{-}max}$) as one of the main inputs to later estimate the rainfall (intensity) value associated with a selected return period: the design rainfall.

IDEAM has lately made many efforts in compiling the majority of the hydrometeorological information freely available for all. The amount of analyzed information on record has considerably increased in the last decade. For instance, total annual average rainfall and temperature were modeled via regional climate models to try to quantify their behavior over the years 2011–2100 by taking into account climate change [4]. Furthermore, during the years 2015 and 2016, IDEAM updated the Intensity-Duration-Frequency (IDF) curves of 130 rain gauges (only 14 of them were in the Caribbean region) by using pluviographs with rainfall observations up to 2010 [5]. On the other hand, MinVivienda [6] recently mandated to both utilize updated rainfall observations that include data of the last five years on record and evaluate the influence of climate change on the rainfall pattern of the area of interest whenever a stormwater system is to be designed. It also recommends to check regularly for the bulletins IDEAM issues (and updates) on climate change and the influence on rainfall. All this represents, undoubtedly, a significant step towards a better understanding (and analysis) of the hydrometeorological variables and their use either in the design of stormwater systems or watershed management plans. Nonetheless, there is information still waiting to be processed, analyzed, and presented in different formats. Because of this, hydrologists and other water-related professionals and scientists sometimes spend a considerable amount of time on rainfall analyses. For frequency analysis, multiple probability functions with two and/or three parameters have been developed to fit the extreme data, among which are: Gumbel, log-normal, gamma, exponential, Pearson 3 (P3), Log-Pearson 3 (LP3), and Generalized Extreme Value (GEV) [1,2]. The variable analyzed is considered both random and independent [1,2]. Some countries have opted to officially recommend the use of one probability distribution function so as to unify criteria. Several studies have been conducted in order to improve the results obtained from frequency analysis. Li et al. [7] and Chowdhury et al. [8] assessed the performance of various distributions (gamma, exponential, mixed-exponential, log-normal) and proposed enhancements by means of stochastic models. Furthermore, regional studies have utilized different probability distribution functions to analyze rainfall data. Pizarro et al. [9] developed a web-based platform to develop IDF curves in Chile by using three distribution functions (Gumbel, GEV, and P3). Burgess et al. [10] updated the existing IDF curves of Jamaica by means of a frequency analysis under the Gumbel distribution. Seo et al. [11] derived design rainfall values via Gumbel and GEV distributions, and the parameter estimation was made through the minimum density power divergence estimator. Nguyen and Nguyen [12] developed a tool to evaluate the performance of ten probability distributions (beta-K, beta-P, GEV, generalized logistic, generalized normal, generalized Pareto, Gumbel, LP3, P3, and Wakeby) over rainfall data in Ontario (Canada). Likewise, isohyetal maps for different durations for various countries have been developed using various probability functions to fit the datasets [13–17].

Independently of the probability distribution function used to derive the isohyetals, having a map, where the design rainfall values for different return periods can be easily selected, would both substantially reduce the time dedicated to this activity and help with the estimation of design rainfalls, especially in ungauged areas, necessary for projects and studies (both local and foreign) with a hydrological and hydraulic component such as flood risk evaluation and mitigation, environmental impact assessments, land development, stream restoration, and the design of hydraulic structures for stormwater management. Unfortunately, there is no such map in Colombia. The lack of readily-available and processed information might become an obstacle in the understanding and development of these projects. Furthermore, in the absence of data, detailed isohyetal maps such as the ones developed in this research can be utilized for both regional and global analyses of extreme rainfall event proxies, hydrological regime changes, climate studies, water balance estimation under various scenarios, and the development of water management strategies.

This study intends to contribute to these tasks by: (a) first carrying out rainfall stationary frequency analyses by means of three different Cumulative Distribution Functions (CDF) for extreme values analysis (Gumbel, GEV, and LP3) so as to confirm whether or not the Gumbel distribution is indeed the most suitable for the rainfall data of this study, as it is the most commonly used in Colombia despite the fact that the other two have been also assessed in various studies [18–23]; (b) secondly, evaluating which spatial interpolation method is most suitable given the highly-dense spatial distribution of the rain gauges; and (c) lastly, drawing isohyetal maps of $P_{24h\text{-}max}$—via Geographical Information System (GIS)—for return periods of 2, 5, 10, 20, 25, 50, and 100 years for the Colombian Caribbean region as the first step in a more ambitious project of elaborating maps for the remaining regions (Pacific, Andean, Orinoco, and Amazon). For that, 318 pluviometric stations (rain gauges) operated by IDEAM—with at least 30 years of data—were used. The rain gauges are distributed as follows: 313 throughout the seven departments that compose the Colombian Caribbean region (Guajira, Magdalena, Cesar, Atlántico, Bolívar, Sucre, and Córdoba) and five from neighboring departments (Antioquia, Santander, and Norte de Santander).

1-2. Study Area and Data

The Caribbean region of Colombia is comprised of seven political and administrative territorial units (called departments), namely Guajira, Magdalena, Cesar, Atlántico, Bolívar, Sucre, and Córdoba, which sum up a total area of 132,244 km^2 (accounting for approximately 12% of the country's total surface area). It has an average annual precipitation that ranges from 0–1500 mm (the region's northern portion) and from 1500 mm up to 5000 mm (in some areas of the southern portion of the departments of Bolívar and Córdoba) [4]. The region is mostly composed of plains, with the exception of the mountain ranges of San Jacinto (located within the departments of Sucre and Bolívar) and Santa Marta (department of Magdalena). The rainiest departments are Bolívar and Sucre, while the driest is Guajira. The average annual temperature is about 30°C with some areas where it may increase or decrease depending on the climatological season and altitude. The rainfall climate regime of the Colombian Caribbean region has three seasons [24]: dry (December–March), transition—also known as Veranillo de San Juan—(June–July), and rainy (April–June and August–November). The duration of these seasons is affected by the El Niño Southern Oscillation (ENSO) phenomenon [25–29].

The data used in this study correspond to multiannual series of $P_{24h\text{-}max}$ that include a total of 12,828 observations till the year 2015 from 318 pluviometric stations (the oldest station in this study started to operate in 1931). Years 2016 and 2017 were not included because the data from some of the stations have not been officially released by IDEAM. The pluviometric stations selected had to comply with the following criteria: (a) being still operative and (b) having at least 30 years of observations [30]. Additionally, $P_{24h\text{-}max}$ values were eliminated if they came from a year not having a minimum of 150 days of data [31–33] and/or missing any of the months of the rainy season. The resulting rainfall data are summarized in Table 1-1. Figure 1-1 shows the departments and the geographical location of the rain gauges. Out of the 318 rain gauges, 183 have 30–40 years of data, 113 have 41–50 years of data, and 22 have more than 50 years of rainfall observations. It may also be observed that the southern areas of the departments of Bolívar and Córdoba have no rain gauges that fit the selection criteria. To fill these gaps, it is necessary to improve the isohyetal alignment, so five additional rain gauges were used. The rain gauges are located within the three neighboring departments of Antioquia (three rain gauges), Santander (one rain gauge), and Norte de Santander (one rain gauge). Despite the fact that these three departments do not belong to the Caribbean region, the rain gauges selected are located close to the southern portion of the Caribbean region. Table 1-2 summarizes the names of the rain gauges analyzed in this study.

Table 1-1. Summary of rainfall data analyzed.

Department	No. of Rain Gauges	Total $P_{24h\text{-}max}$ observations	$P_{24h\text{-}max}$ value (mm)			Year of installation of the oldest rain gauge
			Max	Min	Avg.	
Guajira	44	1834	247.6	5.4	77.6	1937
Cesar	60	2478	271.0	20.0	99.8	1931
Magdalena	55	2159	267.0	15.0	98.7	1956
Atlántico	13	568	250.0	30.0	83.8	1941
Bolívar	57	2153	280.0	24.5	104.4	1941
Sucre	32	1232	301.0	32.0	101.9	1945
Córdoba	53	2184	250.0	34.0	96.4	1959
Antioquia	3	115	254.0	54.0	106.4	1974
Santander	1	61	100.0	20.0	45.48	1956
Norte de Santander	1	44	152.0	38.4	77.0	1974
Total	**319**	**12828**				

Gray cells indicate the maximum and minimum values (of all) recorded, respectively.

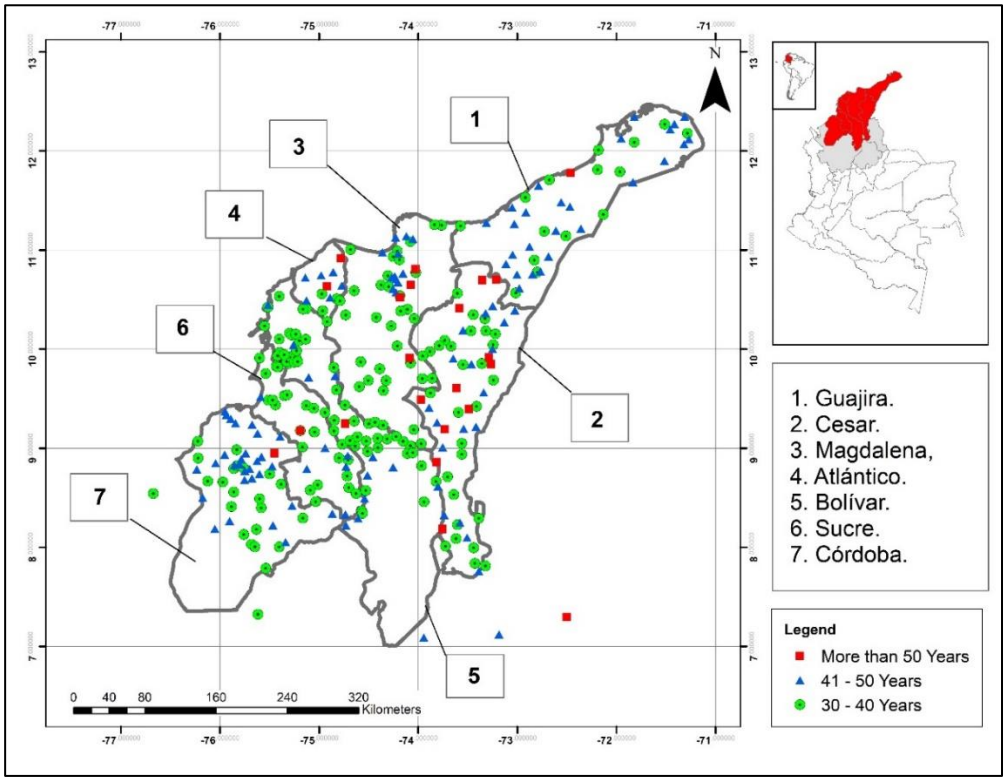

Figure 1-1. Study area and location of pluviometric stations (gray areas in the upper-right map are, from left to right, the departments of Antioquia, Santander, and Norte de Santander)

Table 1-2. Rain gauges of the area of study

Dept.	Rain Gauge Names
Atlántico	Hibaracho, Lena, Polo Nuevo, Pto. Giraldo, Casa de Bombas, Repelón, Sabanalarga, Los Campanos, Hda. El Rabón, Apto. Ernesto Cortissoz, Ponedera, San Pedrito Alerta, and Usiacurí.
Bolívar	Bayunca, Apto. Rafael Núñez, Escuela Naval-CIOH, Santa Ana, Guacamayo, Guaranda, Buenavista, Rionuevo, Arenal, Arjona, Rocha, Sincerín, Barranco Loba, El Limón, La Esperanza, Córdoba, Carmen de Bolívar, Camarón, Pozón, Aguadas La Alerta, San Antonio, Barraco Yuca, Coyongal Alertas, Barbosa, Baracoa, Gamero, San Basilio, El Viso, Chilloa, Flamenco, La Calma, Níspero, Plátano, Mampuján, Presa Arroyo Grande, Nueva

Dept.	Rain Gauge Names
	Florida, San Pablo, Sta. Cruz, Candelaria, Guaymaral, Mompox, Pinillos, Regidor, San Estanislao, Sta. Rosa, El Jolón, San Cristobal, Casa Piedra, Caimital, La Candelaria, Astilleros, La Raya, San Cayetano, Playitas, Zambrano, Hda. Indugan, and Cañaveral.
Cesar	Villa Marlene, Patillal, Atanquez, París de Francia, La Esperanza, Caracolí, San Ángel, Villa Rosa, El Callao, Apto. Alfonso López, Guaymaral, Barranca Lebrija, Totumal, Aguas Claras, Hda. Las Playas, Hda. Sta. Teresa, Codazzi DC, Hda. Centenario, El Retorno, Motilonia Codazzi, Astrea, El Yucal, Socomba, Bosconia, Palmariguaní, Hda. Manature, El Canal, Saloa, Hda. El Terror, Chimichagua, Rincón Hondo, Chiriguaná, Curumaní, Zapatoza, Poponte, La Primavera, La Loma, El Paso, Puerto Mosquito, Gamarra, La Gloria, La Vega, La Jagua, Manaure, La Raya, Sta. Isabel, Pueblo Bello, San Sebastián de Rábago, Río de Oro, Los Ángeles, Hda. San Daniel, El Líbano, San Alberto, Los Planes, San Benito, San Gabriel, Leticia, El Rincón, La Dorada, and Tamalameque.
Córdoba	Sta. Lucía, Hda. Sta. Cruz, Loma Verde, Galán, San Anterito, Buenos Aires, Maracayo, Boca de la Ceiba, Sabanal, Universidad de Córdoba, Apto. Los Garzones, Los Pájaros, Cecilia, Ayapel, Buenavista, Rabolargo, Canalete, Cereté, Turipana, Chimá, Chinú, Turipana, El Salado, La Apartada, La Doctrina, Lorica, Momil, Pica Pica, San Francisco, Hda. Cuba, Centro Alegre, Planeta Rica, Cintura, Hda. Sajondía, Jaramagal, Cristo Rey, Hda. Las Acacias, Sahagún, Jobo El Tablón, Trementino, Colomboy, El Limón, San Bernardo del Viento, San Carlos, Sta. Rosa, Carrizal, Callemar, Corozal 2, San Antonio, Carrillo, Uré, Tierra Alta, and Carmelo.
Guajira	Matitas, Camarones, Los Remedios, Apto. Almirante Padilla, La Arena, Cuestecita, Hda. La Esperanza, Lagunitas, Sabanas de Manuela, Dibulla, Las Lomitas, El Juguete, El Conejo, La Paulina, Escuela Ceura, Paraguachón, Escuela Agropecuaria Carraipía, El Pájaro, Mayapo, Caracas, Manaure, Cañaverales, Hatico de los Indios, San Juan del Cesar, Santana Urraich, Nuevo Ambiente, Buenos Aires, Kauraquimaná, Irraipa, Perpana, Carrizal, Jojoncito, Caimito, Puerto Estrella, Orochón, Sipanao, Siapana, Sillamaná, Jasay, Puerto López, Nazareth, Rancho Grande, Urumita, and Villanueva.
Magdalena	Vista Nieves, Buritaca, Minca, Apto. Simón Bolívar, Guacacha, San Lorenzo, Palomino, Cenizo, La María, Villa Concepción, Camp. El Difícil, Hda. La Cabaña, San Pablo, La Ye, La Palma, Menchiquejo, El Palmor, Sevillano, San Roque, Tiogollo, Negritos, Las Flores, El Bongo, El Destino , Gavilán, La Florida, Bellavista, Bayano, Fundación Rosa de Lima, Nueva Granada, Irán, Doña María, Monterrubio, Garrapata, Apure El Agrado, Tasajera, La Esperanza, Palo Alto, San Rafael, San Ángel, San Sebastián, Salamina, San Zenón, El Brillante, Tierra Grata, La Mecha, El Pueblito, Los Cocos, El Carmen, El Enano, Prado Sevilla, Los Proyectos, and La Unión.
Sucre	Hda. La Frontera, Caimito, Primates, Hato Nuevo, Apto. Rafael Bravo, Galeras, Villanueva, Pto. Asis, Palmarito, Zapata, Majagual, Las Tablitas, Santiago Apóstol, San Benito de Abad, Hda. Eureka, Hda. El Torno, Tolú, Hda. Santa Ángela, Tolú Viejo, San Onofre, Sabanas de Mucacal, Sabanatica, Hda. La Argentina, Chalán, Hda. Belén, Villa Cecilia, San Pedro, Palo Alto, Campo Alegre, San Luis, Berrugas, and Isla de Coco.
Antioquia	Yondó, El Mellito, and San Rita.
Santander	Apto. Palonegro.
Norte de Santander	Labateca.

1-3. Methodology

After having initially selected the pluviometric stations and the $P_{24h\text{-}max}$ data, further data analysis was required, which is explained in the next sub-sections. Figure 1-2 depicts the flowchart of the methodology proposed. The preprocessing (pluviometric station selection and $P_{24h\text{-}max}$ data selection) for the rainfall data selection was already explained in the previous section.

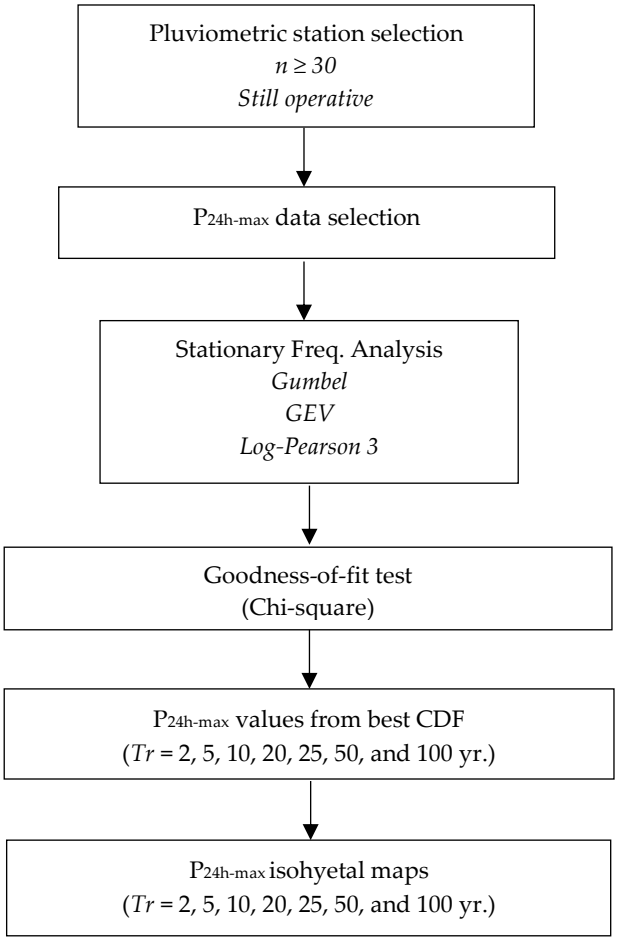

Figure 1-2. Flowchart of the proposed methodology

1-3.1. Stationary Frequency Analysis

In hydrology, there are several CDFs for the analysis of extreme values, namely: gamma, Extreme Value (EV) or Fisher–Tippett (Types 1, 2, and 3), Generalized Extreme Value (GEV), log-normal, Pearson 3, and log-Pearson 3, among others. When a frequency analysis assumes that the CDF used does not change over time, it is called stationary [34,35]. The CDF represents the probability of no-exceedance (probability that the value analyzed is less than or equal to the rest of the values in the dataset). With respect to the variable (or variate) analyzed, it must be random (uncertainty in its prediction) and independent (its occurrence is not affected by other variables) [36]. Extensive literature exists on this topic [1,2,37–40].

1-3.1.1. Gumbel Distribution (Extreme Value Type 1 or Fisher–Tippett Type 1)

Gumbel is a two-parameter unbounded distribution (the shape parameter, k, is zero for this distribution), which uses a double exponential function to estimate the probability of exceedance [$F(Z)$] [41,42]. In Equations (1), (2), and (3), z is the random variable (rainfall, streamflow, wind, etc.), β is the mode (location parameter), α is the dispersion (scale parameter), and z and σ_z are the mean and the variance of the random variable, respectively. It is one of the most-used CDFs by hydrologist and other water-related professionals in Colombia. It is also used in New Zealand for rainfall frequency analysis.

$$F(Z) = 1 - e^{-e^{\left[\frac{z-\beta}{\propto}\right]}} \quad \text{(for maximum values)} \tag{1}$$

$$\beta = \frac{\sigma_z\sqrt{6}}{\pi} \quad (2)$$

$$\alpha = \bar{z} - 0.5772\beta \quad \text{(for maximum values)} \quad (3)$$

1-3.1.2. Generalized Extreme Value Distribution

The GEV is a three-parameter distribution that compiles all three types of the EV distributions into one formula (Equation (4)). In Equation (4), *F(Z)* is the CDF, *z* is the random variable, *k* is the shape (or shift) parameter, β is the mode (location parameter), and α is the dispersion (scale parameter, always assumed to be greater than zero). The GEV distribution may adopt one of the three EV distributions depending on the value of *k* [1,2,40]: (a) when *k* equals zero, EV is Type 1 (Gumbel) [41,42]; (b) when *k* is less than zero, EV is Type 2 (Fréchet) [43,44]; and (c) when *k* greater than zero, EV is Type 3 (Weibull)[45].

$$F(Z) = \exp\left[-\left(1 - k\frac{z-\beta}{\alpha}\right)^{1/k}\right] \quad (4)$$

This distribution is one of the most widely used. Countries like the United States (especially in the eastern portion), the United Kingdom, Australia, Bangladesh, Canada, South Africa, and New Zealand have adopted it in some areas [46–51].

1-3.1.3. Log-Pearson 3

This occurs when the logarithms of the variable analyzed fit the Pearson 3 distribution (P3) (Equation (5)). The P3 consists of a gamma distribution with three parameters (Equations (5)–(8)), namely β (shape parameter), λ (scale parameter), and G (location parameter).

$$F(Z) = \frac{\lambda^{\beta}(y-\epsilon)^{\beta}e^{-\lambda(y-\epsilon)}}{z\Gamma(\beta)} \quad \text{(where } y = log\ (z)\text{)} \quad (5)$$

$$\lambda = \frac{S_y}{\sqrt{\beta}} \quad (6)$$

$$\beta = \left[\frac{2}{C_s(y)}\right]^2 \text{ (assuming that } Cs(y) > 0) \quad (7)$$

$$\epsilon = \bar{y} - S_y\sqrt{\beta} \quad (8)$$

LP3 is the recommended distribution in the United States (typically for flood analysis), Australia, Taiwan, Pakistan, and Nigeria [52–57].

1-3.2. Goodness-of-Fit Test

The goodness-of-fit of the three CDFs used in the frequency analysis was evaluated via the chi-squared test (X^2) with a significance level of 0.05.

$$X^2 = \frac{\sum_i^n (O_i - P_i)^2}{P_i} \quad (9)$$

In Equation (9), O_i and P_i are the observed and predicted distributions, respectively. The theory behind this test may be found throughout the literature on statistical hydrology [1,2,38,40]. In

general, when testing several CDFs for frequency analysis, the lower the value of X^2, the better the CDF fits the dataset.

1-3.3. Estimation of $P_{24h\text{-}max}$ for Different Return Periods

All datasets for each of the 318 rain gauges were subjected to a stationary frequency analysis by using the above-described distributions. The return period (*Tr*) or recurrence interval is a concept commonly misinterpreted, as some describe it as the time (in years) it takes an event (rainfall, streamflow, etc.) to occur again. Instead, *Tr* must be understood as the occurrence of a given rainfall event, in any particular year, that may be equal to or exceeded by some percentage. The return period and the probability of exceedance (*Pe*) are inversely proportional ($Tr = 1/Pe$). The *Tr* is used in many fields: hydrology, hydraulic structures design, protection of water bodies receiving wastewater discharges (low flow indices' estimation), and ecology, just to mention some. The parameters of the Gumbel and GEV distributions were estimated via the maximum likelihood method [1,2,40,58–60], and the Sundry Averages Method (SAM) method was used for LP3 [1,2,40,52–54].

The values of $P_{24h\text{-}max}$ selected (to be later used in the drawing of the isohyetals) for the return periods of 2, 5, 10, 20, 25, 50, and 100 years were those that came from the CDF showing the best result in the goodness-of-fit test. Additionally, a test for outliers was performed ([1], pp. 403–405). Two rain gauges were found to have outliers, namely San Cayetano (department of Bolívar) and Irán (department of Magdalena). The outliers were eliminated, and a new frequency analysis was made for these two rain gauges.

1-3.4. Drawing of Isohyetals for Different Return Periods

A spreadsheet with the geographical location (latitude and longitude) of the 318 rain gauges along with their corresponding estimated $P_{24h\text{-}max}$ values for the different return periods was exported into ArcGIS (Version 10.4.1, ESRI Inc., Redlands, CA, USA) to create a layer for further processing. Given the large density of rain gauges in some areas, three interpolation methods were used to generate the isohyetals: Inverse Distance Weighting (IDW), Ordinary Kriging (OK), and Spline (SP), in order to evaluate their performance prior to selecting one of the methods [61–63]. Default ArcGIS inputs were used in all methods since a sensitivity analysis done for each of the methods by changing the various inputs showed no major changes or improvements in the areas with noticeable alignment discrepancies. The ArcGIS inputs for the three methods are shown in Table 1-3.

Table 1-3. ArcGIS Inputs for each interpolation method.

Interpolation Method	Z-Value	Cell Size	Search Radius
Spline (Regularized)	2	0.021	Variable Number of points: 12. Weight: 0.1
Ordinary Kriging	2	0.021	Variable Number of points: 12.
IDW	2	0.021	Variable. Number of points: 12.

1-3.5. Assessing the Interpolation Methods

The accuracy of each interpolation method in predicting a $P_{24h\text{-}max}$ value for a given return period was evaluated by means of the Root Mean Squared Error (RMSE) (Equation (10)), the Relative Error (REr) (Equation (11)), the Bias or Mean Deviation (MDv) (Equation (12)), and the Nash–

Sutcliffe Coefficient (NSC) (Equation (13)). In Equations (10) – (13), P_{sim} is the simulated areal precipitation from each of the Interpolation Methods ($P_{24h\text{-}max}$-IM), P_{sim} is the average simulated areal precipitation, and P_{true} is $P_{24h\text{-}max}$-RG, which has been considered the true value due to the proximity to the rain gauges. RMSE and REr measure the accuracy, whereas MDv tests the bias. The lower the values of RMSE, REr, and MDv, the better the interpolation method. The NSC, in particular, is widely used in hydrology to assess the prediction power of a model, and it ranges from −∞–one, where negative values indicates that it is better to use the mean of the measured data (true value) than the predicted/simulated value; a value of zero (or close to zero) indicates that either the mean of the measured values or the predicted/simulated value can be used indistinctively; and a value equal to one indicates good agreement between the predicted/simulated and the measured data (true value) [9,64,65].

$$\text{RMSE} = \sqrt{\frac{\sum_{i=1}^{n}(P_{sim}-P_{true})^2}{n}} \quad (10)$$

$$\text{REr (\%)} = \left|\frac{P_{true}-P_{sim}}{P_{true}}\right| x100 \quad (11)$$

$$\text{MDv (Bias)} = \frac{\sum_{i=1}^{n}(P_{true}-\overline{P_{sim}})}{n} \quad (12)$$

$$\text{NSC} = 1 - \frac{\sum_{i=1}^{n}(P_{true}-P_{sim})^2}{\sum_{i=1}^{n}(P_{true}-\overline{P_{sim}})^2} \quad (13)$$

1-4. Results and Discussion

1-4.1. Multiannual Time Series of $P_{24h\text{-}max}$ Values

Scatter plots of the multiannual series of $P_{24h\text{-}max}$ of each rain gauge revealed that there might be regionalization of the daily maximum rainfall trends within the departments that need to be further explored and analyzed, as it was observed that rainfall observations showed a noticeable increasing or decreasing trend line over time, which may indicate (a) a change in the rainfall pattern due to, among others, anthropogenic factors and (b) that a non-stationary frequency analysis is more suitable for the rainfall data of those rain gauges at a local level [66,67]. Figure 1-3 shows the scatter plot and the trend lines of the rain gauges Puerto Giraldo and Los Campanos located in the department of Atlántico.

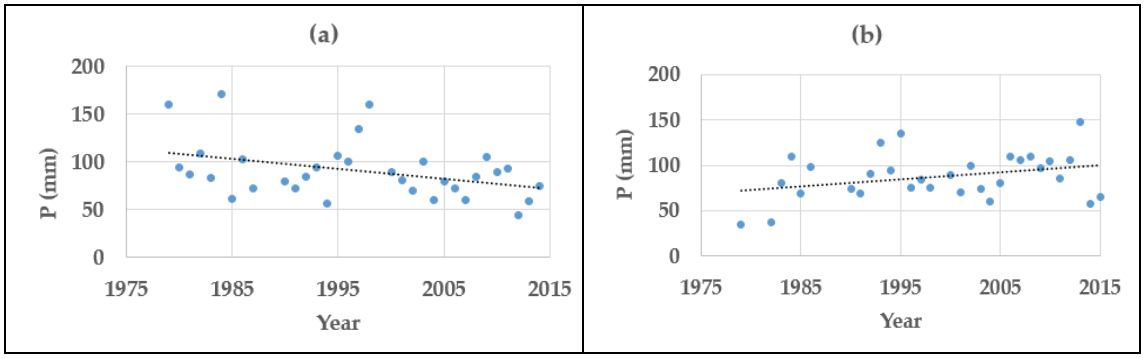

Figure 1-3. (a) Rain Gauge Puerto Giraldo exhibiting a decreasing P24h-max trend line (slope of −1.0563); (b) Rain Gauge Los Campanos showed an increasing P24h-max trend line (slope of 0.7518).

1-4.2. CDFs and Frequency Analysis

As previously mentioned, in Colombia, it is a common practice among hydrologist to use the Gumbel distribution solely for rainfall frequency analysis. However, results presented in Table 1-4 show that GEV is the CDF that best fit the majority of the rain gauges analyzed in this study with 47.2%, followed by Gumbel with 34.3% and LP3 with 18.5%.

Furthermore, based on the value obtained for the shape parameter (k), the 150 rain gauges where GEV was found to be the best fit were further analyzed to determine whether the GEV corresponded to a Type 2 (Fréchet) or Type 3 (Weibull) Extreme Value (EV) distribution. Table 1-5 summarizes the EV Type 2 and 3 totals for each department.

Table 1-4. Best CDFs per department. GEV, Generalized Extreme Value; LP3, Log-Pearson 3

Department	Best-fit CDF			Total
	GEV	Gumb	LP3	
Guajira	21	18	5	44
Cesar	27	21	12	60
Magdalena	26	15	14	55
Atlántico	7	6	0	13
Bolívar	23	22	12	57
Sucre	16	14	2	32
Córdoba	26	12	15	53
Antioquia	3	0	0	3
Santander	0	1	0	1
Norte de Santander	1	0	0	1
Total	**150**	**109**	**60**	**319**

Table 1-5. EV distribution equivalence.

Department	EV type equivalence of the GEV		Total
	EV-3 (Weibull) ($k > 0$)	EV-2 (Fréchet) ($k < 0$)	
Guajira	12	9	21
Cesar	17	10	27
Magdalena	19	7	26
Atlántico	6	1	7
Bolívar	19	4	23
Sucre	10	6	16
Córdoba	16	10	26
Antioquia	1	2	3
Santander	0	1	1
Norte de Santander	N/A	N/A	0
Total	**100**	**50**	**150**

Taking for granted that all rainfall time series fit the Gumbel distribution could lead to either under- or over-estimation of the design rainfall. This is clearly shown in Table 1-6, where, according to the chi-squared test, the Gumbel distribution was not the best fit in any of the cases. The situation became more critical at higher return periods such as 50 years and 100 years (two of the most-used return periods in hydrological analysis for stormwater management and in consideration for flood studies). For the 100-year return period, the differences observed between GEV and Gumbel distributions at rain gauges Santa Ana and Palo Alto were 54.1 mm and 15.2 mm, respectively. Not selecting the most appropriate distribution can negatively impact, for instance,

the design of hydraulic structures for stormwater management and/or the delineation of flood-prone areas.

Table 1-6. $P_{24h\text{-}max}$ values for different return periods.

Rain Gauge Name (Department)	$P_{24h\text{-}max}$ (mm)							CDF	Chi Square (X^2)
	Return period (yr)								
	2	5	10	20	25	50	100		
Santa Ana (Bolívar)	101.1	124.7	135.9	144.3	146.6	152.5	157.2	GEV	2.15
	96.0	126.9	147.3	166.9	173.1	192.3	211.3	Gum	6.52
	99.2	124.7	138.2	149.1	152.2	161.0	168.5	LP3	3.12
Palo Alto (Magdalena)	95.4	126.8	149.0	171.5	178.8	202.2	226.7	GEV	2.91
	96.5	127.3	147.7	167.2	173.4	192.5	211.5	Gum	6.04
	96.1	127.5	148.9	169.9	176.6	197.7	219.3	LP3	4.48

In general, the GEV and Gumbel distributions were demonstrated to be the most suitable for rainfall frequency analysis in the Caribbean region of Colombia. The LP3 distribution showed both poor performance (in some cases, the datasets did not even fit) in most of the rain gauges analyzed and a tendency to underestimate when compared to the values obtained by either GEV or Gumbel distributions, irrespective of being (or not) the best fit of the three.

1-4.3. Interpolation Methods Assessment

After visually inspecting the isohyetal alignments, it was observed that the IDW method had less inconsistencies, among all. Nonetheless, in some areas, it was necessary to adjust manually the isohyetals' alignment generated by the IDW method (the manually-adjusted IDW method will be referred to as IDW adjusted). Figure 1-4 depicts the differences among the interpolation methods. Isohyetals by the OK method (Figure 1-4c) evidenced: (a) the presence of small oval-shaped isohyetals with the same rainfall value of the larger oval they were within and (b) large areas between neighboring rain gauges with no isohyetals ("dead or no-variation zones"), which could affect the estimation of the areal precipitation for a given watershed (the problem was most evident as the return period decreased). The spline method (Figure 1-4d) generated, in some cases, isohyetals with negative values. Isohyetals drawn by the IDW method (Figure 1-4b), despite the fact that a few minor adjustments were manually made in some areas, did not show the setbacks of the other two methods. The IDW method, in spite of its simplicity compared to other interpolation methods like the OK method, is recommended when the data are irregularly distributed like the rain gauges used in this study [68,69].

In addition to the visual inspection, the accuracy of all generated maps (by each of the interpolation methods) to estimate $P_{24h\text{-}max}$ values for a given return period was evaluated in eight watersheds with various area sizes and located at different distances from neighboring rain gauges. Five watersheds are located in the northern part of the department of Bolívar. Watersheds 1, 2, and 3 (W-1, W-2, and W-3) are close to the rain gauges Bayunca, Cañaveral, and Escuela Naval-CIOH, respectively. The rain gauges Bayunca and Cañaveral are located within Watersheds 4 and 5 (W-4 and W-5). Furthermore, three watersheds (W-6, W-7, and W-8) located in the vicinity of the rain gauge Loma Grande (department of Atlántico) were selected to validate the performance of the isohyetal methods in areas with nearby rain gauges not included in this study (Loma Grande had less than thirty years of observations). Table 1-7 summarizes the watersheds' area and distance from the centroid to the nearest rain gauge. Figure 1-5 depicts the location and the isohyetals at each of the watersheds for a 100-year return period.

Watersheds areal $P_{24h\text{-}max}$ for return periods of 2, 5, 10, 20, 25, 50, and 100 years were estimated from each of the isohyetal maps ($P_{24h\text{-}max}$-IM) and compared to the resulting $P_{24h\text{-}max}$ values calculated via frequency analysis of the time series of each of the nearby rain gauges ($P_{24h\text{-}max}$-RG).

The estimated values of $P_{24h\text{-}max}$-RG and $P_{24h\text{-}max}$-IM are presented in Table 1-8. $P_{24h\text{-}max}$-RG is the value obtained via frequency analysis of the precipitation data for all return periods at each of the rain gauges used for validation. $P_{24h\text{-}max}$-IM is the estimated areal precipitation of each watershed by means of the isohyetal method. The observed two-year $P_{24h\text{-}max}$-RG values ranged from 75.4 mm (Loma Grande) to 100.5 mm (Bayunca). Among all rain gauges, Loma Grande had the lowest $P_{24h\text{-}max}$-RG for almost all return periods, except for 100 years. The highest $P_{24h\text{-}max}$-RG values calculated were for the rain gauges of Bayunca (for 2 years, 5 years, and 10 years) and Cañaveral (for 20 years, 25 years, 50 years, and 100 years). The minimum two-year $P_{24h\text{-}max}$-IM values estimated were 91.8 mm (spline), 76.5 mm (spline), 75.0 mm (spline), 95.0 mm (OK), 80.0 mm (OK and spline), 70.0 mm (spline and IDW adjusted), 70.0 mm (spline), and 75.0 mm (IDW adjusted and spline) for W-1, W-2, W-3, W-4, W-5, W-6, W-7, and W-8, respectively. With the IDW adjusted method, the maximum values for the 100-year $P_{24h\text{-}max}$-IM were 165.0 mm, 187.1 mm, 180.1 mm, and 165 mm for W-1, W-2, W-3, and W-4, respectively. With the spline method, the maximum values computed for 100 years were 206.0 mm for W-5 and 178.1 mm for W-6. With the OK method, the maximum values of $P_{24h\text{-}max}$-IM for 100 years were 160.0 mm and 164.0 mm for W-7 and W-8, respectively.

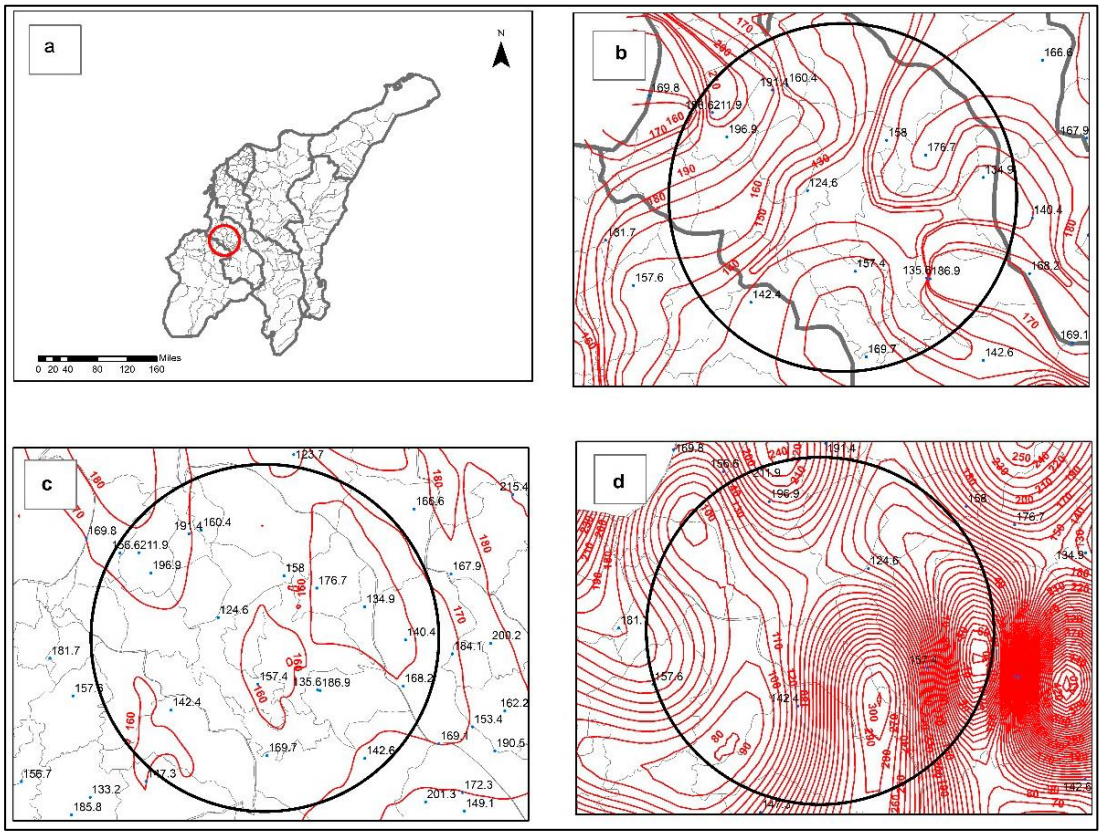

Figure 1-4. (a) Area showing isohyetal alignment discrepancies; (b) isohyetal IDW method; (c) isohyetal ordinary kriging method; (d) isohyetal spline method.

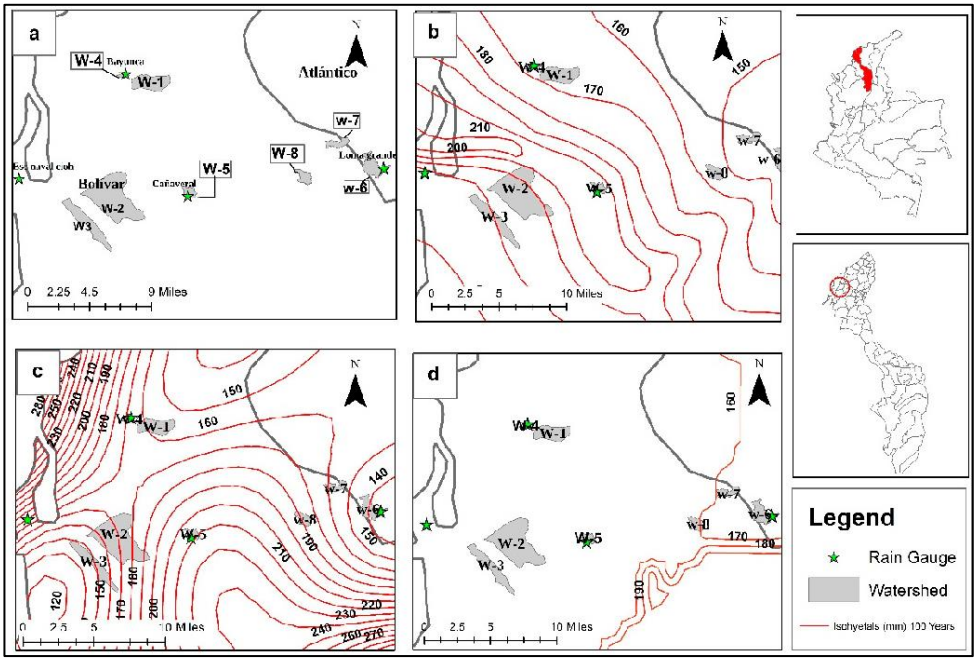

Figure 1-5. (a) Location of the watersheds and rain gauges; (b) areal precipitation of isohyetals by IDW adjusted; (c) areal precipitation by the spline method; (d) areal precipitation of isohyetals by the OK method.

Table 1-7. Watersheds (W) information.

Watershed	Area (ha)	Distance to Nearest Rain Gauge in km
W-1	651.7	3.3 (Bayunca)
W-2	2146.5	9.2 (Cañaveral)
W-3	710.7	11.2 (Escuela Naval-CIOH)
W-4	52.4	0.0 (rain gauge Bayunca is within the watershed)
W-5	154.0	0.0 (rain gauge Cañaveral is within the watershed)
W-6	460.4	0.0 (rain gauge Loma Grande is within the watershed)
W-7	200.6	6.0 (Loma Grande)
W-8	204.6	9.2 (Loma Grande)

Table 1-8. Values of P24h-max-RG and areal $P_{24h\text{-}max}$-Interpolation Method (IM).

Rain Gauge		$P_{24h\text{-}max}$ RG (mm)						
		Tr (yr)						
		2	5	10	20	25	50	100
Bayunca		100.5	127.6	140.6	150.5	153.5	160.5	166.3
Cañaveral		86.6	115.7	136.4	157.2	164.1	185.8	208.5
Esc. Naval-CIOH		87.5	116.7	133.7	148.6	153.0	165.9	177.6
Int. Method	**Watershed**	**Areal $P_{24h\text{-}max}$-IM (mm)**						
IDW Adjusted	W-1	95.0	125.0	135.0	146.2	155.0	155.4	165.0
	W-2	89.9	115.0	135.0	162.4	169.0	181.4	187.1
	W-3	85.0	115.0	135.0	155.5	156.5	170.7	180.1
	W-4	96.7	125.0	138.8	154.0	155.0	163.7	165.0
	W-5	85.0	115.0	135.0	155.0	165.0	175.0	205.0
	W-6	70.0	100.0	110.0	120.0	122.2	136.9	155.0
	W-7	75.0	100.0	110.0	124.9	129.0	145.0	155.0
	W-8	75.0	100.0	114.2	135.0	137.1	149.1	155.0

Spline	W-1	91.8	116.7	128.8	138.7	141.4	149.8	157.1
	W-2	76.5	100.7	115.1	129.9	133.9	149.7	161.6
	W-3	75.0	91.9	104.4	115.2	117.0	129.3	140.9
	W-4	103.8	127.1	144.0	154.1	155.0	164.3	167.7
	W-5	80.0	115.0	139.0	155.0	165.0	185.0	206.8
	W-6	70.0	95.0	110.0	120.0	123.2	133.1	178.1
	W-7	70.0	95.9	110.0	125.0	125.0	142.3	156.5
	W-8	75.0	100.0	115.0	135.0	142.4	158.8	142.4
Ordinary Kriging	W-1	95.0	125.0	125.0	136.3	145.0	155.0	165.0
	W-2	86.0	116.9	125.4	145.0	145.0	155.0	165.0
	W-3	95.0	119.3	127.0	145.0	145.0	155.0	165.0
	W-4	95.0	125.0	125.0	145.0	145.0	155.0	165.0
	W-5	85.0	115.0	125.0	135.0	145.0	155.0	165.0
	W-6	80.0	100.0	120.0	130.0	140.0	150.0	160.0
	W-7	80.0	100.0	120.0	131.4	140.0	150.0	160.0
	W-8g	80.5	100.0	121.2	135.0	140.0	153.1	164.0

With the values estimated in Table 1-8, the performance of the interpolation methods at each of the watershed was tested via REr, and the overall performance of each interpolation method in predicting $P_{24h\text{-}max}$ for a given return period in all watersheds (n = 8) was tested via RMSE, MDv, and NSC (Table 1-9).

Table 1-9. Interpolation method performance at each watershed.

Int. Method	Watershed	Relative Error						
		Tr (Years)						
		2	5	10	20	25	50	100
IDW Adjusted	W-1	5.8%	2.1%	4.2%	3.0%	1.0%	3.3%	0.8%
	W-2	3.7%	0.6%	1.0%	3.2%	2.9%	2.4%	11.4%
	W-3	3.0%	1.5%	1.0%	4.5%	2.3%	2.8%	1.4%
	W-4	4.0%	2.1%	1.3%	2.3%	1.0%	1.9%	0.8%
	W-5	1.8%	0.6%	1.0%	1.4%	0.5%	6.2%	1.7%
	W-6	7.8%	1.3%	7.6%	12.3%	14.6%	14.0%	11.0%
	W-7	0.6%	1.3%	7.6%	7.9%	8.5%	7.7%	11.0%
	W-8	0.6%	1.3%	3.7%	0.1%	2.1%	4.7%	11.0%
Spline	W-1	9.5%	9.4%	9.2%	8.5%	8.6%	7.1%	5.8%
	W-2	13.2%	14.9%	18.5%	21.0%	22.6%	24.1%	29.0%
	W-3	16.7%	17.0%	28.1%	29.0%	30.7%	28.3%	26.1%
	W-4	3.2%	0.4%	2.3%	2.3%	1.0%	2.3%	0.8%
	W-5	8.2%	0.6%	1.9%	1.4%	0.5%	0.4%	0.8%
	W-6	7.8%	6.6%	7.6%	12.3%	13.6%	17.3%	3.4%
	W-7	7.8%	6.6%	7.6%	7.8%	12.0%	9.7%	9.9%
	W-8	0.6%	1.3%	3.0%	0.1%	1.7%	1.7%	20.8%
Ordinary Kriging	W-1	5.8%	2.1%	12.5%	10.5%	5.9%	3.6%	0.8%
	W-2	0.6%	1.0%	8.7%	8.4%	13.2%	19.9%	26.4%
	W-3	7.9%	2.2%	5.2%	2.5%	5.5%	7.0%	7.6%
	W-4	5.8%	2.1%	12.5%	3.8%	5.9%	3.5%	0.8%
	W-5	1.8%	0.6%	9.1%	16.4%	13.2%	19.9%	26.4%
	W-6	5.7%	1.3%	1.3%	3.7%	0.0%	4.1%	7.5%
	W-7	5.7%	1.3%	1.3%	2.6%	0.0%	4.1%	7.5%
	W-8	6.2%	1.3%	2.3%	0.1%	0.0%	2.0%	4.9%

		Root Mean Squared Error (RMSE)						
IDW Adjusted	All Watersheds	0.37	0.15	0.45	0.62	0.66	0.76	0.96
Spline		0.80	1.06	1.23	1.40	1.53	1.60	1.78
Ord. Kriging		0.52	0.17	0.85	0.86	0.85	1.22	1.62
		Mean Deviation (Bias)						
IDW Adjusted	All Watersheds	2.05	1.53	3.74	1.93	2.43	6.21	9.50
Spline		5.74	8.23	9.59	11.95	13.16	14.32	16.52
Ord. Kriging		−1.07	0.75	6.79	8.21	7.90	12.34	16.78
		Nash–Sutcliffe Coefficient (NSC)						
IDW Adjusted	All Watersheds	0.88	0.97	0.76	0.39	0.37	0.49	0.54
Spline		0.56	0.26	−0.11	−0.29	−0.36	−0.26	−0.09
Ord. Kriging		0.76	0.97	0.27	0.24	0.23	0.08	0.03

Gray cells indicate that a method different from IDW adjusted performed best. Green cells indicate a Relative Error (REr) value above five percent.

The REr values in Table 1- 9 show how the IDW adjusted outperformed the other two methods in almost all watersheds except in 18 cases (gray cells) out of 168 (nine of those 18 cases occurred in watersheds where the rain gauge was within them). With respect to the watersheds having a rain gauge within them (W-4, W-5, and W-6), better REr results were obtained in the IDW adjusted method, except for W-6, where the OK method predicted values closer to the ones calculated via frequency analysis. The IDW adjusted method showed REr estimates ranging from 0.8–4% for W-4, 0.6–6.2% for W-5, and 1.3–14.6% for W-6. The spline method had REr estimates that oscillated from 0.4–3.2% for W-4, 0.4–8.2% for W-5, and 3.4–17.3%. The REr values obtained through the OK method ranged from 0.8–12.5% for W-4, from 0.6–26.4% for W-5, and from 0.0–7.5% for W-6. The IDW adjusted method reported fifteen REr values above 5%, of which only two cases were greater than 10% (the highest was 14.6%). The spline method reported 36 cases where REr values were above 5%, with 17 values above 10% (the highest was 20.8%). Finally, the OK method had 27 cases where REr estimates were above 5%, with 11 values above 10% (the highest was 26.4%). When the performance of the interpolation methods was evaluated based on the distance between the watershed and the rain gauge, once again, the IDW adjusted method exhibited better results, with a few exceptions observed (gray cells in W-2, W-7, and W-8). For W-1 and W-3 (respectively, the closest and the furthest), lower REr values were obtained with the IDW adjusted method. For W-2, located at 9.2 km of its corresponding closest rain gauge, the IDW adjusted method had lower estimates of REr for all return periods, except at two years, where the OK method was best. However, the IDW adjusted method reported an error of only 3.7%. For W-8, also located at 9.2 km, for return periods of 10 years, 25 years, and 50 years, the OK and spline methods were best. Nonetheless, all REr values observed for the IDW adjusted method were lower than 5%, except for the return period of 100 years with a value of 11%. For W-7, located at 6.0 km from the rain gauge Loma Grande, the OK method reported lower REr values, which ranged from 0.0–7.5%. The IDW adjusted and spline methods reported similar REr values (less than 5%) in most of the return periods, except for the return period of 100 years, where values of 11% and 20.8% were obtained for the IDW adjusted and spline methods, respectively. As for the return periods of 50 years and 100 years, two of the most-used return periods when evaluating the performance of hydraulic structures (e.g., culverts, bridges, and open channels) and in flood mitigation and stream restoration projects, the IDW adjusted method reported better results, with only six cases (four for the spline method and two for the OK method) out of 42, where the other two methods outperformed. The IDW adjusted method reported four cases above 10% (the highest was 14%), while spline had six cases (the highest was 20.8%). Although the OK method also reported four cases with REr values greater than 10%, the maximum value was 26.4%, which is the largest of the three methods. Irrespective of the watershed size and/or distance from a nearby rain gauge, these results are not only indicative that the IDW adjusted method performed best in the majority of the watersheds where the rain gauge was within them (W-4, W-5, and W-6), but also—and most

importantly—in areas distant from a rain gauge where the design rainfall estimation was most needed, since in watersheds where a rain gauge is within them, it is always recommended to calculate the design rainfall directly from the rainfall observations.

As for the overall performance of the interpolation methods, the IDW adjusted method had the best results (RMSE, MDv, and NSC) in the majority of the cases. The OK method showed lower bias (MDv) values for two occasions (−1.07 mm and 0.75 mm for return periods of two and five years; negative values indicate that average simulated value was higher than the true value). This notwithstanding, the IDW adjusted method estimates were low as well (2.05 mm and 1.53 mm for return periods of two and five years). A closer look at the isohyetal alignment of both methods within the assessed area revealed that the OK method alignment for isohyetals of 70 mm, 80 mm, 90 mm, and 100 mm did not pass through several rain gauges they were supposed to have (dead or no-variation zones). This would have resulted in high error values for the OK method had other watersheds been selected. In general, the results indicate that the values from the IDW adjusted method showed less bias (2.5 mm–9.5 mm) than the other two methods (5.74–16.52 mm and −1.07–16.78 mm for the spline and OK methods, respectively), where the bias was more noticeable as the return period increased. This can lead to serious implications, especially at return periods of 50 years and 100 years, which are two of the most used in the design of hydraulic structures for both stormwater management and flood mitigation projects. As for the prediction power, the IDW adjusted method outperformed the other two methods with NSC values greater than or equal to 0.39, indicating good agreement between the true and simulated variables. For the spline method, the NSC was above zero only in return periods of two and five years. The remaining return periods showed negative values, implying that the average value was a better predictor. Similar results were observed for the OK method, with values closer to zero as the return period increased, which signifies that either the average or the true values were better predictors. The NSC values for the spline and OK methods are consistent with the bias results: poor performance in predicting $P_{24h\text{-}max}$ when compared with the IDW adjusted method.

In sum, the results above confirm that the performance of an interpolation method should always be assessed prior to its selection [68–75]. This is of great importance, especially, because the OK method has become one of the most widely-preferred interpolation methods to the point that some do not even question its adequacy due to it typically showing good results.

1-4.4. Isohyetal Maps for Different Return Periods

The seven isohyetals maps of daily maximum precipitation for return periods of 2, 5, 10, 20, 25, 50, and 100 years drawn by means of the IDW adjusted method for the Colombian Caribbean region are shown in Figures 1-6 to 1-12. The statistical analysis results demonstrated that areal $P_{24h\text{-}max}$ can be estimated by means of the isohyetal maps proposed in this study. However, the final decision of using the maps shall be at the user's discretion based on his/her experience and knowledge of the area where the areal $P_{24h\text{-}max}$ is intended to be estimated. It is then recommended that a frequency analysis of the multiannual series be performed, and the results shall be compared to those estimated through the isohyetal maps in order to rule out any major discrepancies that could potentially affect the calculation of the design streamflow value and subsequent sizing of hydraulic structures.

For the department of Guajira, $P_{24h\text{-}max}$ isohyetals ranged from 50–120 mm for two years, 70–150 mm for 5 years, 90–160 mm for 10 years, from 100–180 mm for 20 years, 120–200 mm for 25 years, from 120–240 mm for 50 years, and from 120–280 mm for 100 years. The lowest and highest values were observed in the northeastern and northwestern areas, respectively.

For the department of Magdalena, $P_{24h\text{-}max}$ isohyetals ranged from 80–130 mm for two years, 90–160 mm for five years, 110–170 mm for 10 years, from 120–180 mm for 20 years, 120–200 mm for 25 years, from 120–240 mm for 50 years, and from 120–260 mm for 100 years. The lowest and highest values were observed in the eastern and northern areas, respectively.

For the department of Cesar, $P_{24h\text{-}max}$ isohyetals ranged from 80–120 mm for two years, 90–150 mm for five years, 100–170 mm for 10 years, from 120–180 mm for 20 years, 120–200 mm for 25 years, from 120–220 mm for 50 years, and from 120–260 mm for 100 years. The lowest and highest values were observed in the northeastern and southern areas, respectively.

For the department of Atlántico, $P_{24h\text{-}max}$ isohyetals ranged from 70–90 mm for two years, 100–110 mm for five years, 100–120 mm for 10 years, from 120–140 mm for 20 years, 120–140 mm for 25 years, from 140–160 mm for 50 years, and from 120–180 mm for 100 years. The lowest and highest values were observed in the central-eastern and southern areas, respectively. This was the department with the smallest ranges of P24h-max values mainly due to its total area (3385.1 km^2) and topography.

For the department of Bolívar, $P_{24h\text{-}max}$ isohyetals ranged from 90–140 mm for two years, 90–170 mm for five years, 100–190 mm for 10 years, from 120–200 mm for 20 years, 120–200 mm for 25 years, from 120–240 mm for 50 years, and from 140–270 mm for 100 years. The lowest and highest values were observed in the northern and southwestern areas, respectively.

For the department of Sucre, $P_{24h\text{-}max}$ isohyetals ranged from 90–130 mm for two years, 90–160 mm for five years, 100–190 mm for 10 years, from 120–200 mm for 20 years, 120–200 mm for 25 years, from 120–240 mm for 50 years, and from 140–250 mm for 100 years. The lowest and highest values were observed in the northeastern and southeastern areas, respectively.

For the department of Córdoba, $P_{24h\text{-}max}$ isohyetals ranged from 80–130 mm for two years, 100–160 mm for five years, 110–190 mm for 10 years, from 120–200 mm for 20 years, 120–200 mm for 25 years, from 120–220 mm for 50 years, and from 140–240 mm for 100 years. The lowest and highest values were observed in the northwestern and southeastern areas, respectively.

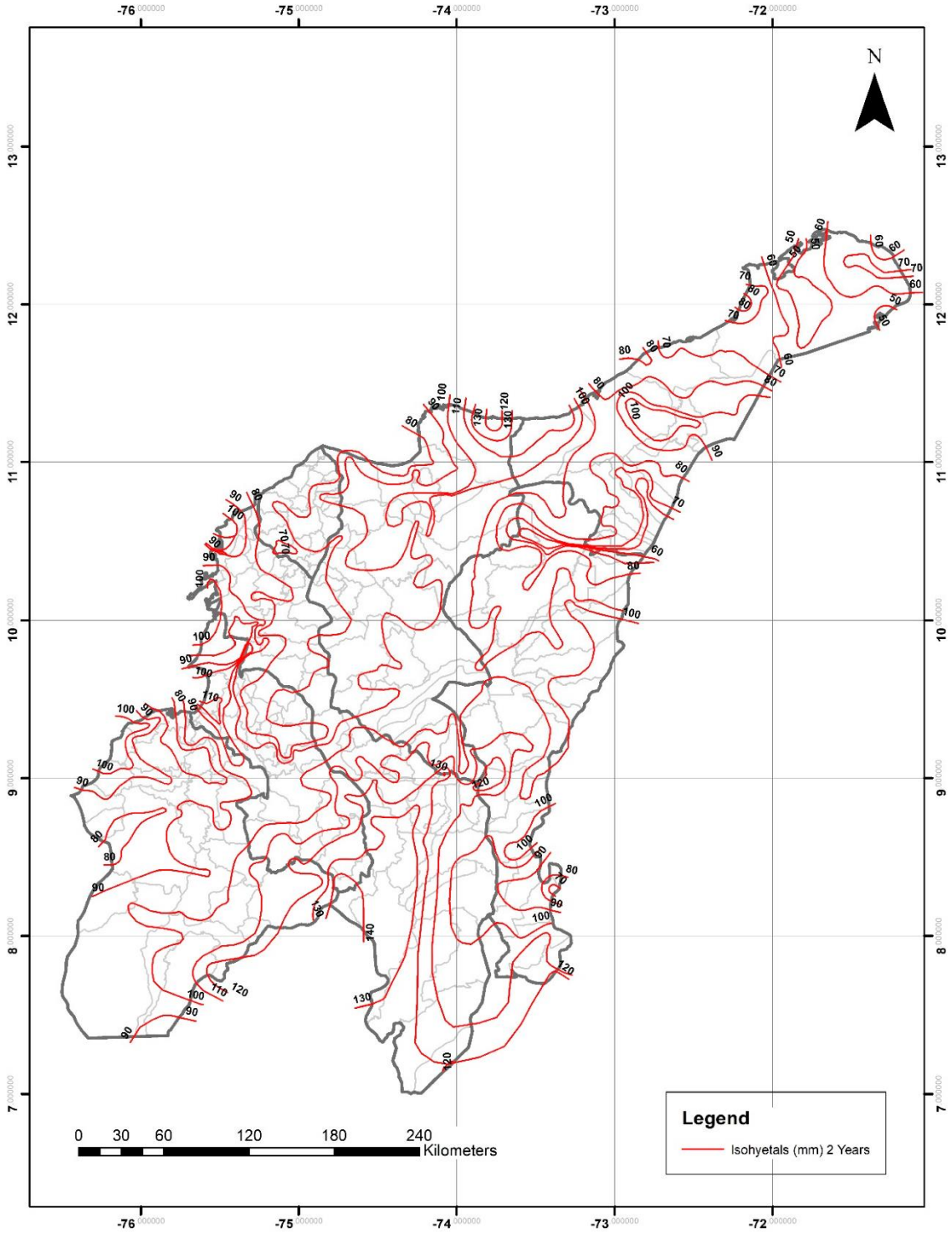

Figure 1-6. Daily maximum precipitation for a two-year return period ($P_{24h\text{-}max}$ in mm). IDW adjusted method. Light-gray lines are the boundaries of the different municipalities within the departments.

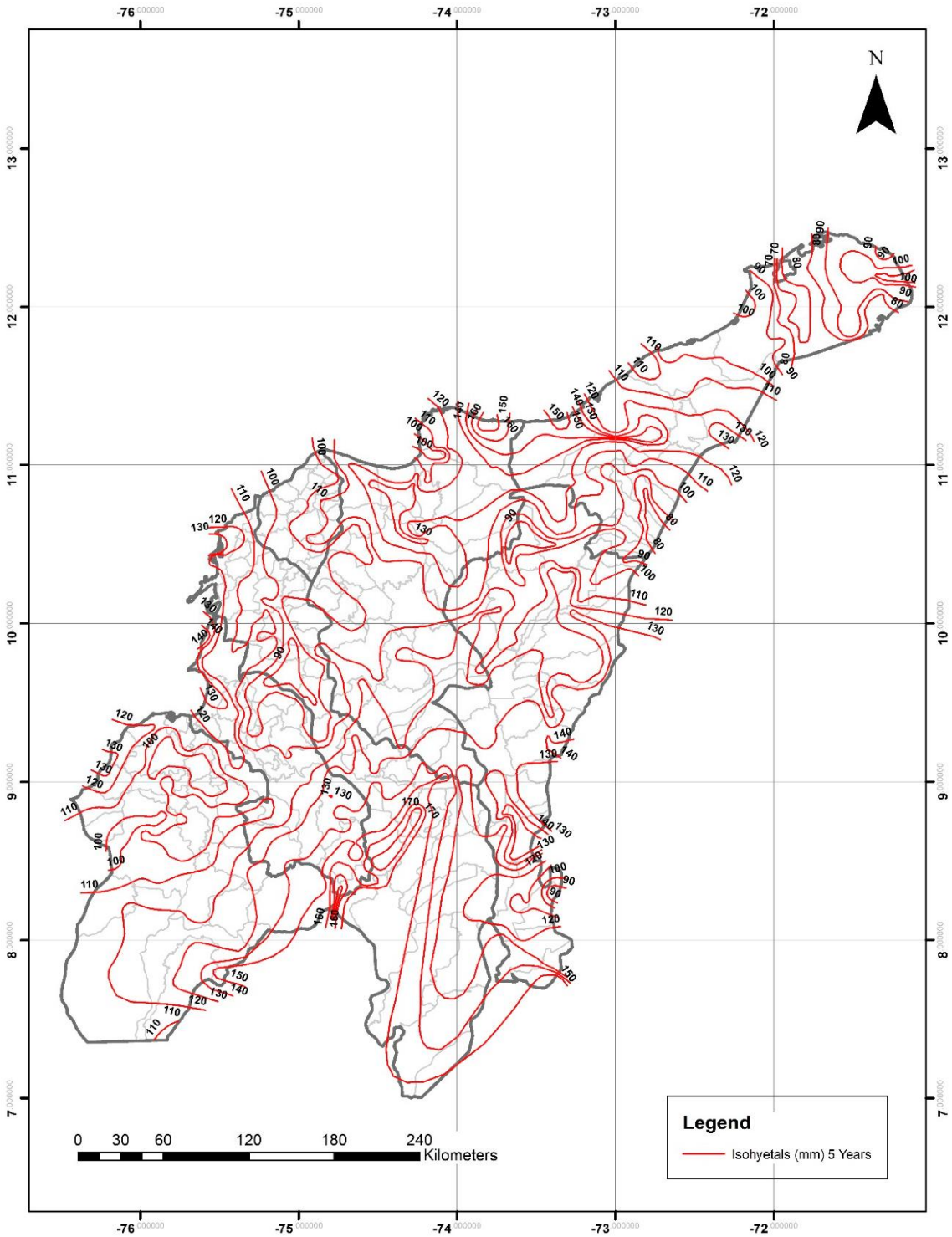

Figure 1-7. Daily maximum precipitation for a five-year return period (P24h-max in mm). IDW adjusted method. Light-gray lines are the boundaries of the different municipalities within the departments

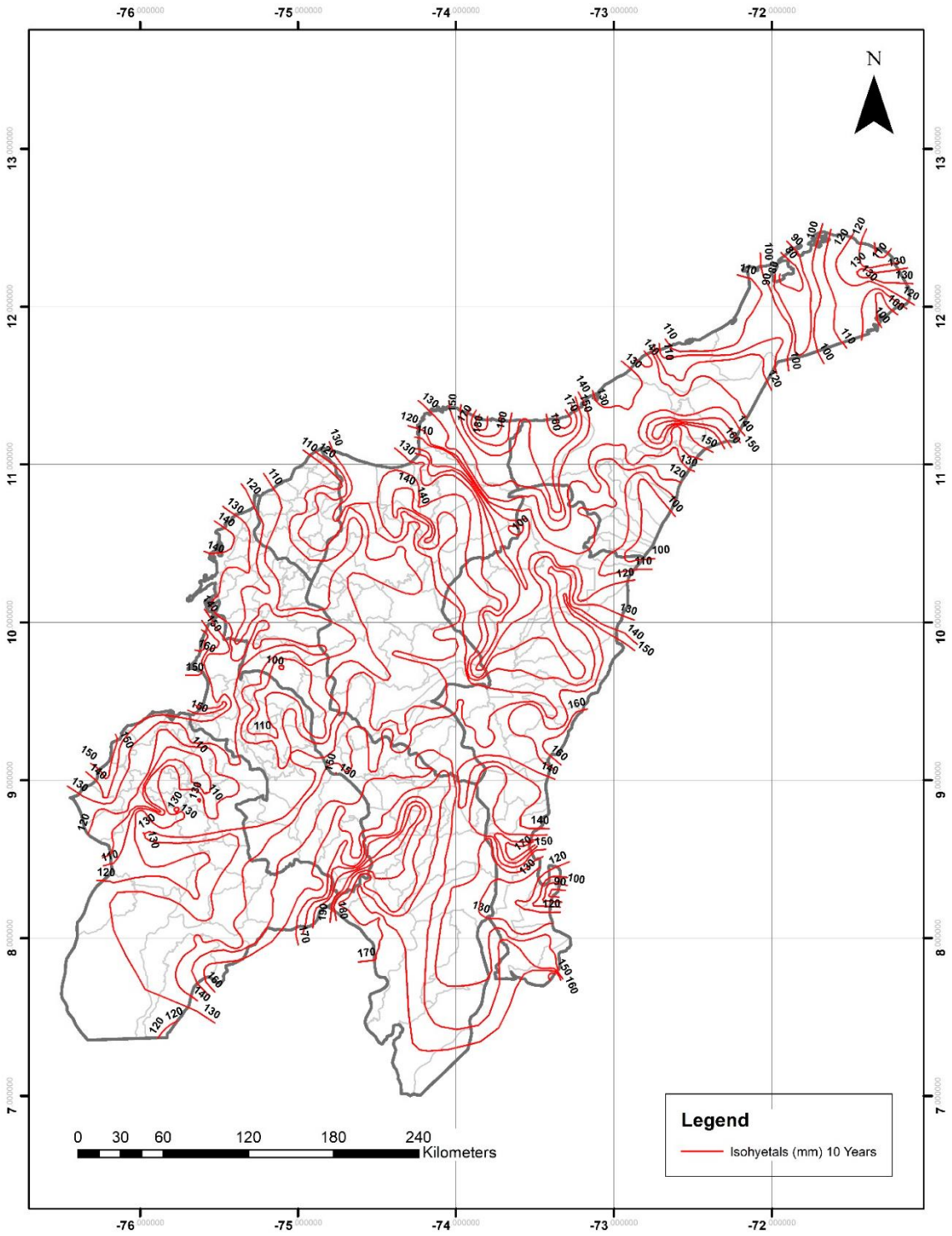

Figure 1-8. Daily maximum precipitation for a 10-year return period (P24h-max in mm). IDW adjusted method. Light-gray lines are the boundaries of the different municipalities within the departments.

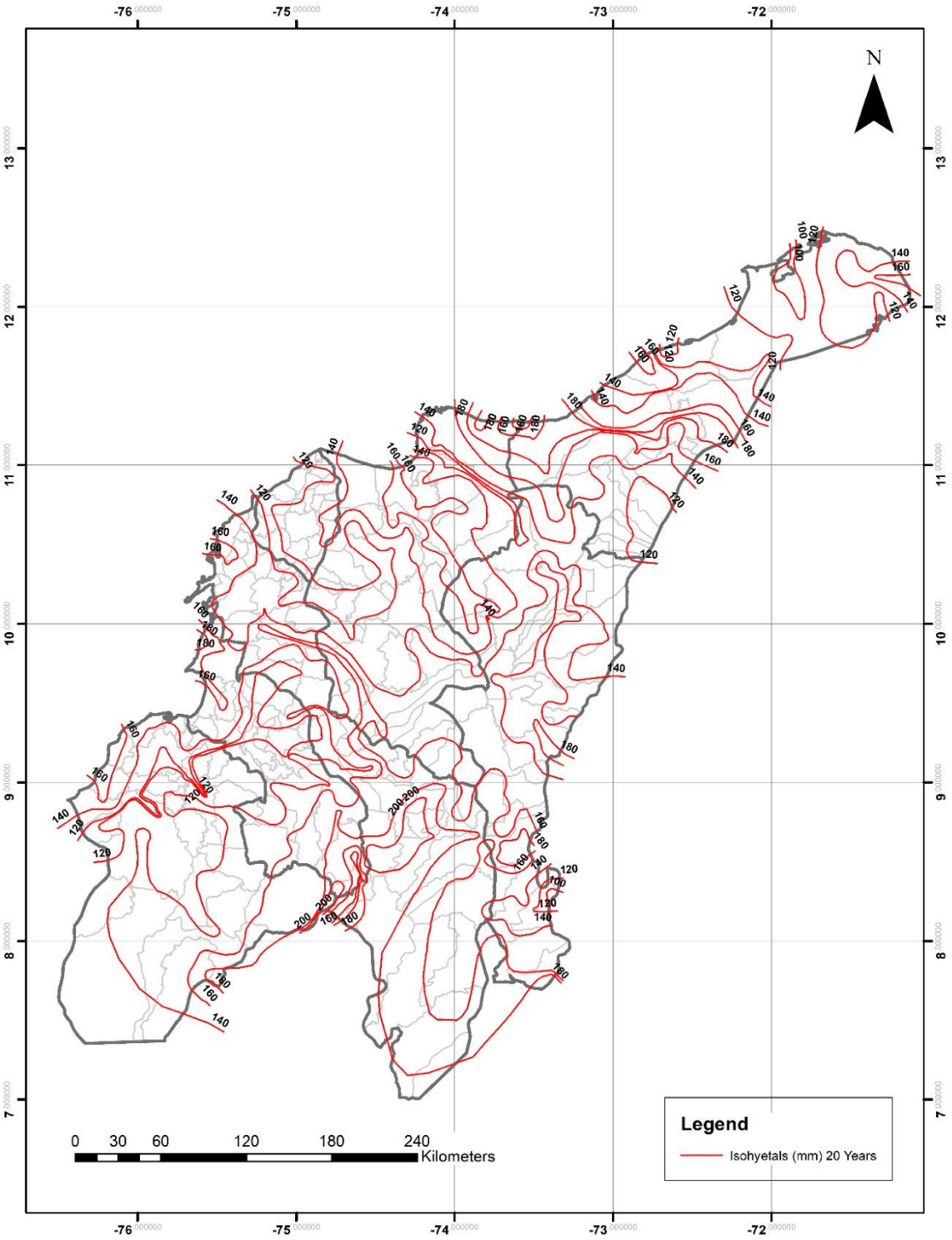

Figure 1-9. Daily maximum precipitation for a 20-year return period (P24h-max in mm). IDW adjusted method. Light-gray lines are the boundaries of the different municipalities within the departments.

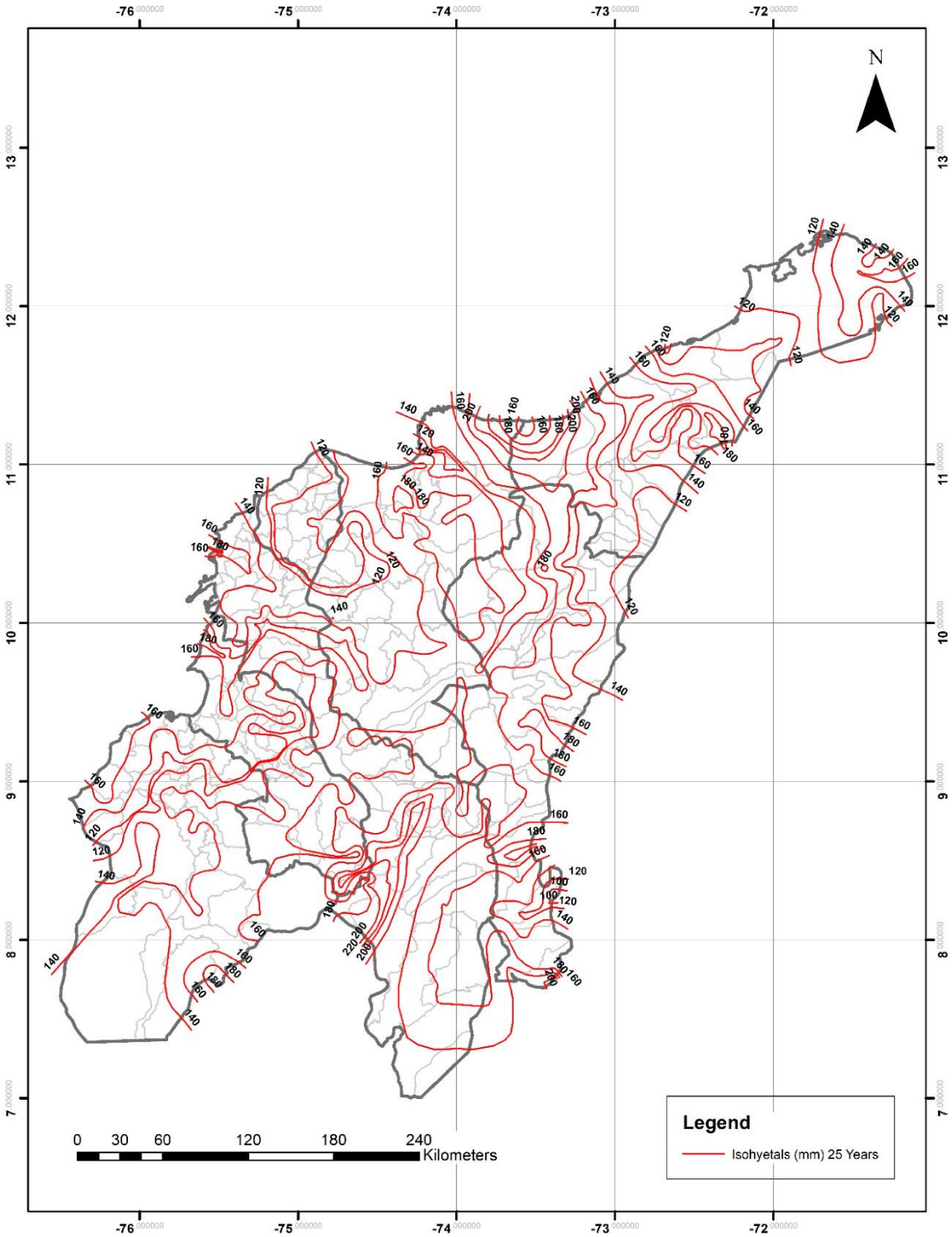

Figure 1-10. Daily maximum precipitation for a 25-year return period (P24h-max in mm). IDW adjusted method. Light-gray lines are the boundaries of the different municipalities within the departments.

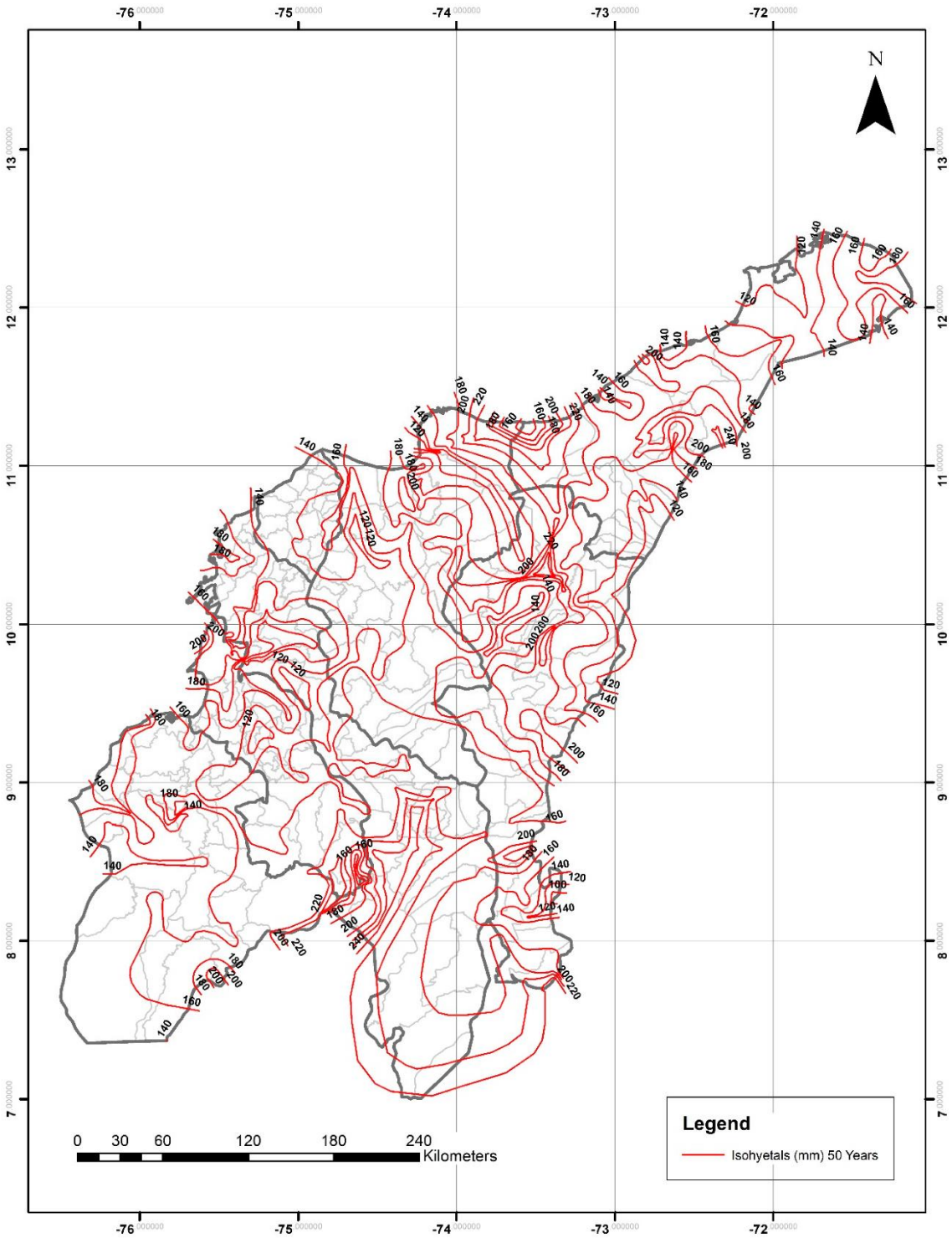

Figure 1-11. Daily maximum precipitation for a 50-year return period (P24h-max in mm). IDW adjusted method. Light-gray lines are the boundaries of the different municipalities within the departments.

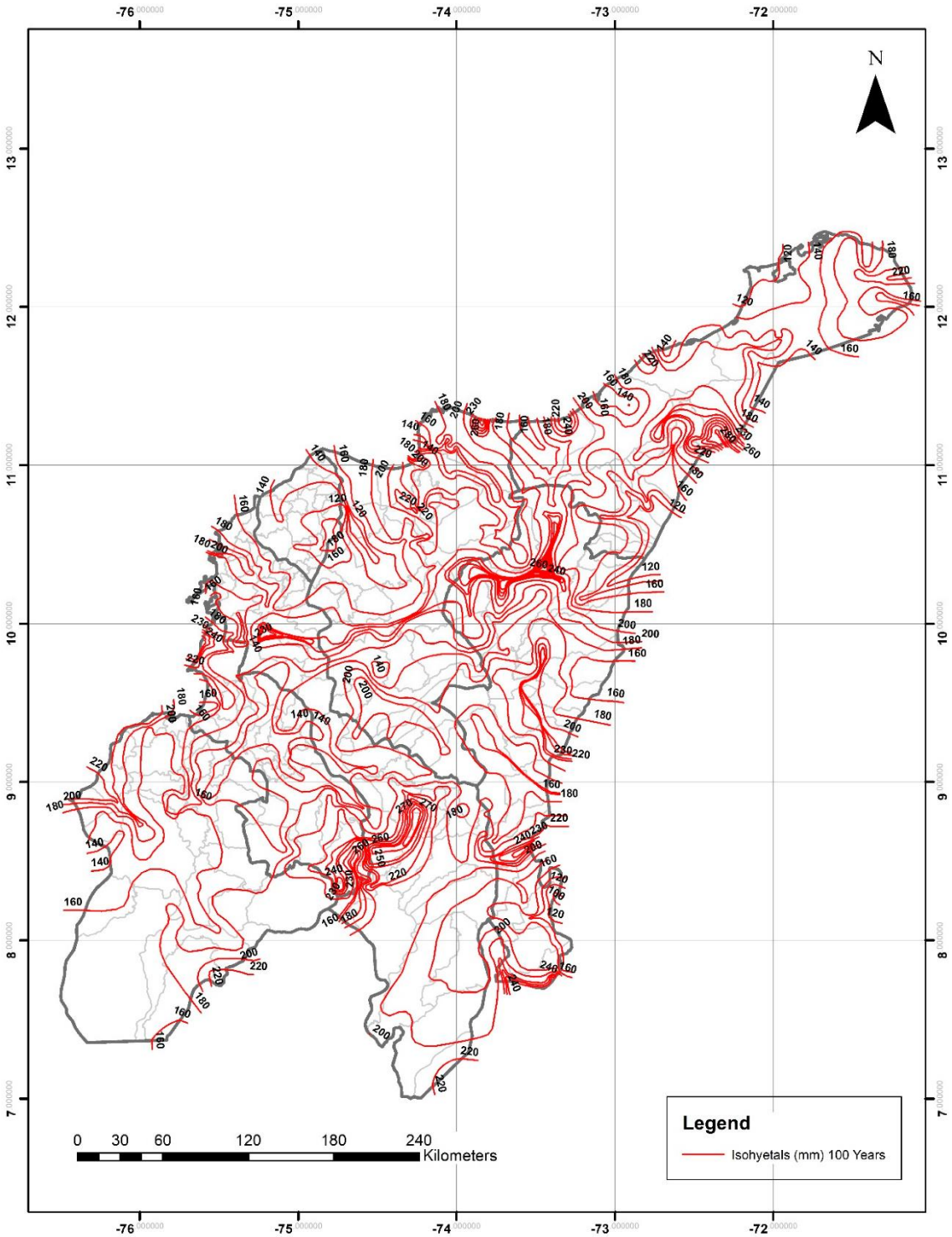

Figure 1-12. Daily maximum precipitation for a 100-year return period (P24h-max in mm). IDW adjusted method. Light-gray lines are the boundaries of the different municipalities within the departments.

1-5. Conclusions

Unlike other countries, Colombia, currently, does not have any official document that compiles a series of recommended methodologies for frequency analysis for a particular region. In this context and contrary to what is the common practice, the Gumbel distribution was not the best fit for most of the time series analyzed. Instead, and according to the chi-squared test, the GEV distribution was shown to be the best fit among the three CDFs used in majority of the datasets. Only 34.3% of the rain gauges fit the Gumbel distribution, while 47.2% of them fit the GEV

distribution. LP3, on the other hand, did not work well among the rain gauges analyzed. Based on the results of this study, GEV and Gumbel are the most recommended distributions for the Caribbean region of Colombia.

With respect to the best interpolation method for generating isohyetals in the study area, the IDW method outperformed both the spline and the ordinary kriging methods. These results demonstrate that geostatistically-based interpolation methods (e.g., ordinary kriging) are not always the best selection as many typically take for granted.

According to the results of the REr, RMSE, MDv, and NSC, the areal $P_{24h\text{-}max}$ estimated with the resulting isohyetal maps (by the IDW adjusted method) of this study were close to the true value and can be used to select a design rainfall for a given return period. This is of particular significance given the large amount of ungauged areas within the Colombian Caribbean region where many hydrological studies (made by either international or local consulting companies) are based on the utilization of neighboring rain gauges that sometimes are located at remote distances that do not guarantee the reliability and/or accuracy of the derived design rainfall. The isohyetal maps generated in this study are the first step in developing similar ones for the remaining four regions of Colombia. The 318 multiannual $P_{24h\text{-}max}$ time series analyzed were assumed to be stationary. However, increasing and decreasing trends were observed in some of the time series, suggesting the presence of non-stationarity, which, if confirmed, could result in higher or lower values of point $P_{24h\text{-}max}$ (at the rain gauge). The possible modifications of the isohyetal alignments in certain areas may or may not alter the total areal $P_{24h\text{-}max}$ of a given watershed, since, unlike point rainfall, the areal rainfall is calculated differently. It depends on both the isohyetal alignment (which, in this case, will vary based on the stationary versus the non-stationary $P_{24h\text{-}max}$ value obtained) and the watershed size and distance from the nearest rain gauges, which define how much area of the watershed is covered by each isohyetal (the weighted area). In other words, a change in the value of point rainfall does not necessarily imply a major change in the areal rainfall. Because of that, the authors' future work will address: (a) $P_{24h\text{-}max}$ regionalization at each of the seven departments of the Colombian Caribbean region, (b) the monotonic trend of the multiannual $P_{24h\text{-}max}$ time series via Mann–Kendall and Spearman's rho tests, and (c) the stationarity and non-stationarity of the time series of the rain gauges analyzed in this study so as to compare point versus areal rainfall values and their impact on the design rainfall selection for different return periods at the local and regional level.

Finally, rather than being considered as the sole source for $P_{24h\text{-}max}$ estimation, these maps are intended to be used as a reference in the hydrological and hydraulic analysis, mainly for stormwater management and flood mitigation projects.

1-6. References

1- Chow, V.T.; Maidment, D.R.; Mays, L.W. *Applied Hydrology*, 1st ed.; McGraw-Hill: New York, NY, USA, 1988; pp. 350–376.
2- Bedient, P.B.; Huber, W.C. *Hydrology and Floodplain Analysis*; Prentice-Hall: Upper Saddle River, NJ, USA, 2002; pp. 168–224.
3- Vargas, M.R.; Díaz-Granados, M. Colombian Regional Synthetic IDF Curves. Master's Thesis, University of Los Andes, Bogotá, Colombia, 1998.
4- IDEAM; PNUD; MADS; DNP; CANCILLERÍA. New Scenarios of Climate Change for Colombia 2011–2100 Scientific Tools for Department-Based Decision Making—National Emphasis: 3rd National Bulletin on Climate Change. 2015.
5- IDEAM. Intensity-Duration-Frequency Curves (IDF).

6- Ministry of Housing, City, and Development (MinVivienda), Republic of Colombia. Resolution 0330 of 8 June 2017, Technical Guidelines for the Sector of Potable Water and Basic Sanitation (RAS). 2017.
7- Liu, Y.; Zhang, W.; Shao, Y.; Zhang, K. A Comparison of Four Precipitation Distribution Models Used in Daily Stochastic Models. *Adv. Atmos. Sci.* **2011**, *28*, 809–820.
8- Chowdhury, A.F.M.K.; Lockart, N.; Willgoose, G.; Kuczera, G.; Kiem, A.S.; Parana Manage, N. Development and evaluation of a stochastic daily rainfall model with long-term variability. *Hydrol. Earth Syst. Sci.* **2017**, *21*, 6541–6558.
9- Pizarro, R.; Ingram, B.; Gonzalez-Leiva, F.; Valdés-Pineda, R.; Sangüesa, C.; Delgado, N.; García-Chevesich, P.; Valdés, J.B. WEBSEIDF: A Web-Based System for the Estimation of IDF Curves in Central Chile. *Hydrology* **2018**, *5*, 40.
10- Burgess, C.P.; Taylor, M.A.; Stephenson, T.; Mandal, A. Frequency analysis, infilling and trends for extreme precipitation for Jamaica (1895–2100). *J. Hydrol.* **2015**, *3*, 424–443.
11- Seo, Y.; Hwang, J.; Kim, B. Extreme Precipitation Frequency Analysis Using a Minimum Density Power Divergence Estimator. *Water* **2017**, *9*, 81.
12- Nguyen, V.-T.-B.; Nguyen, T.-H. Statistical Modeling of Extreme Rainfall Processes (SMExRain): A Decision Support Tool for Extreme Rainfall Frequency Analyses. In Proceedings of the 12th International Conference on Hydroinformatics, Incheon, Korea, 21–26 August 2016; Volume 154, pp. 624–630.
13- Ngoc Phien, H.; Arbhabhirama, A.; Sunchindah, A. Rainfall distribution in northeastern Thailand. *Hydrol. Sci. J.* **2009**, *25*, 167–182.
14- Ministry of Public Development, General Department of Water, Republic of Chile. Maximum Precipitations for 1, 2, and 3 Days. 1990.
15- Ministry of Development. State Secretary of Infrastructure and Transport, General Direction of Roads. Daily Maximum Rainfall in Peninsular Spain. 1999.
16- Liaw, C.-H.; Chiang, Y.-C. Dimensionless Analysis for Designing Domestic Rainwater Harvesting Systems at the Regional Level in Northern Taiwan. *Water* **2014**, *6*, 3913–3933.
17- U.S. Department of Commerce (USDOC). *Technical Paper No. 40 (TP-40), Rainfall Frequency Atlas of the United States for Durations from 30 Minutes to 24 Hours and Return Periods from 1 to 100 Years*; Weather Bureau Technical Papers: Washington, DC, USA, 1961.
18- Jaramillo-Robledo, A. Lluvias máximas en 24 horas para la región Andina de Colombia (24-hour maximum rainfall for the Colombian Andean region). *Cenicafé* **2005**, *56*, 250–268.
19- Gutiérrez Jaraba, J.; Pérez Márquez, F.; Angulo Blanquicett, G.; Chiriboga Gavidia, G.; Valdés Cervantes, L. Determination of the Intensity-Duration-Frequency (IDF) Curves for the City of Cartagena de Indias for the period between 1970 and 2015. In Proceedings of the Fifteenth LACCEI International Multi-Conference for Engineering, Education, and Technology: Global Partnerships for Development and Engineering Education, Boca Raton, FL, USA, 19–21 July 2017.
20- Pulgarín Dávila, E.G. Regional Equations for the Estimation of the Intensity-Duration-Frequency Curves based on the Rainfall Scale Properties (Colombian Andean Region). Master's Thesis, National University of Colombia, Bogotá, Colombia, 2009.
21- Acosta Castellanos, P.M.; Sierra Aponte, L.X. IDF construction methods' evaluation, from probability distributions and adjustment's parameters. *Revista Facultad Ingeniería* **2013**, *22*, 25–33.
22- Becerra-Oviedo, J.A.; Sánchez-Mazorca, L.F.; Acosta-Castellanos, P.M.; Díaz-Arévalo, J.L.

Regionalization of IDF curves for the use of hydrometeorological models in the Western Sabana of Cundinamarca department. *Revista Ingeniería Región* **2015**, *14*, 143–150.

23- Muñoz, B.J.E.; Zamudio, H.E. Regionalización de Ecuaciones Para el Cálculo de Curvas de Intensidad, Duración y Frecuencia Mediante Mapas de Isolíneas en el Departamento de Boyacá (Regionalization of the Equations for the Calculation of the IDF Curves through Isohyetals Maps in the Department of Boyacá).

24- Hydrographic and Oceanographic Research Center (CIOH). General Circulation of the Atmosphere in Colombia. 2010.

25- Poveda, G.; Jaramillo, A.; Gil, M.M.; Quinceno, N.; Mantilla, R.I. Seasonality in ENSO-related precipitation, river discharges, soil moisture, and vegetation index in Colombia. *Water Resour. Res.* **2001**, *37*, 2169–2178.

26- Waylen, P.; Poveda, G. El Niño-Southern Oscillation and aspects of western South American hydro-climatology. *Hydrol. Process* **2002**, *16*, 1247–1260.

27- Poveda, G.; Álvarez, D.M.; Rueda, O.A. Hydro-climatic variability over the Andes of Colombia associated with ENSO: A review of climatic processes and their impact on one of the Earth's most important biodiversity hotspots. *Clim. Dyn.* **2011**, *36*, 2233–2249.

28- Hoyos, N.; Escobar, J.; Restrepo, J.C.; Arango, A.M.; Ortiz, J.C. Impact of the 2010–2011 La Niña phenomenon in Colombia, South America: The human toll of an extreme weather event. *Appl. Geogr.* **2013**, *39*, 16–25.

29- Ramírez-Cerpa, E.; Acosta-Coll, M.; Vélez-Zapata, J. Analysis of the climatic conditions for short term precipitation in urban areas: A case study Barranquilla, Colombia. *Idesia* **2017**, *32*, 87–94.

30- Schneider, L.E.; McCuen, R.H. Statistical guidelines for curve number generation. *J. Irrig. Drain. Eng.* **2005**,*131*, 282–290.

31- Macvicar, T.H. *Frequency Analysis of Rainfall Maximums for Central and South Florida, Technical Publication # 81-3*; South Florida Water Management District: West Palm Beach, FL, USA, 1981.

32- Ali, A.; Abtew, W. *Regional Rainfall Frequency Analysis for Central and South Florida. Technical Publication WRE#380*; South Florida Water Management District: West Palm Beach, FL, USA, 1999.

33- Pathak, C.S. *Frequency Analysis of Rainfall Maximums for Central and South Florida, Technical Publication EMA # 390*; South Florida Water Management District: West Palm Beach, FL, USA, 2001.

34- Obeysekera, J.; Salas, J.D. Quantifying the uncertainty of design floods under nonstationary conditions.*J. Hydrol. Eng.* **2014**, *19*, 1438–1446.

35- Salas, J.D.; Obeysekera, J.; Vogel, R.M. Techniques for assessing water infrastructure for nonstationary extreme events: A review. *Hydrol. Sci. J.* **2018**, *63*, 325–352.

36- Faber, B. Current methods for hydrologic frequency analysis. In Proceedings of the Workshop on Nonstationarity, Hydrologic Frequency Analysis, and Water Management, Colorado Water Institute Information Series No. 109, Boulder, CO, USA, 13–15 January 2010; pp. 33–39.

37- Haan, C.T. *Statistical Methods in Hydrology*; The Iowa State University Press: Ames, IA, USA, 1977; pp. 97–158.

38- McCuen, R.H. *Microcomputer Applications in Statistical Hydrology*; Prentice Hall: Englewood Cliffs, NJ, USA, 1993; pp. 58–69.

39- Singh, V.P. *Entropy-Based Parameter Estimation in Hydrology*; Kluwe Academic Dordrecht: London, UK, 1988.
40- Chin, D.A. *Water-Resources Engineering*, 3rd ed.; Pearson: London, UK, 2013; pp. 344–395.
41- Gumbel, E.J. The return period of flood flows. *Ann. Math. Stat.* **1941**, *2*, 163–190.
42- Gumbel, E.J. *Statistical Theory of Extreme Values and Some Practical Applications: A Series of Lectures*; U.S. Dept. of Commerce, National Bureau of Standards Applied Mathematics Series 33; U.S. Govt. Print. Office: Springfield, VA, USA, 1954.
43- Jenkinson, A.F. The frequency distribution of the annual maximum (or minimum) values of meteorological elements. *Q. J. R. Meteorol. Soc.* **1955**, *81*, 158–171.
44- Frechet, M. Sur la loi de probabilité de l'ecart máximum (On the probability law of máximum values). *Annales Societe Polonaise Mathematique* **1927**, *6*, 93–116.
45- Weibull, W. A statistical theory of the strength of materials. *Proc. Ing. Vetensk Akad.* **1939**, *51*, 5–45.
46- Lazoglou, G.; Anagnostopoulou, C. An Overview of Statistical Methods for Studying the Extreme Rainfalls in Mediterranean. In Proceedings of the 2nd International Electronic Conference on Atmospheric Sciences, Basel, Switzerland, 16–31 July 2017.
47- Selaman, O.S.; Said, S.; Putuhena, F.J. Flood Frequency Analysis for Sarawak using Weibull, Gringorten and L-moments Formula. *J. Inst. Eng.* **2007**, *68*, 43–52.
48- Chikobvu, D.; Chifurira, R. Modelling of Extreme Minimum Rainfall Using Generalised Extreme Value Distribution for Zimbabwe. *S. Afr. J. Sci.* **2015**, 111.
49- Millington, M.; Das, S.; Simonovic, S.P. *The Comparison of GEV, Log-Pearson Type 3 and Gumbel Distributions in the Upper Thames River Watershed under Global Climate Models*; Water Resources Research Report (Report # 077); The University of Western Ontario, Department of Civil and Environmental Engineering: London, ON, Canada, 2011.
50- Koutsoyiannis, D. Statistics of extremes and estimation of extreme rainfall: II. Empirical investigation of long rainfall records. *J. Hydrol. Sci. J.* **2004**, *49*, 610.
51- Alam, M.A.; Emura, K.; Farnham, C.; Yuan, J. Best-Fit Probability Distributions and Return Periods for Maximum Monthly Rainfall in Bangladesh. *Climate* **2018**, *6*, 9.
52- U.S. Geological Survey (USGS). *Flood-Frequency Analyses, Manual of Hydrology: Part 3, Flood-Flow Techniques*; U.S. Government Printing Office: Washington, DC, USA, 1960.
53- U.S. Geological Survey (USGS). *Theoretical Implications of under Fit Streams, Flood-Flow Techniques*; U.S. Government Printing Office: Washington, DC, USA, 1965.
54- Lumia, R.; Freehafer, D.A.; Smith, M.J. Magnitude and Frequency of Floods in New York: U.S. Geological Survey Scientific Investigations Report 2006–5112. 2006.
55- Webster, V.L.; Stedinger, J. Log-Pearson Type 3 Distribution and Its Application in Flood Frequency Analysis. I: Distribution Characteristics. *J. Hydrol. Eng.* **2007**, *12*.
56- Greis, N.P. Flood frequency analysis: A review of 1979–1982. *Rev. Geophys.* **1983**, *21*, 699–706.
57- Vogel, R.M.; McMahon, T.A.; Chiew, F.H.S. Floodflow frequency model selection in Australia. *J. Hydrol.* **1993**,*146*, 421–449.
58- Jam, P.; Singh, V.J. Estimating parameters of EV 1 distribution for flood frequency analysis. *J. Am. Water Resour. Assoc.* **1987**, *23*, 59–71.
59- Ngoc Phien, H. A review of methods of parameter estimation for the extreme value type-1 distribution.*J. Hydrol.* **1987**, *90*, 251–268.
60- Fathi, K.; Bagheri, S.F.; Alizadeh, M.; Alizadeh, M. A study of methods for estimating in the exponentiated Gumbel distribution. *J. Stat. Theory Appl.* **2017**, *16*, 81–95.

61- Sarangi, A.; Cox, C.A.; Madramootoo, C.A. Geostatistical Methods for Prediction of Spatial Variability of Rainfall in a Mountainous Region. *Trans. ASAE* **2005**, *48*, 943–954.
62- Bhunia, G.S.; Shit, P.K.; Maiti, R. Comparison of GIS-based interpolation methods for spatial distribution of soil organic carbon (SOC). *J. Saudi Soc. Agric. Sci.* **2018**, *17*, 114–126.
63- Boer, E.P.J.; De Beursl, K.M.; Hartkampz, A.D. Kriging and thin plate splines for mapping climate variables.*J. Appl. Genet.* **2001**, *3*, 146–154.
64- Gonzalez, A.; Temimi, M.; Khanbilvardi, R. Adjustment to the curve number (NRCS-CN) to account for the vegetation effect on hydrological processes. *Hydrol. Sci. J.* **2015**, *60*, 591–605.
65- Moriasi, D.N.; Arnold, J.G.; Van Liew, M.W.; Bingner, R.L.; Harmel, R.D.; Veith, T.L. Model evaluation guidelines for systematic quantification of accuracy in watershed simulations. *Trans. ASABE* **2007**, *50*, 885–900.
66- Gonzalez-Alvarez, A.; Coronado-Hernández, O.E.; Fuertes-Miquel, V.S.; Ramos, H.M. Effect of the Non-Stationarity of Rainfall Events on the Design of Hydraulic Structures for Runoff Management and Its Applications to a Case Study at Gordo Creek Watershed in Cartagena de Indias, Colombia. *Fluids* **2018**, *3*, 27.
67- Wang, D.; Hagen, S.C.S.; Alizad, K. Climate change impact and uncertainty analysis of extreme rainfall events in the Apalachicola River basin, Florida. *J. Hydrol.* **2012**, *480*, 125–135.
68- Li, J.; Heap, A.D. *A Review of Spatial Interpolation Methods for Environmental Scientists*; Geoscience Australia: Canberra, ACT, Australia, 2008. (accessed on 23 August 2018).
69- Mitas, L.; Mitasova, H. Spatial Interpolation. In *Geographic Information Systems: Principles, Techniques, Management and Applications*, 2nd ed.; Wiley: Longley, PA, USA, 2005; Volume 1, pp. 481–492.
70- Ikechukwu, M.N.; Ebinne, E.; Idorenyin, U.; Raphael, N.I. Accuracy Assessment and Comparative Analysis of IDW, Spline and Kriging in Spatial Interpolation of Landform (Topography): An Experimental Study. *Earth Environ. Sci.* **2017**, *9*, 354–371.
71- Curtarelli, M.; Leão, J.; Ogashawara, I.; Lorenzzetti, J.; Stech, J. Assessment of Spatial Interpolation Methods to Map the Bathymetry of an Amazonian Hydroelectric Reservoir to Aid in Decision Making for Water Management. *Int. J. Geo-Inf.* **2015**, *4*, 220–235.
72- Simpson, G.; Wu, Y.H. Accuracy and Effort of Interpolation and Sampling: Can GIS Help Lower Field Costs? *Int. J. Geo-Inf.* **2014**, *3*, 1317–1333.
73- Di Piazza, A.; Lo Conti, F.; Viola, F.; Eccel, E.; Noto, L.V. Comparative Analysis of Spatial Interpolation Methods in the Mediterranean Area: Application to Temperature in Sicily. *Water* **2015**, *7*, 1866–1888.
74- Phillips, D.L.; Dolph, J.; Marks, D. A comparison of geostatistical procedures for spatial analysis of precipitation in mountainous terrain. *Agric. For. Meteorol.* **1992**, *58*, 119–141.
75- Luo, W.; Taylor, M.C.; Parker, S.R. A comparison of spatial interpolation methods to estimate continuous wind speed surfaces using irregularly distributed data from England and Wales. *Int. J. Clim.* **2008**, *28*, 947–959.

Chapter 2: Analysis of the Behavior of Daily Maximum Rainfall within the Department of Atlántico, Colombia

The final result of this stage of the research was a manuscript already published (shown below) in the Journal Water (MDPI) under the same title with the following citation:

Viloria-Marimón, O.M.; González-Álvarez, Á.; Mouthón-Bello, J.A. Analysis of the Behavior of Daily Maximum Rainfall within the Department of Atlántico, Colombia. Water 2019, 11, 2453. (available at: https://www.mdpi.com/2073-4441/11/12/2453)

Abstract: In the Colombian Caribbean region, there are few studies that evaluate the behavior of one of the most commonly used variables in hydrological analyses: the maximum daily rainfall ($P_{max\text{-}24h}$). In this study, multiannual $P_{max\text{-}24h}$ time series from 19 rain gauges, located within the department of Atlántico, were analyzed to: (a) determine possible increasing/decreasing trends over time, (b) identify regions with homogeneous behavior of $P_{max\text{-}24h}$, (c) assess whether the time series are better suited under either a stationary or non-stationary frequency analysis, (d) generate isohyetal maps under stationary, non-stationary and mixed conditions, and (e) evaluate the isohyetal maps by means of the calculation of areal rainfall (P_{areal}) in nine watersheds. In spite of the presence of both increasing and decreasing trends, only Puerto Giraldo rain gauge showed a significant decreasing trend. Also, three regions (east, central, and west) with similar $P_{max\text{-}24h}$ behavior were identified. According to the Akaike Information Criterion test, 79% of the rain gauges showed better fit under stationary conditions. Finally, statistical analysis revealed that under stationary conditions, the errors in the calculation of P_{areal} were more frequent, while the magnitude of the errors were larger under non-stationary conditions, especially in the central-south region.

2-1. Introduction

Globally, changes in the pattern of behavior of hydrometeorological variables (e.g., precipitation, temperature, runoff, relative humidity, etc.) are influenced, among others, by population growth, watershed land-use/land-cover (LULC) changes, and the increase in greenhouse gases emissions [1,2]. In Colombia, the Institute of Hydrology, Meteorology, and Environmental Studies (IDEAM, in Spanish) conducted several studies focused on evaluating the changes in the behavioral patterns of some hydrometeorological variables [3–7]. IDEAM [3] analyzed the annual average rainfall trend over the periods 2011–2040, 2041–2070, and 2071–2100 for the different departments (political and administrative territorial units) that compose the five regions of Colombia (Caribbean, Pacific, Andean, Orinoco, and Amazon). According to the study, the department of Atlántico (located within the Caribbean region) will experience an annual average rainfall decrease ranging from 7.39% through 11.26% during the 2011–2100 period. In addition, it was predicted that some of the municipalities located in the southeast of the department will be the most affected.

Such changes in the hydrological cycle can lead to (a) decreases in the water supply (both for human consumption and for the different sectors of the economy), (b) possible water supply cost increase, and (c) under- or oversized hydraulic structures for stormwater management [8]. Several studies analyzed the rainfall behavior within the department of Atlántico [9–13]. However, none analyzed the maximum daily rainfall ($P_{max\text{-}24h}$) time series trends or whether they (the trends) have regional behavior within the department. González-Álvarez et al. [14] detected increasing and decreasing linear trends in some of the multiannual $P_{max\text{-}24h}$ time series of the 13 rain gauges analyzed in the department of Atlántico, which further suggested the presence of

non-stationarity. Despite the findings, the scope of the study did not cover a detailed analysis of trends using non-parametric tests (e.g., Mann–Kendall and Spearman's rho) and the possible presence of different regions exhibiting similar rainfall behavior. Furthermore, the study did not determine whether a non-stationary frequency analysis was more convenient than a stationary one when estimating the $P_{max\text{-}24h}$ associated with the different return periods and their possible impact on (a) the isohyetal alignments, and (b) the subsequent computation of the areal rainfall of a given watershed.

Several municipalities, within the department of Atlántico, experience different affectations that go from severe and prolonged droughts [15] to more recurrent and devastating floods [13,16,17]. During the rainy season of 2010–2011, a great portion of the southern part of the department was flooded, causing a dyke breakage that exacerbated the problem with 185,236 people affected and total losses (infrastructure, habitat, etc.) estimated to be approximately United States dollars (USD) $491 million, of which infrastructure accounted for 11% [18]. All these extreme events could indicate a change in the rainfall regime (particularly $P_{max\text{-}24h}$) that needs to be analyzed, especially for the design of stormwater management infrastructure. Thus, this study uses multiannual time series of $P_{max\text{-}24h}$ from 19 rain gages within the department of Atlántico to (a) analyze the time series trends by means of the Mann–Kendall (MK), Spearman's rho (SR), and Theil–Sen estimator as a first step to identify possible changes in the rainfall pattern over time, (b) determine and delineate regions with homogeneous $P_{max\text{-}24h}$ behavior, which contributes to the understanding of rainfall behavior mainly in ungauged areas, (c) perform both a stationary and a non-stationary rainfall frequency analysis in order to calculate $P_{max\text{-}24h}$ for return periods of five, 10, 25, 50, and 100 years, (d) determine, via Akaike information criterion (AIC) test, whether a stationary or a non-stationary frequency analysis better fits the time series analyzed, and (e) draw isohyetal maps for different return periods by using the $P_{max\text{-}24h}$ under both stationary and non-stationary conditions, as well as mixed (stationary and non-stationary $P_{max\text{-}24h}$ based on the AIC test results), so as to evaluate the possible implications of not taking into account pattern shifts observed in a variable such as $P_{max\text{-}24h}$ commonly used in water resource-related projects (e.g., flood risk evaluation, design of hydraulic structures for stormwater management, water balances, and water scarcity, among others). Ultimately, the findings herein are intended to show the importance of adapting those projects to climate changes through a thorough analysis that permits a better understanding of the hydrological variables as part of the decision-making process.

2-2. Study area and data

The department of Atlántico, located in the Caribbean region, is one of the 32 departments in which Colombia is politically divided [19,20]. This department has an extension of 3386 km^2 and consists of 23 municipalities, grouped into five (5) regions: Metropolitan Area, Coastal, Eastern, Central, and South (Table 2-1 and Figure 2-1) [21].

Table 2-1. Political-administrative regions and municipalities within the department of Atlántico

Region	Municipality
Metropolitan Area	Barranquilla, Puerto Colombia, Soledad, Malambo, and Galapa.
Coastal	Tubará, Juan de Acosta, Piojó, and Usiacurí.
Eastern	Sabanagrande, Santo Tomás, Palmar de Varela, and Ponedera.
Central	Baranoa, Polonuevo, Sabanalarga, and Luruaco.
South	Repelón, Manatí, Candelaria, Campo de la Cruz, Santa Lucía, and Suan.

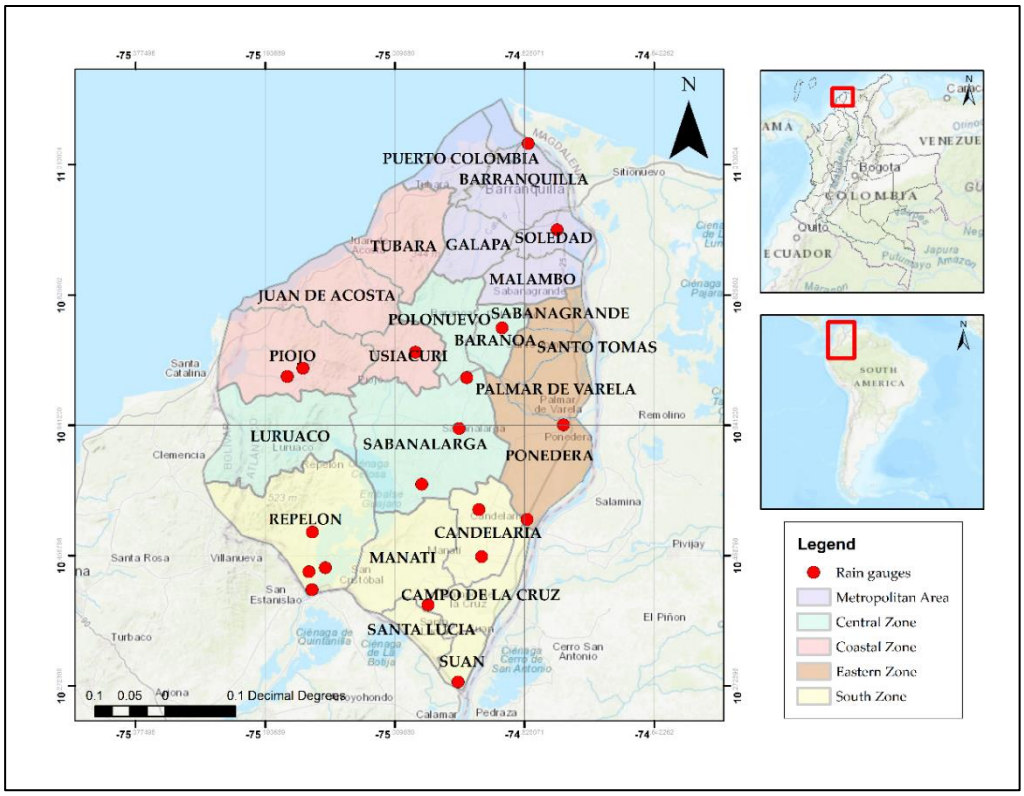

Figure 2-1.Political distribution of the department of Atlántico

The department of Atlántico has a warm and dry climate, with an average annual temperature of approximately 28 °C and maximum temperatures that can reach up to 40 °C. The average annual rainfall ranges from 500 mm to 1500 mm [15]. The rainfall regime has three seasons: dry (December to March), transition (late April to June), and rainy (August to early December) [22].

In this research, multi-annual series of maximum daily rainfall were used, from 19 rain gauges operated by IDEAM (Table 2), totaling 728 observations from 1940 to 2015 (records from 2016–2019 were not included as some rain gauges do not yet have the information available for those years). The rain gauges used in this study were selected under the following criteria: (a) time series with a minimum of 20 years of data, (b) exclusion of rain gauges with less than 25% of the rainfall information in any given year, (c) exclusion of rain gauges that did not have information from the months corresponding to the rainy season [23], and (d) elimination of outliers by means of the Water Resources Council method [24]. The selected rain gauges are shown in Table 2.).

Table 2-2. Rain gauges selected in the department of Atlántico

Rain gauge	Municipality	Latitude	Longitude	No. of rainfall observations	$P_{max-24h}$ (mm)			Year of installation
					Max	Min	Avg	
Aeropuerto (Apto) Ernesto Cortissoz	Soledad	10.91778	–74.77972	72	140.7	30.0	79.0	1940
Candelaria	Candelaria	11.04000	–74.82083	28	125.0	40.0	82.5	1978
Casa de Bombas	Repelón	10.40833	–75.12722	30	122.0	37.0	77.2	1978
El Porvenir	Piojó	10.71022	–75.16228	27	175.0	42.0	90.6	1988
Hacienda (Hda) El Rabón	Santa Lucía	10.38694	–74.96278	33	115.0	50.0	79.3	1978
Hibaracho	Piojo	10.72189	–75.14011	45	145.0	44.0	84.5	1963
Las Flores	Barranquilla	10.52172	–74.89078	28	151.3	44.6	86.4	1971
Lena	Candelaria	10.43383	–75.13158	46	150.0	39.0	90.7	1969

Loma Grande	Repelón	10.55778	–74.97178	27	167.0	33.5	80.2	1968
Los Campanos	Sabanalarga	10.70850	–74.90783	31	148.0	35.0	87.7	1985
Montebello	Baranoa	10.77900	–74.85792	26	140.0	49.0	80.8	1985
Polo nuevo	Polo Nuevo	10.64178	–74.77072	49	150.0	50.0	93.0	1959
Ponedera	Ponedera	10.50789	–74.82228	46	157.3	42.0	91.2	1959
Puerto Giraldo	Ponedera	10.49000	–75.12694	33	171.0	44.0	90.8	1978
Repelón	Repelón	10.63672	–74.91889	48	160.3	32.0	73.1	1963
Sabanalarga	Sabanalarga	10.43944	–75.10833	52	250.0	42.0	86.9	1959
San José	Luruaco	10.27789	–74.92022	24	135.6	45.0	78.0	1987
San Pedrito Alerta	Suán	10.74472	–74.98056	34	115.0	44.4	78.4	1978
Usiacurí	Usiacurí	10.91778	–74.77972	49	130.0	37.0	78.5	1964
Total				**728**	**250.0**	**30.0**	**83.6**	

2-3. Methodology

After selecting the rain gauges that met the above-mentioned criteria, the rainfall time series underwent further analysis. Figure 2-2 shows the steps that make up the methodology proposed in this research.

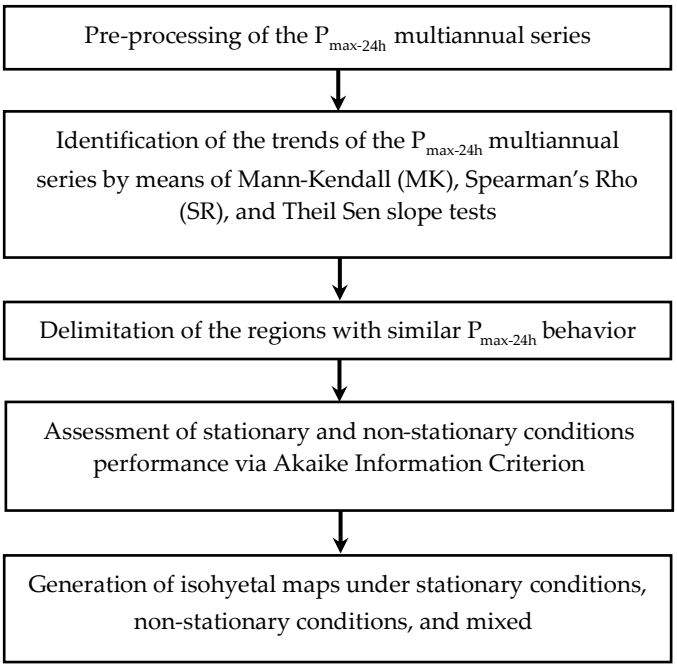

Figure 2-2. Research methodology flowchart

2-3.1. Trend Analysis

In this study, the monotonic trend detection was performed through the nonparametric tests of Mann-Kendall and Spearman's Rho [25], with significance levels of 5%. Nonparametric testing has the advantage of being able to detect trends, independently of whether the data has a normal distribution or not, as with hydrometeorological variables [26]. In addition, the analysis was complemented by determining the magnitude of the trends' slopes identified in the $P_{max-24h}$ series using the Theil-Sen Slope [27].

2-3.1.1. Mann-Kendall (MK) Test

The test considers both a null hypothesis (H_0) when no trend (to increase or decrease) exists and, as alternative hypothesis (H_1), that there is a trend. The calculation of Mann-Kendall's statistics S and standardized Z uses the following set of formulas (Equation (1)):

$$S = \sum_{i=1}^{n-1} \sum_{j=i+1}^{n} Sig(X_j - X_i),$$

$$Sgn(X_j - X_i) = \begin{cases} +1 \ if \ (X_j - X_i) > 0 \\ 0 \ \ if \ (X_j - X_i) = 0 \\ -1 \ if \ (X_j - X_i) < 0, \end{cases}$$

$$V(S) = \frac{1}{18}\left[n(n-1)(2n+5) - \sum_{p=1}^{q} t_p(t_p-1)(2t_p+5)\right],$$

$$Z_{MK} = \begin{cases} \frac{S-1}{\sqrt{VAR(S)}} \text{ if S} > 0 \\ 0 \qquad \text{if S} = 0 \\ \frac{S+1}{\sqrt{VAR(S)}} \text{ if S} < 0. \end{cases} \quad (1)$$

Where, X_i and X_j represent the time series data in chronological order, n the number of data in the time series, t_p the number of links for the p-th value and q the number of links. Positive Z values (MK statistic) indicate the presence of increasing trends and negative values indicate decreasing trends. If $|Z|>Z_{1-\alpha/2}$, the null hypothesis will be rejected, indicating a statistically significant trend. The critical value of $Z_{1-\alpha/2}$ for a significance level of 5% is 1.96 [26]. That is, a trend will be considered increasing or decreasing, at a significance level of 5%, only if Z_{MK} is greater than |1.96|. Otherwise, it is considered trendless (constant).

2-3.1.2. Spearman's Rho (SR) Test

This test assumes that the data is independent and identically distributed. Null and alternative hypotheses are defined the same way as in the Mann-Kendall test [28]. The R_{SR} and Z_{SR} statistical variables are calculated using Equations (2) and (3).

$$R_{SR} = 1 - \frac{6*\sum_{i=1}^{n}(D_i - i)^2}{n(n^2-1)} \quad (2)$$

$$Z_{SR} = R_{sp}\sqrt{\frac{n-2}{1-{R_{SR}}^2}} \quad (3)$$

D_i represent the i-th observation, i the chronological order of the number, n the number of observations, Z_{SR} is the value of the t-student distribution with n–2 degrees of freedom. Positive and negative Z_{SR} values represent increasing and decreasing trends, respectively. If $|Z_{SR}| > t_{(n-2,1-\alpha/2)}$, the null hypothesis will be rejected, demonstrating statistically significant trends [10,29].

2-3.1.3. Estimator of Theil-Sen Slope

This estimator allows to determine the actual slope of the trends of a given time series. The principle of this estimator is based on the assumption that when a series of data shows a linear trend, the median of the slope of the linear trend can be calculated using the slopes of several data points and this value will represent the slope of its trend (Equation (4)) [30,31].

$$\beta_{TS} = \text{median}\left(\frac{x_j - x_k}{j-k}\right), j = 1, 2, \ldots, n; k = 1, 2, \ldots, j-1 \quad (4)$$

β_{TS} represents the slope between the Xj and Xk points in the time series (which corresponds to the time points j and k, with $j > k$).

2-3.2. Delimiting homogeneous regions

The delimitation of regions with similar hydrometeorological conditions involved a statistical analysis of the data observed in the study area [32,33] by means of the regionalization method suggested by Hosking and Wallis [15]. This method defines statistical parameters similarly to the traditional L-moments, which, in turn, involves the calculation of the β estimators (Equations (5) to (8)).

$$\beta_0 = \frac{1}{n}\sum_{i=1}^{n} x_i \quad (5)$$

$$\beta_1 = \frac{\sum_{i=1}^{n-1}(n-i)x_i}{n(n-1)} \quad (6)$$

$$\beta_2 = \frac{\sum_{i=1}^{n-2}(n-i)(\text{n}-\text{i}-1)x_i}{n(n-1)(\text{n}-2)} \quad (7)$$

$$\beta_3 = \frac{\sum_{i=1}^{n-3}(n-i)(\text{n}-\text{i}-1)(\text{n}-\text{i}-2)x_i}{n(n-1)(\text{n}-2)(\text{n}-3)} \quad (8)$$

X_i represents the value of the $P_{max\text{-}24h}$ series, i the rank of each data arranged from highest to lowest and n the number of data in the series of each rain gauges j. Subsequently, the L-moments (represented with λ) are obtained using Equations (9) to (12).

$$\lambda_1 = \beta_0 \quad (9)$$

$$\lambda_2 = 2\beta_1 - \beta_0 \quad (10)$$

$$\lambda_3 = 6\beta_2 - 6\beta_1 + \beta_0 \quad (11)$$

$$\lambda_4 = 20\beta_3 - 30\beta_2 + 12\beta_1 - \beta_0 \quad (12)$$

Finally, the dimensionless L-moments were calculated via Equations (13) to (15), where τ_2 represents the coefficient of variation; τ_3, the asymmetry coefficient; and τ_4, the kurtosis coefficient.

$$\tau_2 = \frac{\lambda_2}{\lambda_1} \quad (13)$$

$$\tau_3 = \frac{\lambda_3}{\lambda_2} \quad (14)$$

$$\tau_4 = \frac{\lambda_4}{\lambda_2} \quad (15)$$

Homogeneous regions were then formed via cluster analysis by means of the K-means method [35], which allows the dimensional L-moments to be related to the elevation and location parameters of each of the rain gauges. This way, the clusters sharing similar characteristics are detected so that the homogeneous regions can be defined. Additionally, varying the number of clusters in the K-means method helps with finding a geographically consistent configuration. Finally, the selected cluster configuration was reassessed using the methodology used by Hosking et al. [36] in order to corroborate the regions homogeneity.

2-3.3. Stationary and non-stationary rainfall frequency analysis

The point rainfall values used for the $P_{max\text{-}24h}$ isohyetals were estimated via frequency analysis for both stationary (SC) and non-stationary (NSC) conditions for return periods of 5, 10, 25, 50 and 100 years.

Based on the results obtained by González-Alvarez et al [14] for the Colombian Caribbean region, Generalized Extreme Value (GEV) [61] (Equations (16)) and Gumbel [62] (Equations (17) to (19)) were used for the stationary frequency analysis. The theoretical basis for these two cumulative distributions functions (CDF) can be widely found in the literature [39-41]. In Equations (17)-(19), k is the shape parameter, β is the mode (or location) and α the scale (always greater than zero). GEV can take one of three extreme value (EV) distributions depending on the value of k: (a) if k equals zero, takes the form of Type 1 EV (Gumbel); (b) if less than zero, Type 2 (Fréchet); and (c) Type 3 (Weibull), if greater than zero. The $P_{max\text{-}24h}$ value selected for the stationary frequency analysis was the one that came from the function showing the best Chi-square test [42] result.

$$F(Z) = \exp\left[-\left(1 - k\frac{z-\beta}{\alpha}\right)^{1/k}\right] \quad (16)$$

$$F(Z) = 1 - e^{-e^{\left[\frac{z-\beta}{\propto}\right]}} \quad (17)$$

$$\beta = \frac{\sigma_z\sqrt{6}}{\pi} \quad (18)$$

$$\alpha = \bar{z} - 0.5772\beta \quad (19)$$

The non-stationary frequency analysis was carried out according to the methodology proposed by Obeysekera and Salas [1,43,44], which uses: (a) the GEV function by varying the location parameter over time and maintaining the constant parameters of scale and shape (called GEVmu) and (b) a definition of the return period (Tr) according to the geometric distribution given by Equation (20), where Pj is the probability of leave and j represents the year to be projected [1,45]. The GEVmu function was already tested by Gonzalez-Alvarez et al. [45] in the Colombian Caribbean region, where a sensitivity analysis showed that varying the shape and/or scale parameters did not bring any improvement in the performance of either GEV or Gumbel distributions.

$$Tr, NSC = 1 + \prod_{X=1}^{\infty}\sum_{J=1}^{\infty}\left(1 - p_J\right) \quad (20)$$

Subsequently, a linear trend model of each parameter (location, shape, and scale) was defined to estimate its value using a code programmed in the R software (Version 3.3.1, R Development Core Team, Auckland, New Zealand) with the library nsextremes [46].

After the $P_{max\text{-}24h}$ values were calculated for stationary and non-stationary conditions, the Akaike Information Criterion (AIC) goodness-of-fit test [47] was used to determine which of the two conditions (stationary and non-stationary) better represented the multiannual series for each of the rain gauges analyzed. The $P_{max\text{-}24h}$ values for SC, NSC, and the better of the two conditions were later used for the generation of the stationary, non-stationary, and mixed isohyetal maps, respectively (Section 3.4).

2-3.4. Generation of isohyetals maps

After obtaining the $P_{max\text{-}24h}$ values (for stationary and non-stationary conditions) for each of the rain gauges, three different types of $P_{max\text{-}24h}$ isohyetals (for return periods 5, 10, 25, 50 and 100 years) were generated (Table 2-3), using ArcGIS (Version 16.1, ESRI Inc., Redlands, CA, US). For this, the Inverse Distance Weighting (IDW) interpolation method with manual adjustment was utilized, based on the findings of González-Álvarez et al. [14] for the Colombian Caribbean region (inputs: Z-Value = 2; Cell Size = 0.021; Search Radius variable, and Number of Points = 12).

Table 2-3. Type of isohyetal maps

Condition	Description
Stationary	Isohyetal maps generated from $P_{max\text{-}24h}$ values under stationary conditions.
Non-stationary	Isohyetal maps generated from $P_{max\text{-}24h}$ values under non-stationary conditions.
Mixed	Isohyetal maps generated from the $P_{max\text{-}24h}$ value corresponding to the best fit according to the AIC test.

2-3.5. Evaluation of the different isohyetals maps

The performance of the isohyetal maps was tested in nine watersheds (three watersheds per homogeneous regions) by estimating their corresponding areal precipitation under SC, NSC, and mixed for return periods of 5, 10, 20, 50, and 100 years. The selected watersheds had various sizes and were located at different distances from the nearest rain gauge.

After estimating the areal $P_{max\text{-}24h}$ of each of the watersheds, a statistical analysis was performed using the Relative Error Percentage (REr), RMSE and Standard Deviation Ratio (RSR) (Equation (22)), the Bias Percentage (PBIAS) (Equation (23)), and the Nash–Sutcliffe Efficiency (NSE) (Equation (24)) [14,48–51].

$$REr\ (\%) = \left|\frac{P_{true}-P_{sim}}{P_{true}}\right| x\ 100 \tag{21}$$

$$RSR = \left[\frac{\sqrt{\sum_{i=1}^{n}(P_{true}-P_{sim})^2}}{\sqrt{\sum_{i=1}^{n}(P_{true}-\overline{P_{sim}})^2}}\right] \tag{22}$$

$$PBIAS = \left[\frac{\sum_{i=1}^{n}(P_{true}-P_{sim})}{\sum_{i=1}^{n}(P_{true})}\right] * 100 \tag{23}$$

$$NSE = 1 - \frac{\sum_{i=1}^{n}(P_{true}-P_{sim})^2}{n\sum_{i=1}^{n}(P_{true}-\overline{P_{sim}})^2} \tag{24}$$

RErr measures the error percentage between the true and simulated values; its optimal value is zero. RSR also evaluates the error, with an optimal value of zero; however, it does so in a standardized manner by dividing the mean square error (RMSE) of the true and simulated values by the standard deviation. PBIAS estimates the bias as a percentage, with an optimal value of zero; negative values indicate overestimation, while positive underestimation. NSE is an indicator of the predictive power of a model (range of values from $-\infty$ to one); it measures how the simulated values resemble true values (dispersion around the 1:1 line). The optimal value of NSE is one (perfect fit). Negative values indicate that it is better to use the average of true values than simulated values. Values of zero (or close to zero) indicate that either the average of true values or the simulated value could be used.

For this study, areal $P_{max\text{-}24h}$ values from the mixed isohyetals were assumed to be the true value, given that these (the isohyetals) were derived from the point $P_{max\text{-}24h}$ data of the distribution functions that performed best according to the AIC test. In Equations (21)–(24), P_{true} represents the true areal $P_{max\text{-}24h}$, P_{sim} corresponds to the areal $P_{max\text{-}24h}$ estimated from both the stationary and non-stationary isohyetals, n the number of watersheds analyzed, and i the watershed analyzed.

2-4. Results and Discussion

2-4.1. Trend detection

The results of the MK and SR tests (Table 2-4) showed that only the $P_{max\text{-}24h}$ time series of Puerto Giraldo rain gauge (gray cell in Table 2-4) had a significant trend at a 5% level of confidence (gray cell in Table 2-4). The Theil Sen Slope value of –0.89 corroborated the results obtained from the MK and SR tests.

Table 2-4. Seasonal trends

Rain gauge	Z_{SR}	Z_{MK}	β_{TS}
Apto Ernesto Cortissoz	1.25 (C)	1.22 (C)	0.15
Casa de Bombas	0.43 (C)	–0.02(C)	0.00
Hda El Rabón	–0.26(C)	–0.99(C)	–0.36
Hibaracho	–0.85(C)	0.75 (C)	0.07
Lena	1.16(C)	–0.25(C)	–0.04
Los Campanos	1.24(C)	1.41 (C)	0.79
Polo Nuevo	–0.31(C)	0.84 (C)	0.18
Ponedera	–0.27(C)	0.49 (C)	0.10
Puerto Giraldo	1.35 (DC)	–2.06 (DC)	–0.89
Repelón	0.96 (C)	1.08 (C)	0.18
Sabanalarga	0.74 (C)	–1.52 (C)	–0.36
San Pedrito Alerta	–2.12 (C)	–0.07 (C)	–0.02
Usiacurí	1.08 (C)	–0.32 (C)	–0.07
Candelaria	–1.51 (C)	0.24 (C)	0.00
Loma Grande	0.14 (C)	–0.17 (C)	–0.13
Las Flores	–0.23 (C)	1.38 (C)	0.78
Montebello	1.54 (C)	1.41 (C)	0.76
San José	–1.28 (C)	–1.36 (C)	–0.88
El Porvenir	0.16 (C)	0.19 (C)	0.13

C = Constant or no significant trend; DC = Significant decreasing trend; IC = Significant increasing trend

Despite the fact that Puerto Giraldo was the only rain gauge with significant trend, there were also other rain gauges with either increasing or decreasing trends. Out of the 19 rain gauges, ten showed increasing trend, five of which had Z_{MK} values greater than one. Likewise, eight rain gauges had decreasing trend, three of them with values below one. The trends of these time series, although currently considered as not significant, should be evaluated in the coming years to determine any increment of the estimated values. With respect to the Theil Sen Slope results, San José and Hda El Rabón had values less than one. These two rain gauges are both located in the southern part of the department, where IDEAM [3] predicted the rainfall decrease. These findings help with: (a) a better understanding of the rainfall regime (both annual and daily maximum) and (b) confirming the hypothesis raised by González-Álvarez et al. [37] as to the existence of $P_{max\text{-}24h}$ trends in within the Colombian Caribbean coast.

2-4.2. Identification and delimitation of homogeneous regions

Table 2-5 presents the results of the dimensionless L-moments τ_2, τ_3 y τ_4 for each of the rain gauges analyzed, which were used for identifying the homogeneous regions.

Table 2-5. Dimensionless L-moments

Rain gauge	Elevation (m)	Latitude	Longitude	τ_2	τ_3	τ_4
Apto Ernesto Cortissoz	14.0	10.918	–74.780	–0.157	–0.066	0.138
Candelaria	20.0	10.455	–74.887	–0.135	–0.153	0.234
Casa de Bombas	10.0	10.408	–75.127	–0.162	–0.134	0.119
El Porvenir	40.0	10.710	–75.162	–0.181	–0.191	0.174
Hda El Rabón	4.0	10.387	–74.963	–0.149	–0.086	–0.005
Hibacharo	80.0	10.722	–75.140	–0.146	–0.193	0.354
La Pintada	200.0	10.955	–74.995	–0.237	–0.462	0.439
Las Flores	2.0	11.040	–74.821	–0.161	–0.172	0.219
Lena	45.0	10.522	–74.891	–0.167	–0.115	0.111
Loma Grande	15.0	10.434	–75.132	–0.194	–0.225	0.293
Los Campanos	100.0	10.558	–74.972	–0.161	–0.276	0.249
Montebello	100.0	10.709	–74.908	–0.140	–0.128	0.216
Polo Nuevo	80.0	10.779	–74.858	–0.133	–0.108	0.144
Ponedera	8.0	10.642	–74.771	–0.167	–0.112	0.116
Puerto Giraldo	5.0	10.508	–74.822	–0.175	–0.228	0.229
Repelón	10.0	10.490	–75.127	–0.170	–0.198	0.226
Sabanalarga	100.0	10.637	–74.919	–0.203	–0.386	0.427
San José	20.0	10.439	–75.108	–0.158	–0.082	0.126
San Pedrito Alerta	8.0	10.278	–74.920	–0.135	–0.072	0.062
Usiacurí	70.0	10.745	–74.981	–0.147	–0.137	0.152

Subsequently and with the purpose of defining the best homogeneous region, the K-means method was performed using clusters with different set-ups of rain gauge groups. Groups of three, four, and five clusters were defined with respect to the homogeneity presented in the variables shown in Table 5. Finally, the best configuration was selected using (a) the Hosking et al. [36] methodology, and (b) a geographical comparison among the homogeneous group distributions.

Figures 2-3a–c depict the rain gauge spatial distribution grouped into three, four, and five clusters, respectively. In Figures 2-3b, c, the green ovals show how a rain gauge belonging to another group (yellow diamond) is within a different cluster (blue circles). This indicates that grouping rain gauges into either a four- or five-rain-gauge cluster introduces geographically inconsistent distributions. In fact, Hosking et al. [37] affirmed that these types of plots (those that relate τ_2, τ_3, and τ_4) can sometimes contain overlapping groups, which makes it difficult to select the number of clusters that adequately represent rain gauges with similar characteristics. The three-rain-gauge cluster group (Figure 2-3a) did not show that problem. Also, the adequacy of the three-rain-gauge cluster was further verified by analyzing the behavior of the geographic location variables (latitude and longitude) with respect to the coefficient asymmetry (τ_3). Figure 2-4 evidences three well-defined clusters, which represent those rain gauges with similar characteristics.

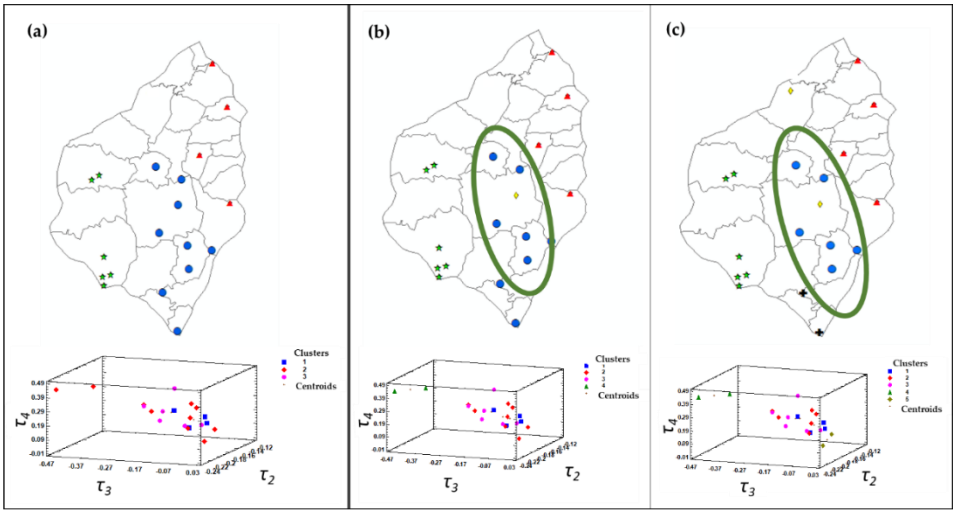

Figure 2-3. Geographical distribution of clusters and scatter plots of τ2, τ3 vs τ4

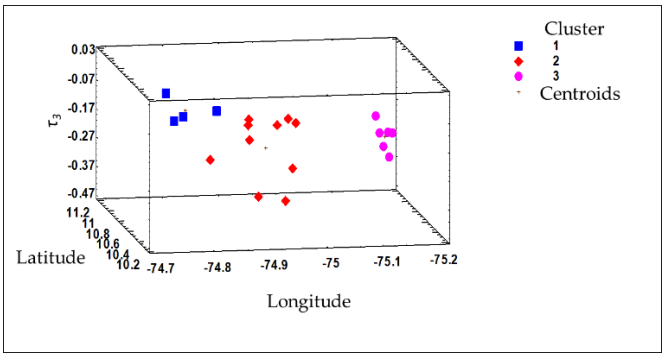

Figure 2-4. Latitude and longitude vs asymmetry coefficient

Once the clusters were defined, three homogeneous regions were delineated through the IDW interpolation method (via ArcGIS) (Figure 2-5), namely East (Cluster 1), Central (Cluster 2), and West (Cluster 3). Table 2-6 summarizes the rain gauges that make up each of the regions.

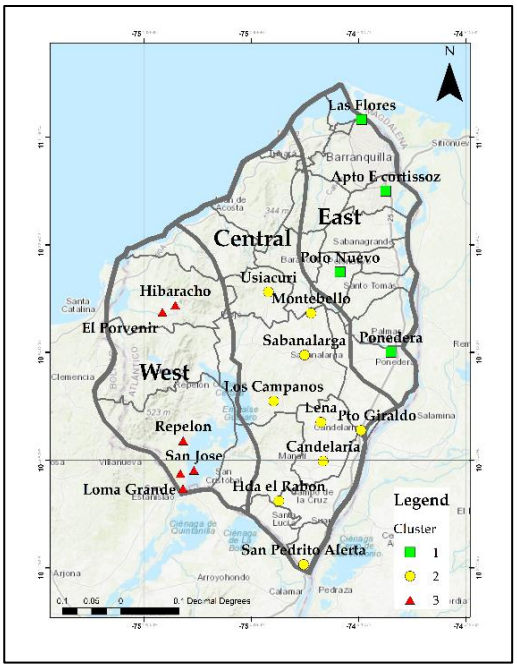

Figure 2-5. Delimited homogeneous zones

Table 2-6. Homogeneous regions and corresponding rain gauges

Region	Rain gauge
East	Apto Ernesto Cortissoz, Las Flores, Polo Nuevo y Ponedera.
Central	Candelaria, Hda El Rabón, Lena, Los Campanos, Montebello, Puerto Giraldo, Sabanalarga, San Pedrito Alerta y Usiacurí.
West	Casa de Bombas, El Porvenir, Hibaracho, Loma Grande, Repelón y San José.

2-4.3. Rain frequency analysis

2-4.3.1 Stationary frequency analysis

Table 2-7 and Figure 2-6 show the rain gauges (in each of the regions) where CDFs Gumbel and GEV better represented the time series. Overall, the Gumbel distribution was the best fit in 63.2% of the 19 rain gauges analyzed, while GEV was the best fit in only 36.8%. These results represent a shift from the findings by González-Álvarez et al. [45], where GEV was best in 53.8% of the 13 rain gauges assessed. This is due to the fact that the Gumbel distribution was the best CDF among the new additional six rain gauges analyzed in this study. Based on the findings and despite the fact that the Gumbel distribution was best in the majority of the cases, there was not a unique CDF that better represented all the time series within a particular region. $P_{max\text{-}24h}$ values under stationary conditions for each of the 19 rain gauges are presented in Table A1 (Appendix A).

Table 2-7. cumulative distribution function (CDF) per homogeneous zone. GEV—generalized extreme value.

Homogeneus region	Best-fit CDF		Total
	GEV	Gumbel	
East	2	2	**4**
Central	3	6	**9**
West	2	4	**6**
Total	**7**	**12**	**19**

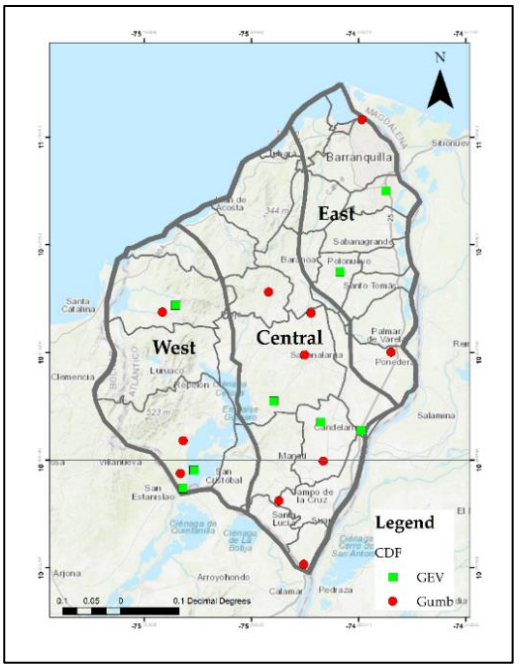

Figure 2-6. Geographical distribution of best cumulative distribution function (CDF) for stationary conditions

2-4.3.2 Non-stationary frequency analysis

$P_{max\text{-}24h}$ estimates under non-stationary conditions (by means of the GEVmu distribution) for the 19 rain gauges are compiled in Table A1 (Appendix A). Differences of up to 58.9 mm were observed at the El Porvenir rain gauge between the $P_{max\text{-}24h}$ values under stationary and non-stationary conditions for a 100-year return period.

2-4.3.3 Selecting the best $P_{max\text{-}24h}$ value

After the estimation of the $P_{max\text{-}24h}$ under both stationary and non-stationary conditions, it was necessary to determine—via AIC test—which of the two conditions better represented the time series (Table 8). The values obtained in this section were later used for the generation of isohyetal maps called mixed (derived from the best rainfall value of the two conditions) explained in the next section. Table 8 shows the best condition (stationary or non-stationary) and CDF, as well as the AIC test values obtained. Figure 2-7 depicts the time series of rain gauges at Casa de Bombas, Hda El Rabón, Puerto Giraldo, and Los Campanos. For the first two rain gauges, a stationary condition frequency analysis is best, according to the AIC test, while the last two suit a non-stationary one.

Table 2-8. Best scenario for each rain gauge

Rain gauge	Best condition	Best CDF	AIC value
Apto Ernesto Cortissoz	NSC	GEVmu	650.7842
Candelaria	SC	Gumbel	249.7441
Casa de Bombas	SC	GEV	257.7023
El Porvenir	SC	Gumbel	258.1377
Hda El Rabón	SC	Gumbel	312.5542
Hibacharo	SC	GEV	400.6611
Las Flores	SC	Gumbel	435.5705

Rain gauge	Best condition	Best CDF	AIC value
Lena	SC	GEV	435.8551
Loma Grande	SC	Gumbel	256.2291
Los Campanos	NSC	GEVmu	291.8771
Montebello	SC	Gumbel	231.1521
Polonuevo	SC	GEV	442.7164
Ponedera	SC	Gumbel	433.9843
Puerto Giraldo	NSC	GEVmu	311.2199
Repelón	SC	Gumbel	432.4012
Sabanalarga	NSC	GEVmu	470.3504
San José	SC	Gumbel	217.7901
San Pedrito Alerta	SC	Gumbel	298.327
Usiacurí	SC	Gumbel	435.5705

SC = stationary conditions; NSC = non-stationary conditions

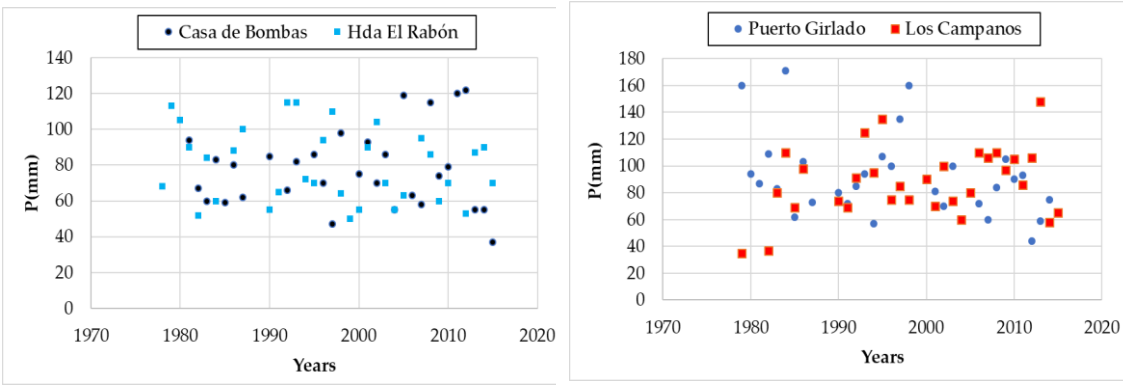

(**a**) (**b**)

Figure 2-7. Rainfall time series: (a) stationary conditions and (b) non-stationary conditions

2-4.4. Isohyetal maps

With the $P_{max\text{-}24h}$ values of the 19 rain gauges obtained in Sections 4.3.1–4.3.3, maps of stationary (Figure 2-8), non-stationary (Figure 2-9), and mixed (the best value of the two conditions according to the AIC test, Figure 2-10) isohyetals were drawn for return periods of five, 10, 25, 50, and 100 years.

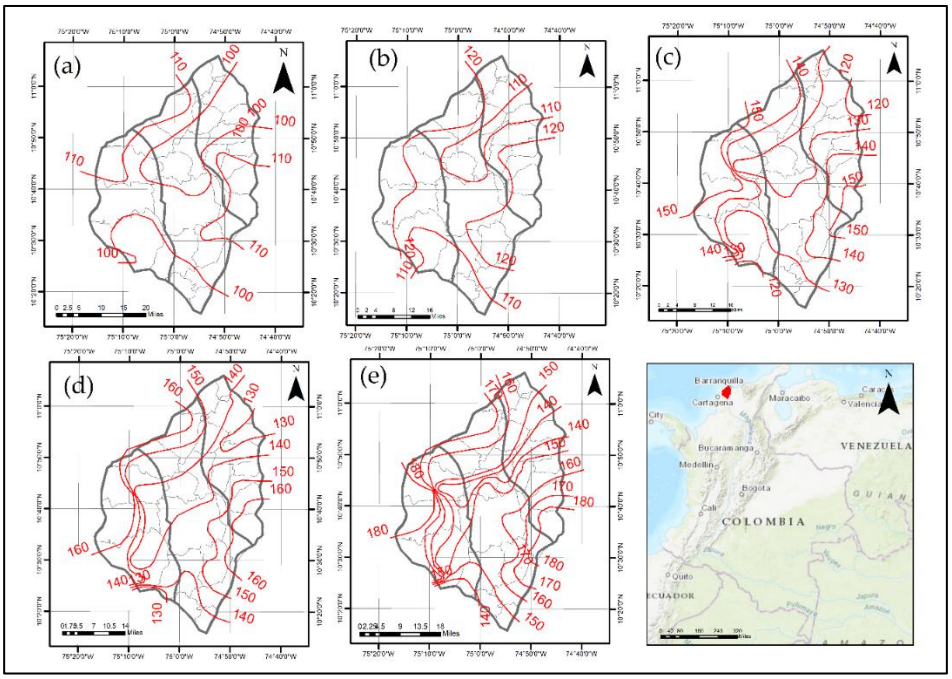

Figure 2-8. SC isohyetal maps (a) 5 years, (b) 10 years, (c) 25 years, (d) 50 years, and (e) 100 years

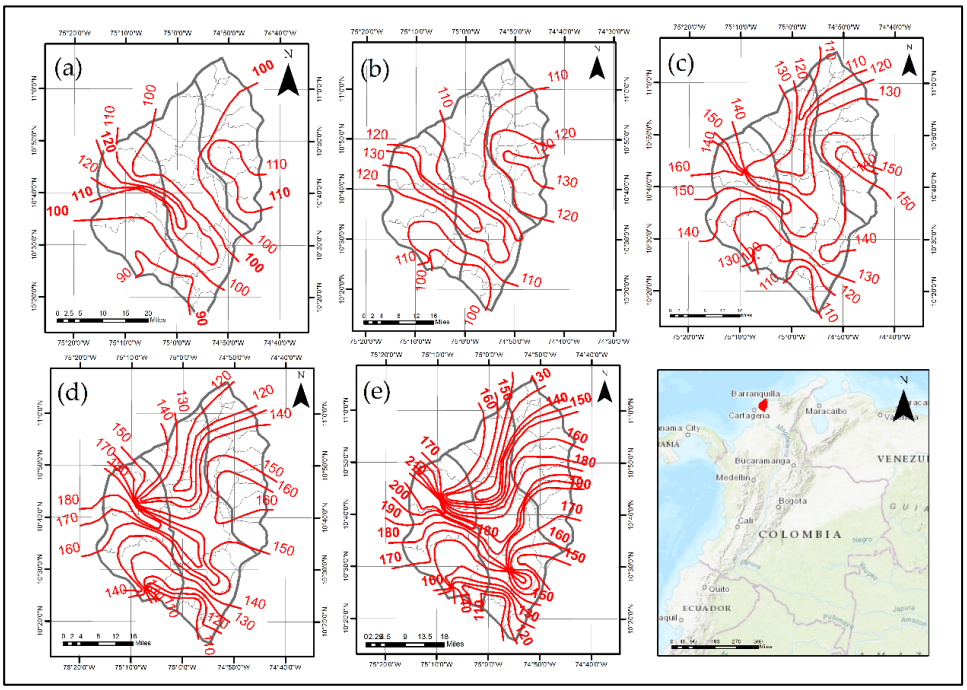

Figure 2-9. NSC isohyetal maps (a) 5 years, (b) 10 years, (c) 25 years, (d) 50 years, and (e) 100 years

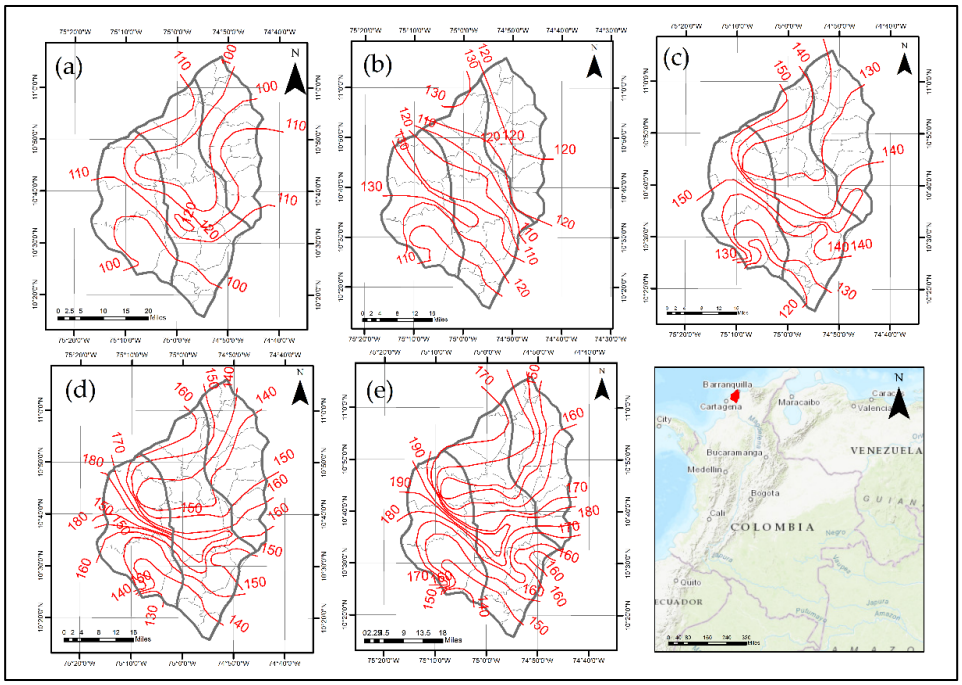

Figure 2-10. Mixed isohyetal maps. (a) 5 years, (b) 10 Years, (c) 25 years, (d) 50 years, and (e) 100 years

Figure 2-8 shows that isohyetal values ranged from 100–110 mm for five years, from 110–120 mm for 10 years, from 120–150 mm for 25 years, from 130–160 mm for 50 years, and from 140–180 mm for 100 years.

Figure 2-9 shows values of 90–120 mm for a return period of five years, 100–130 mm for 10 years, 110–160 mm for 25 years, 110–180 mm for 50 years, and 110–210 mm for 100 years.

Finally, in Figure 2-10, it can be observed that the isohyetals ranged from 100–120 mm for five years, from 110–130 mm for 10 years, from 120–150 mm for 25 years, from 130–180 mm for 50 years, and from 140–190 mm for 100 years. The highest values were observed in the south zone and the lowest values were observed in the north

4.5. Isohyetal maps assessment

In order to assess how the use of stationary and/or non-stationary isohyetals maps could affect the calculation of the areal rainfall in a given watershed (W), nine watersheds were selected, three at each of the three homogeneous regions (light green areas in Figure 2-11). W1, W2, and W3 are located in the north, central, and southern areas of the west homogeneous region, respectively. W4, W5, and W6 are within the central region, located in the northern, central and southern areas, respectively. Finally, W7 (north), W8 (center) and W9 (south) are located within the east region. Table 2-9 summarizes the watersheds area, the nearest rain gauge, and its distance to each of the watersheds.

Table 2-9. Information about watershed used

Watershed ID	Area (ha)	Nearest rain gauge	Distance to rain gauge (km)
1	2552.9	Hibacharo	0.0
2	4788.3	El Porvenir	11.3
3	2153.6	Repelón	0.0
4	4677.7	Usiacurí	12.4

Watershed ID	Area (ha)	Nearest rain gauge	Distance to rain gauge (km)
5	4697.6	Los Campanos	6.3
6	4596.0	Hda. El Rabón	0.0
7	1528.5	Apto Ernesto Cortissoz	5.5
8	1955.8	Polo Nuevo	9.5
9	1260.0	Ponedera	4.9

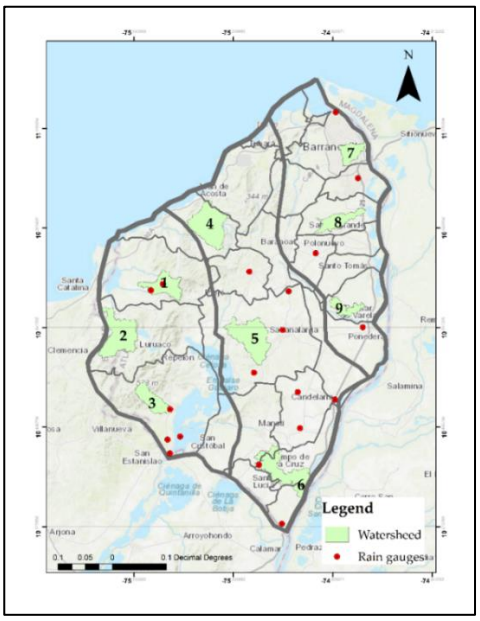

Figure 2-11. Delimited homogeneous regions

The P_{areal} values for all watersheds (return periods of five, 10, 25, 50, and 100 years) for stationary and non-stationary conditions, as well as mixed ones, are shown in Table 2-10. Likewise, stationary and non-stationary P_{areal} values were compared, through their differences (mixed minus the SC and NSC values), with P_{areal} values of mixed isohyetal maps (Table 2-10).

Table 2-10. Areal $P_{max\text{-}24h}$ values for different isohyetals maps

Type of Isohyetals	Region	Watershed	Areal $P_{24h\text{-}max}$ (mm)					Mixed – SC and NSC (mm)				
			Tr (years)					Tr (years)				
			5	10	25	50	100	5	10	25	50	100
Mixed	West	W1	104.7	118.0	136.2	142.8	158.6					
		W2	105.0	126.7	145.2	168.9	173.7					
		W3	95.0	107.6	127.3	141.2	153.1					
	Central	W4	104.7	112.9	134.9	147.4	162.6					
		W5	108.0	118.6	139.4	158.1	179.2					
		W6	96.0	112.7	129.3	142.0	153.3					
	East	W7	100.3	115.0	132.5	143.6	155.0					
		W8	109.2	115.4	135.0	145.0	154.3					
		W9	107.1	120.0	142.6	158.3	172.1					
Stationary	West	W1	105.8	121.3	131.3	141.6	150.9	–1.1	–3.3	4.9	1.2	7.7
		W2	105.0	124.2	147.7	160.0	180.0	0.0	2.5	–2.5	8.9	–6.3
		W3	105.0	113.0	127.1	143.4	159.4	–10.0	–5.4	0.2	-2.2	–6.3

	Central	W4	104.3	120.4	138.4	146.2	157.5	0.4	–7.5	–3.5	1.2	5.1
		W5	100.0	115.0	128.1	144.3	155.0	8.0	3.6	11.3	13.8	24.2
		W6	101.1	113.6	128.8	141.8	154.0	–5.1	–0.9	0.5	0.2	–0.7
	East	W7	100.0	119.7	124.7	135.0	144.4	0.3	–4.7	7.8	8.6	10.6
		W8	104.8	120.0	128.2	136.0	143.1	4.4	–4.6	6.8	9.0	11.2
		W9	109.4	123.8	145.0	157.1	171.7	–2.3	–3.8	–2.4	1.2	0.4
Non-stationary	West	W1	105.8	118.7	133.7	148.2	160.8	–1.1	–0.7	2.5	–5.4	–2.2
		W2	106.1	116.5	145.5	161.2	187.0	–1.1	10.2	–0.3	7.7	–13.3
		W3	95.0	105.0	125.8	139.9	158.1	0.0	2.6	1.5	1.3	–5.0
	Central	W4	100.0	115.0	134.1	136.3	158.3	4.7	–2.1	0.8	11.1	4.3
		W5	111.7	119.5	141.3	161.7	185.2	–3.7	–0.9	–1.9	–3.6	–6.0
		W6	94.8	101.6	115.4	120.1	126.8	1.2	11.1	13.9	21.9	26.5
	East	W7	105.0	115.0	125.3	136.6	152.8	–4.7	0.0	7.2	7.0	2.2
		W8	107.3	122.4	138.3	152.5	173.8	1.9	–7.0	–3.3	–7.5	–19.5
		W9	109.6	125.0	145.0	160.4	175.0	–2.5	–5.0	–2.4	–2.1	–2.9

Note: The values of the difference between the mixed and SC and NSC in red and black indicate, respectively, overestimation and underestimation. Gray cells indicate a difference less than or equal to 5.0 mm.

P_{areal} values of the mixed isohyetals for the five-year return period were in a range of 95.0 mm (W3) to 109.2 mm (W8). For the 10-year return period, the value range was between 107.6 mm (W3) and 126.7 mm (W2). For the 25-year return period, values ranged from 127.3 mm (W3) to 145.5 mm (W2). For the return period of 50 years, the range was between 141.2 mm (W3) and 168.9 mm (W2). For the 100-year return period, values ranged from 153.1 mm (W3) to 179.2 mm (W5).

P_{areal} values of the stationary isohyetals for the five-year return period were in a range of 100.0 mm (W5) to 109.4 mm (W9). For the 10-year return period, the minimum and maximum values were between 113.0 mm (W3) and 124.2 mm (W2). For the 25-year return period, values ranged from 124.7 mm (W7) to 147.7 mm (W2). For the 50-year return period, the value range was between 135.0 mm (W7) and 160.0 mm (W2). For the 100-year return period, values ranged from 143.1 mm (W8) to 180.0 mm (W2).

P_{areal} values of the non-stationary isohyetals for the five-year return period were in a range of 94.8 mm (W6) to 117.7 mm (W5). For the 10-year return period, the value range was given between 101.6 mm (W6) and 125.0 mm (W9). For the 25-year return period, values ranged from 115.4 mm (W6) to 145.5 mm (W2). For the 50-year return period, values ranged from 120.1 mm (W6) to 161.7 mm (W5). For the 100-year return period, the values were between 126.8 mm (W6) and 187.0 mm (W2).

The frequency analysis under stationary conditions is most commonly used by hydrologists to estimate the design rainfall for hydraulic structures for stormwater management. Nonetheless, the differences observed in Table 2-10 show that the stationary frequency analysis underestimated the values of areal $P_{max\text{-}24h}$ for the study area. This behavior occurred in 60% of the cases evaluated (27 out of 45) throughout the department of Atlántico. This implies that, if a designer decides to use a stationary design rainfall, the subsequent estimation of the design flow for a given hydraulic structure could end up as an underestimated value. It can also be observed that these underestimations reach their most critical values within the central region, where the highest areal $P_{max\text{-}24h}$ differences range from 11.3 to 24.2 mm (both in W5) for return periods of 25, 50, and 100 years (which are the most used in the design of drainage hydraulic structures). The west region exhibited only two cases where the difference in P_{areal} had values greater than 5 mm

(7.7 mm in W1 and 8.9 mm in W2). In the eastern region, underestimations occurred in 60% of cases (six cases out of 10) with values ranging from 6.8 to 11.2 mm (W7 and W8). Like the central region, these values came from return periods of 25, 50, and 100 years. These results also show that, for stationary conditions, the probability of underestimating the values of P_{areal} is higher in these three return periods, with values of 66%, 88%, and 66%, respectively. Rainfall differences with values less than 5 mm occurred in 57.8% of the cases (26 cases distributed as follows: nine for the west region, nine for the east region, and eight for the central region, where two values of 5.1 mm were given that could be considered within the rank).

For the non-stationary scenario, the tendency to underestimate P_{areal} occurred in 46.7% of the cases (21 out of 45): seven cases for the west region, nine for the central region, and five for the east region. It was also noted that, for this scenario, more P_{areal} values with differences less than or equal to 5 mm are estimated, which was observed in 66.7% of the cases (11 for the west region, nine for the central region, and 10 for the eastern region). On the other hand, when each of the regions was analyzed individually, the western region showed a slight tendency to overestimate the P_{areal} values (eight out of 15, negative values in red in Table 2-10). This behavior was more noticeable for the 100-year return period, where the three watersheds evaluated presented values ranging from 2.2 mm (W2) to 13.3 mm (W3). In the central region, underestimated values of P_{areal} (60% of the cases or nine out of 15) were observed, particularly in the southern part of this region (W6), with values ranging from 11.1 to 26.5 mm for return periods 10, 25, 50, and 100 years. For the eastern region, there was also a tendency to overestimate the P_{areal} (66.7% of the cases, 10 of 15), with values ranging from 2.1 mm (W9) to 19.5 mm (W8).
Regarding the real values of P_{areal} (mixed isohyetals), the southern area of the department of Atlántico exhibited the lowest values, specifically in W3 (located in the south of the west region) and W6 (located in the south of the eastern region). This is clearly evident, for example, when comparing the P_{areal} values for the 100-year return period between W6 and W7 (located northeast). W6, despite having an area three times larger than W7, has a lower P_{areal} value (153.3 mm versus the 155.0 mm for W7). These results coincide with the findings of IDEAM [3], who determined that municipalities located in the southeast of the department will likely be the most affected by rainfall decrease.

The isohyetal map (stationary and non-stationary) performance assessment within each of the watersheds was carried out through the relative error percentage (REr). Additionally, the performance of each of the regions was assessed by RSR, PBIAS, and NSE. The results of this statistical analysis are presented in Table 2-11.

Table 2-11. Statistical analysis of isohyetal maps performance

Type of Isohyetal	Watershed	Region	Relative Error, REr (%)				
			Tr (years)				
			5	10	25	50	100
Stationary	W1	West	1.04	2.68	3.72	0.81	5.12
	W2		0.00	2.04	1.71	5.58	3.51
	W3		9.52	4.77	0.13	1.51	3.95
	W4	Central	0.35	6.17	2.58	0.82	3.28
	W5		8.04	3.13	8.84	9.59	15.64
	W6		5.03	0.77	0.46	0.17	0.44
	W7	East	0.33	3.96	6.26	6.36	7.31
	W8		4.15	3.82	5.30	6.60	7.86
	W9		2.06	3.05	1.66	0.75	0.23

Type of Isohyetal	Watershed	Region	Relative Error, REr (%)				
			Tr (years)				
			5	10	25	50	100
Non-stationary	W1	West	1.03	0.60	1.84	3.62	1.36
	W2		1.03	8.75	0.23	4.80	7.11
	W3		0.00	2.46	1.18	0.93	3.13
	W4	Central	4.66	1.81	0.53	8.12	2.71
	W5		3.27	0.75	1.34	2.21	3.23
	W6		1.29	10.93	12.10	18.28	20.85
	W7	East	4.45	0.00	5.73	5.09	1.47
	W8		1.71	5.69	2.35	4.90	11.20
	W9		2.24	4.00	1.66	1.34	1.67
RSR							
Stationary		West	1.25	0.50	0.43	0.42	0.78
Non-stationary			0.19	0.78	0.23	0.43	0.95
Stationary		Central	1.09	1.75	1.67	1.20	1.33
Non-stationary			0.69	2.39	1.98	2.15	1.48
Stationary		East	0.75	1.94	1.43	1.09	1.09
Non-stationary			0.85	2.19	1.11	0.91	1.39
PBIAS (%)							
Stationary		West	–3.64	–1.73	0.61	1.75	–1.01
Non-stationary			–0.72	3.42	0.88	0.81	–4.21
Stationary		Central	1.07	–1.37	2.07	3.41	5.80
Non-stationary			0.72	2.36	3.16	6.58	5.00
Stationary		East	0.77	–3.74	2.97	4.19	4.61
Non-stationary			–1.67	–3.42	0.37	–0.60	–4.19
NSE							
Stationary		West	–0.56	0.75	0.81	0.82	0.39
Non-stationary			0.96	0.39	0.95	0.81	0.09
Stationary		Central	–0.18	–2.07	–1.78	–0.44	–0.78
Non-stationary			0.52	–4.72	–2.91	–3.61	–1.18
Stationary		East	0.44	–2.75	–1.04	–0.19	–0.18
Non-stationary			0.27	–3.78	–0.23	0.17	–0.94

Note: Gray cells indicate values of relative error greater than or equal to 5%; green cells indicate best value of RSR and PBIAS for the two conditions; and light blue cells represent values of NSE above 0.5.

For the stationary isohyetal maps, REr values ranged from 0.00% (W2) to 9.52% (W3) for the five-year return period, 0.77% (W6) to 6.17% (W4) for the 10-yearperiod, 0.13% (W3) to 8.84% (W5) for the 25-year period, 0.17% (W6) to 9.59% (W5) for the 50-year period, and 0.23% (W9) to 15.64% (W5) for the 100-year period. The highest REr values were observed in two of the return periods (50 and 100 years) most commonly used in the design of hydraulic structures for runoff management (50 and 100 years). No relationship was observed between the watershed area and REr.

For non-stationary isohyetal maps, REr values ranged from 0.00% (W3) to 4.66% (W4) for the five-year return period, 0.00% (W7) to 10.93% (W6) for the 10-year period, 0.23% (W2) to 12.10% (W6) for the 25-year period, 0.93% (W3) to 18.28% (W6) for the 50-year period, and 1.36% (W1) to

20.85% (W6) for the 100-year period. The highest REr values were observed in return periods of 50 and 100 years.

In general, for stationary conditions, there were 14 cases where REr was greater than or equal to 5.00% (gray cells). The maximum value was 15.64%, with only one case where REr was greater than or equal to 10%. For the non-stationary conditions, 10 cases were observed where the REr was greater than or equal to 5.00%. The maximum value was 20.85%, with five cases where REr was greater than or equal to 10%. Furthermore, when the stationary and non-stationary conditions were compared one-to-one, it was observed that, in 57.8% of the cases (26 out of 45), the REr values for the non-stationary conditions were lower than their stationary counterparts. These results suggest that (a) the error might be more frequent when using the stationary condition isohyetal maps, and (b) additional attention should be paid during the design of hydraulic structures under stationary frequency analysis, especially as it was also found that this scenario tends to underestimate the P_{areal} (Table 2-10).

With respect to the overall performance of all regions, the stationary conditions resulted in lower values of RSR (10 in total) than those for the non-stationary conditions (five in total). At first glance, this may indicate less error under stationary conditions (which contradicts the results previously obtained when the REr was analyzed for each watershed). Nonetheless, a closer look at Table 2-10 revealed that, despite the fact that each condition had five REr values greater than or equal to 5.00%, the non-stationary condition had REr values of up to 20.85%, which contributed to having an overall larger RSR value. Such large REr values were due to the fact that W6 happened to have a rain gauge (Hda El Rabón) with a time series better suited to a stationary frequency analysis (Table 2-8). As for the individual performance of each region, the west region showed 90% (nine out of 10) of the RSR values below one, followed by the east region with three values. The central region had more stationary condition values (in four out of the five return periods) that outperformed the non-stationary ones.

Regarding the P_{areal} tendency to under- or overestimate, PBIAS values indicate that isohyetal maps under stationary conditions tend to underestimate (black positive values in Table 2-11) in the majority of the cases (66.7% or 10 out of 15), which is more evident in the central region. These results corroborate what was previously found in Table 2-10. The underestimated results also observed in the central region for the non-stationary conditions (which are opposite to the results of both Table 2-10 and REr in Table 2-11) were mainly caused by the large P_{areal} differences found in W6. The non-stationary isohyetal maps tend to underestimate (60% in all regions, or nine out of 15). In the central region, the underestimation occurred in all return periods for both stationary and non-stationary conditions, especially for 50- and 100-year periods, which are two of the return periods most used in the design of hydraulic structures. In the east region, a tendency to overestimate (red values in Table 2-11) was detected for non-stationary conditions in four out of five return periods. A different behavior was observed for the stationary conditions within the same region (east) where underestimation prevailed. Overall, the west region showed less bias when compared with the other two regions, with values ranging from 0.61% (underestimation for the 25-year return period for stationary conditions) to −4.21% (overestimation for the five-year return period for non-stationary conditions). Central and east regions showed values oscillating from 0.72% (underestimation for the five-year return period for non-stationary conditions) to 5.80% (underestimation for the 100-year return period for stationary conditions).

With regard to the prediction power of the isohyetal maps under stationary and non-stationary conditions, better NSE results were obtained within the west region in the majority of cases. Both conditions (stationary and non-stationary) had three return periods with NSE values above 0.5 (blue cells in Table 2-11). Among the return periods most used for the design of hydraulic

structures for stormwater management (25, 50, and 100 years), 25- and 50-year periods showed values close to one (indicator of a good performance), with values above 0.70 for both conditions. For the 100-year period, a value of 0.39 was observed for stationary conditions, denoting good performance as well. However, for non-stationary conditions, a value of 0.09 denotes both that the simulated value is far from the 1:1 line and that the average value of either the simulated or true value better represents the areal rainfall value. For the central and east regions, negative values prevailed in most of the cases for either stationary or non-stationary conditions (only one value was above 0.5). Within the central region for stationary conditions, all return periods had negative values, while, for the non-stationary conditions, this behavior was seen in 80% of the cases. In the east region, four out of five return periods showed negative values for stationary conditions, and three out of five return periods showed negative values for non-stationary conditions. These results indicate that the average of the true value (mixed isohyetal maps) is a better predictor for these two regions.

In general, lower values of REr, RSR, and PBIAS were observed within the west region, especially for stationary conditions, which suggests that a stationary frequency analysis might be used in watersheds within this region. This was also confirmed by the NSE results obtained in four out of five of the return periods. For the central and east regions, the use of a stationary frequency analysis (typically and widely used in hydrology), according to the results obtained, might introduce errors in the calculation of P_{areal}, which could affect, for instance, the magnitude of the estimated runoff for water balances (for agriculture, livestock, and energy water demand, among other uses), hydraulic structures for stormwater management, flash flood guidance, and flood risk assessment.

2-5. Conclusions

With respect to the $P_{max\text{-}24h}$ behavior, three regions were determined, namely east, central, and west. The regionalization will be of great help for the $P_{max\text{-}24h}$ analysis in ungauged areas given the fact the department of Atlántico is, among the remaining six departments of the Colombian Caribbean region, the one with the lowest rain gauges density (only nineteen with statistically representative time series).

Increasing and decreasing trends were identified among the nineteen $P_{max\text{-}24h}$ time series analyzed within the department of Atlántico. Furthermore, only one rain gauge showed a significant decreasing trend with values of Z_{SR}, Z_{MK}, and β_{TS} of 1.36, –2.06, and –0.89, respectively. However, other rain gauges also showed increasing and decreasing trends, which, despite the fact of not being significant, five of them showed Z_{MK} greater than one and three had values less than negative one. This suggests the need for future trend analysis in the coming five-year periods to determine any further trends' increase/decrease. Overall, the southern area of the central and west regions showed the most noticeable decreasing trend. This results are in agreement with IDEAM [3] findings.

As to which frequency analysis –stationary or non-stationary– better represented the nineteen time series analyzed, the AIC revealed that 79% of them suited a stationary one. In terms of the performance of the isohyetal maps under stationary and non-stationary conditions when compared with the mixed (stationary along with non-stationary), the REr values indicate that while the error under stationary conditions can be observed more frequently, under non-stationary conditions could be more significant in terms of magnitude, especially in the southern central region. This was also confirmed by the RSR and PBIAS results, where the non-stationary condition, despite having less cases with REr greater than 10% among the nine watersheds evaluated, results showed how the magnitude of the error impact the overall results within a

given region. In sum, the west region had less cases (watersheds) with REr values above 10% under both stationary and non-stationary conditions. Likewise, RSR, PBIAS, and NSE also indicated that either a stationary or a non-stationary frequency analysis might be performed in the estimation of the areal $P_{max\text{-}24h}$., which represents a contribution to the hydrological analysis given that, according to the results of this study, a stationary frequency analysis (the most commonly used) might be safely performed within the west region. On the other hand, the other two regions presented a tendency for underestimation, especially under stationary conditions, which indicates, for example, that hydraulic structures for stormwater management shall be designed with precaution.

The findings of this study shed some light on the need of both a better understanding of the regional hydrological behavior and the impact of climate change on future water related projects.

Appendix A. $P_{max\text{-}24h}$ values under stationary and non-stationary conditions at each rain gauge

The Table A1 show the $P_{max\text{-}24h}$ values under stationary and non-stationary conditions (by means of the GEVmu distribution) for each of the 19 rain gauges analyzed in this study. Additionally, this table indicate the best value of the two conditions according to the AIC test results (grey cells).

Table A1. $P_{max\text{-}24h}$ values under stationary and non-stationary conditions at each rain gauge

Homogeneous Region	Rain gauge	Condition	Best CDF	$P_{max\text{-}24h}$ (mm)				
				Tr (years)				
				5	10	25	50	100
East	Apto Ernesto Cortissoz	SC	GEV	97.30	108.30	120.30	127.80	134.60
		NSC	GEVmu	111.74	125.88	144.37	160.29	181.33
	Las Flores	SC	Gumbel	106.30	122.10	142.10	156.90	171.60
		NSC	GEVmu	115.94	134.82	161.33	184.70	214.07
	Polo Nuevo	SC	GEV	110.20	121.80	135.20	144.20	152.40
		NSC	GEVmu	91.60	104.40	120.50	131.90	144.90
	Ponedera	SC	Gumbel	112.70	129.90	151.50	167.60	183.60
		NSC	GEVmu	91.97	105.60	123.23	137.13	152.39
Central	Candelaria	SC	Gumbel	100.20	112.60	128.30	139.90	151.40
		NSC	GEVmu	103.64	116.44	135.03	153.65	183.41
	Hda El Rabón	SC	Gumbel	95.34	108.30	124.70	136.90	148.90
		NSC	GEVmu	86.68	93.01	99.88	106.38	123.09
	Lena	SC	GEV	112.20	125.30	139.50	148.60	156.70
		NSC	GEVmu	117.60	131.40	150.20	166.70	188.00
	Los Campanos	SC	GEV	107.50	120.10	135.60	146.90	147.10
		NSC	GEVmu	109.00	129.20	144.40	147.20	150.30
	Montebello	SC	Gumbel	97.00	109.80	126.10	138.10	150.10
		NSC	GEVmu	99.87	116.29	136.65	151.02	164.22
	Puerto Giraldo	SC	GEV	110.60	128.10	151.10	168.90	187.10
		NSC	GEVmu	93.22	110.75	134.56	154.86	187.41
	Sabanalarga	SC	Gumbel	101.80	116.40	134.80	148.40	161.90
		NSC	GEVmu	88.74	94.35	102.10	107.50	111.90
	San Pedrito Alerta	SC	Gumbel	94.30	106.70	122.50	134.10	145.70
		NSC	GEVmu	93.48	101.75	110.32	115.58	120.09
	Usiacurí	SC	Gumbel	95.20	108.40	125.10	137.40	149.70
		NSC	GEVmu	92.98	103.79	115.81	122.10	126.23
West	Casa de Bombas	SC	GEV	94.00	105.60	119.00	128.20	136.60
		NSC	GEVmu	110.50	123.10	135.80	141.80	146.30
	El Porvenir	SC	Gumbel	112.40	130.00	152.40	168.90	185.40
		NSC	GEVmu	96.17	102.88	108.29	112.77	126.51
	Hibaracho	SC	GEV	101.30	111.90	124.00	132.00	139.20
		NSC	GEVmu	101.90	112.60	125.00	133.80	142.50
	Loma Grande	SC	Gumbel	101.30	118.40	140.00	156.10	172.00
		NSC	GEVmu	113.30	127.60	144.50	156.40	168.20

Homogeneous Region	Rain gauge	Condition	Best CDF	$P_{max-24h}$ (mm)				
				Tr (years)				
				5	10	25	50	100
	Repelón	SC	Gumb	90.30	104.00	121.50	134.40	147.20
		NSC	GEVmu	120.40	134.90	155.10	176.20	195.90
	San José	SC	Gumb	106.30	124.30	147.10	164.00	180.00
		NSC	GEVmu	104.40	116.40	131.40	143.60	158.60

For stationary conditions (SC), the values shown represent the ones from the CDF having the best fit. Gray cells indicate the best value of the two conditions according to the AIC test results shown in Table 2-8.

2-6. References

1. Obeysekera, J.; Salas, J.D. Frequency of Recurrent Extremes under Nonstationarity. *J. Hydrol. Eng.* **2016**, *21*, 04016005.
2. Wi, S.; Valdés, J.B.; Steinschneider, S.; Kim, T.-W. Non-stationary frequency analysis of extreme precipitation in South Korea using peaks-over-threshold and annual maxima. *Stoch. Environ. Res. Risk Assess.* **2016**, *30*, 583–606.
3. IDEAM; PNUD; MADS; DNP; CANCILLERÍA. *New Scenarios of Climate Change for Colombia 2011–2100 Scientific Tools for Deparment-based Decision Making—National Emphasis: 3rd National Bulletin on Climate Change*; IDEAM: Bogota, Colombia, 2015.
4. IDEAM; UNAL. *La Variabilidad Climática y el Cambio Climático en Colombia*; Universidad Nacional de Colombia: Bogotá, Colombia, 2018; ISBN 978-958-8067-97-1.
5. IDEAM. *Tercera Comunicación Nacional de Colombia a la Convención Marco de las Naciones Unidas Sobre el Cambio Climático*; IDEAM: Bogotá, Colombia, 2017; ISBN 978-958-8971-73-5.
6. IDEAM; PNUD; Alcaldía de Bogotá; Gobernación de Cundinamarca; CAR; Corpoguavio; Instituto Alexander von Humboldt, Parques; Nacionales Naturales de Colombia; MADS; DNP. *Estrategia Regional de Mitigación y Adaptación al Cambio Climático para Bogotá y Cundinamarca. Plan Regional Integral de Cambio Climático para Bogotá Cundinamarca (PRICC)*; IDEAM: Bogota, Colombia, 2014; ISBN 978-958-8758-99-2.
7. IDEAM; PNUD; MADS; DNP; CANCILLERÍA. Acciones de adaptación al cambio climático en Colombia. In *Tercera Comunicación Nacional de Cambio Climático*; IDEAM: Bogotá, Colombia, 2017; ISBN In process.
8. Murcia, J.F.R. *Cambio Climático en Temperatura, Precipitación y Humedad Relativa para Colombia Usando Modelos Metereologicos de alta Resolución (Panorama 2011-2010)*; IDEAM: Bogotá, Colombia, 2010.
9. Ramírez-Cerpa, E.; Acosta-Coll, M.; Vélez-Zapata, J. Analysis of the climatic conditions for short-term precipitation in urban areas: A case study Barranquilla, Colombia. *Idesia (Arica)* **2017**, *35*, 87–94.
10. Ávila, H. Perspective of the Stromwater Management Facing Climate Change-Case Study: Barranquilla City, Colombia. *Rev. Ing.* **2012**, *36*, 54–59.
11. Ávila, B.; Ávila, H. Spatial and temporal estimation of the erosivity factor R based on daily rainfall data for the department of Atlántico, Colombia. *Ing. Investig.* **2015**, *35*, 23–29.
12. Avila, L.; Ávila, H.; Sisa, A. A Reactive Early Warning Model for Urban Flash Flood Management. In Proceedings of the World Environmental and Water Resources Congress 2017, Sacramento, CA, USA, 21–25 May 2017; pp. 372–382.
13. Coll, M.A.A. Sistemas de Alerta Temprana (SAT) para la Reducción del Riesgo de Inundaciones Súbitas y Fenómenos Atmosféricos en el Área Metropolitana de Barranquilla. *Sci. Tech.* **2013**, *18*, 303–308.
14. González-Álvarez, Á.; Viloria-Marimón, O.; Coronado-Hernández, Ó.; Vélez-Pereira, A.; Tesfagiorgis, K.; Coronado-Hernández, J. Isohyetal Maps of Daily Maximum Rainfall for Different Return Periods for the Colombian Caribbean Region. *Water* **2019**, *11*, 358.
15. Ruiz Cabarcas, A.D.C.; Pabón Caicedo, J.D. Efecto de los fenómenos de El Niño y La Niña en la precipitación y su impacto en la producción agrícola del departamento del Atlántico (Colombia). *Cuad. Geogr. Rev. Colomb. Geogr.* **2013**, *22*, 35–54.
16. Sedano-Cruz, K.; Carvajal-Escobar, Y.; Ávila Díaz, Á.J. Analysis of the aspects which increase the risk of floods in Colombia. *Revista Luna Azul* **2013**, *37*, 219–238.

17. Cama-Pinto, A.; Acosta-Coll, M.; Piñeres-Espitia, G.; Caicedo-Ortiz, J.; Zamora-Musa, R.; Sepúlveda-Ojeda, J. Diseño de una red de sensores inalámbricos para la monitorización de inundaciones repentinas en la ciudad de Barranquilla, Colombia. *Ingeniare Rev. Chil. Ing.* **2016**, *24*, 581–599.
18. CEPAL, N. *Valoración de daños y pérdidas: Ola invernal en Colombia 2010–2011*; CEPAL: Santiago, Chile, 2013; ISBN 958-57544-0-1.
19. *Gobernación del Departamento del Atlántico Plan de Desarrollo del Departamento del Atlántico 2016–2019*; Partido Liberal Colombiano: Barranquilla, Colombia, 2016.
20. Gobernación del Departamento del Atlántico; UNGRD. *Programa de las Naciones Unidas para el Desarrollo Colombia Plan departamental de gestión del riesgo—Atlántico*; UNGRD: Bogotá, Colombia, 2012.
21. Departamento de planeación territorial; Gobernación del Departamento del Atlántico Visión. *Atlántico 2020: La Ruta para el Desarrollo*; Departamento Nacional de Planeación—DNP: Bogotá, Colombia, 2011.
22. Hydrographic and Oceanographic Research Center (CIOH). *General Circulation of the Atmosphere in Colombia;* Hydrographic and Oceanographic Research Center (CIOH): Bogota, Colombia, 2010.
23. Guzmán, D.; Ruiz, J.F.; Cadena, M. *Regionalización de Colombia Según la Estacionalidad de la Precipitación Media Mensual, a Través de Análisis de Componentes Principales*; IDEAM: Bogotá, Colombia, 2014.
24. Chow, V.T.; Maidment, D.R.; Mays, L.W. *Applied Hydrology*, 1st ed.; McGraw-Hill: New York, NY, USA, 1998.
25. Vélez-Pereira, A.M.; De Linares, C.; Delgado, R.; Belmonte, J. Temporal trends of the airborne fungal spores in Catalonia (NE Spain), 1995–2013. *Aerobiología* **2016**, *32*, 23–37.
26. Ahmad, I.; Tang, D.; Wang, T.; Wang, M.; Wagan, B. Precipitation Trends over Time Using Mann-Kendall and Spearman's rho Tests in Swat River Basin, Pakistan. *Adv. Meteorol.* **2015**, *2015*, 1–15.
27. Some'e, B.S.; Ezani, A.; Tabari, H. Spatiotemporal trends and change point of precipitation in Iran. *Atmos. Res.* **2012**, *113*, 1–12.
28. Yue, S.; Pilon, P.; Cavadias, G. Power of the Mann–Kendall and Spearman's rho tests for detecting monotonic trends in hydrological series. *J. Hydrol.* **2002**, *259*, 254–271.
29. Dahmen, E.; Hall, M. *Screening of Hydrological Data. Tests for stationarity and Relative Consistency*; Publication 49; International Institute for Land Reclamation and Improvement/ILRI: Wageningen, The Netherlands, 1990; 58p.
30. Sen, P.K. Estimates of the Regression Coefficient Based on Kendall's Tau. *J. Am. Stat. Assoc.* **1968**, *63*, 1379–1389.
31. Chattopadhyay, S.; Edwards, D.R. Long-Term Trend Analysis of Precipitation and Air Temperature for Kentucky, United States. *Climate* **2016**, *4*, 10.
32. Luna Vera, J.A.; Domínguez Mora, R. Un método para el análisis de frecuencia regional de lluvias máximas diarias: Aplicación en los Andes bolivianos. *Ingeniare Rev. Chil. Ing.* **2013**, *21*, 111–124.
33. Terassi, P. Emerson Galvani Identification of Homogeneous Rainfall Regions in the Eastern Watersheds of the State of Paraná, Brazil. *Climate* **2017**, *5*, 53.
34. Hoskins, J.; Wallis, J. *Regional Frequency Analysis: An Approach Based on l-Moments*; Cambridge University Press: Cambridge, UK, 1997; ISBN 0-521-01940-0.
35. MacQueen, J. *Some Methods for Classification and Analysis of Multivariate Observations*; University of California Press: Oakland, CA, USA, 1967; Volume 1, pp. 281–297.
36. Hosking, J.R.M.; Wallis, J.R.; Wood, E.F. Estimation of the generalized extreme-value distribution by the method of probability-weighted moments. *Technometrics* **1985**, *27*, 251–261.
37. Aitkin, M.; Clayton, D. The fitting of exponential, Weibull and extreme value distributions to complex censored survival data using GLIM. *J. R. Stat. Soc. Ser. C (Appl. Stat.)* **1980**, *29*, 156–163.
38. Fisher, R.A.; Tippett, L.H.C. Limiting forms of the frequency distribution of the largest or smallest member of a sample. *Math. Proc. Camb. Philos. Soc.* **1928**, *24*, 180.
39. U.S. Geological Survey (USGS). *Theoretical Implication of Underfit Streams*; U.S. government printing office: Washington, DC, USA, 1965.
40. Jenkinson, A.F. The frequency distribution of the annual maximum (or minimum) values of meteorological elements. *Q. J. R. Meteorol. Soc.* **1955**, *81*, 158–171.
41. Alam, A.M.; Emura, K.; Farnham, C.; Yuan, J. Best-Fit Probability Distributions and Return Periods for Maximum Monthly Rainfall in Bangladesh. *Climate* **2018**, *6*, 9.
42. Plackett, R.L. Karl Pearson and the Chi-Squared Test. *Int. Stat. Rev. Rev. Int. De Stat.* **1983**, *51*, 59–72.

43. Salas, J.D.; Obeysekera, J.; Vogel, R.M. Techniques for assessing water infrastructure for nonstationary extreme events: A review. *Hydrol. Sci. J.* **2018**, *63*, 325–352.
44. Obeysekera, J.; Salas, J.D. Quantifying the Uncertainty of Design Floods under Nonstationary Conditions. *J. Hydrol. Eng.* **2014**, *19*, 1438–1446.
45. Gonzalez-Alvarez, A.; Coronado-Hernández, O.; Fuertes-Miquel, V.; Ramos, H. Effect of the Non-Stationarity of Rainfall Events on the Design of Hydraulic Structures for Runoff Management and Its Applications to a Case Study at Gordo Creek Watershed in Cartagena de Indias, Colombia. *Fluids* **2018**, *3*, 27.
46. Gilleland, E.; Ribatet, M.; Stephenson, A.G. A software review for extreme value analysis. *Extremes* **2013**, *16*, 103–119.
47. Akaike, H. A new look at the statistical model identification. *IEEE Trans. Autom. Control* **1974**, *19*, 716–723.
48. Haque, A.; Haider, M.R.; Navera, U.K. Developing a semi-distributed hydrological model and rainfall frequency analysis of bangshi river basin. In Proccedings of the 3rd International Conference on Civil Engineering for Sustainable Development (ICCESD 2016), Khulna, Bangladesh, 12–14 February 2016.
49. Bodian, A.; Dezetter, A.; Deme, A.; Diop, L. Hydrological Evaluation of TRMM Rainfall over the Upper Senegal River Basin. *Hydrology* **2016**, *3*, 15.
50. Legates, D.R.; McCabe, G.J., Jr. Evaluating the use of "goodness-of-fit" Measures in hydrologic and hydroclimatic model validation. *Water Resour. Res.* **1999**, *35*, 233–241.
51. Moriasi, D.N.; Arnold, J.G.; Van Liew, M.W.; Bingner, R.L.; Harmel, R.D.; Veith, T.L. Model evaluation guidelines for systematic quantification of accuracy in watershed simulations. *Trans. ASABE* **2007**, *50*, 885–900.

Conclusions

Little information on $P_{max\text{-}24h}$ is readily available for water-related professionals, especially in the Colombian Caribbean region. Even IDEAM has not been able, so far, to process and present all the information they gather, on daily basis, in different formats be it for water-related professional, municipalities, or local, regional, national agencies that typically use this type of data. This study precisely contributes to address this lack of information by thoroughly analyzing the behavior of the daily maximum rainfall, which is one of the variables most used in hydrological analyses for water related project, especially for stormwater management. Each of the stages allowed to tackle these setbacks by analyzing all the available information at regional and more local scale (at department scale) so that municipalities can use it as a reference. The overall main conclusion from each of the stages are shown below:

Chapter 1

The generation of maps of maximum daily precipitation for different return periods, allowed to conclude that:

- Based on the results of this study, GEV and Gumbel are the most recommended distributions for the Caribbean region of Colombia. However, according to the chi-squared test, the GEV distribution was shown to be the best fit among the three CDFs used in majority of the datasets and not the Gumbel distribution function as traditional practices suggest.

- With respect to the best interpolation method for generating isohyetals in the department of Atlántico, the IDW method outperformed both the spline and the ordinary kriging methods. These results demonstrate that geostatistically-based interpolation methods (e.g., ordinary kriging) are not always the best selection as many typically take for granted.

- Increasing and decreasing trends were observed in some of the time series, suggesting the presence of non-stationarity, which, were confirmed in the second chapter of this investigation.

Finally, rather than being considered as the sole source for $P_{24h\text{-}max}$ estimation, the maps developed in this first stage are intended to be used as a reference in the hydrological and hydraulic analysis, mainly for stormwater management and flood mitigation projects.

Chapter 2

The analysis of the Behavior of daily maximum rainfall within the department of Atlántico, Colombia, allowed to obtain the following conclusions:

- The department of Atlántico can be subdivided into three homogeneous regions with respect to the behavior of its $P_{max\text{-}24h}$. These regions were called east, central and west. This finding will make it possible to improve analyzes in areas without rain gauges, taking into account that this department has one of the less dense station networks.

- There are increasing and decreasing trends among the rain gauges of Atlántico, however, only one of the rainfall stations showed a significant trend. This suggests the need for

future trend analysis in the coming five-year periods to determine any further trends 'increase / decrease.

- Overall, the southern area of the central and west regions showed the most noticeable decreasing trend, which is consistent with results previously obtained by IDEAM [1] findings.

- In terms of the performance of isohyetal maps under stationary and non-stationary conditions compared to the mixture (stationary together with non-stationary), the REr values indicate that, although the error in stationary conditions can be observed more frequently, under Stationary conditions could be more significant in terms of magnitude, especially in the south-central region.

- According to the results of the REr, RSR, PBIAS and NSE analyzes, in the western region a stationary frequency analysis (the most used) could be performed safely.

- The central and eastern regions showed a tendency to underestimate, especially in stationary conditions, which indicates, for example, that hydraulic structures for stormwater management should be designed with caution.

The findings in this second stage shed some light on the need of both a better understanding of the regional hydrological behavior and the impact of climate change on future water related projects.